UNIVERSITÀ DEGLI STUDI DI TRENTO

International PhD Program in Biomolecular Sciences

Department of Cellular, Computational
and Integrative Biology – CIBIO

XXXII Cycle

Human cerebellar organoids as an *in vitro* 3D model of Group 3 Medulloblastoma

Supervisor: Pr. Luca Tiberi
CIBIO-University of Trento

Tutor: Pr. Luciano Conti
CIBIO-University of Trento

Ph.D. Thesis of: Marica Anderle
CIBIO-University of Trento

Academic Year 2018-2019

Declaration

I, Marica Anderle, confirm that this is my work and the use of all materials from other sources has been properly and fully acknowledged

Dedicated to my Brother
Daniele P. Anderle

Contents

Abstract

Medulloblastoma (MB) is a heterogeneous tumor that represents the most common malignant brain tumor of childhood. It stands as a cause for a high percentage of morbidity and mortality among cancer patients. Thanks to genome-wide analyses, MB can be divided into four significant subgroups, different from each other for diagnosis, prognosis, and metastatic recurrence. WNT subtype has the best prognosis; SHH subtype has an intermediate prognosis; Group 3 subtype is characterized by a high percentage of metastases and worst prognosis; Group 4 MB is the most common subtype, but the less understood.

Willing to increase the knowledge about the aggressiveness of the Group3 subtype, this work will focus on developing a reliable Human Group 3 MB model based on cerebellar organoids derived from human induced pluripotent stem cells (iPSC).

Three-dimensional (3D) cell culture systems have gained increasing interest in modeling, drug discovery, and tissue engineering due to their evident advantages in providing more reliable information and more predictive data before *in vivo* tests. The field of cell development, differentiation, and cell organization was the first to make use of cerebellar organoids, but these 3D structures are starting to be a novelty in the cancer field.

One of the innovative points of this work is the setup of a new way to modify wild type human cerebellar organoids, electroporating them with strong Group 3 MB inducers, derived from *in vivo* patient-specific NGS data screen. We validate that Gfi1/c-Myc and Otx2/c-Myc oncogenes give rise to MB-like organoids, which (in nude mice) can develop tumors harboring a DNA methylation signature that clusters specifically with human patient Group 3 tumors. Moreover, we identify Smarca4 as an oncosuppressor gene and discover that treatment with an EZH2 specific inhibitor, called Tazemetostat, reduces Otx2/c-Myc tumorigenicity in human organoids.

We speculate that our Medulloblastoma 3D culture system holds great promises for applications in infant tumor research, cancer cell biology, and drug discovery, being a novel human 3D reliable tool for developing personalized therapies.

Introduction

1.1 Medulloblastoma

1.1.1 About it

Cancer is a substantial worldwide health problem and is the second leading cause of death in childhood (5-14 years) (Ward, DeSantis, Robbins, Kohler, & Jemal, 2014). In 2018 were estimated 17.0 million worldwide new cancer cases and 198,700 new cancer cases among children ages 0-14 (John, 2018). The most common cancers in children are acute lymphoblastic leukemia (ALL), brain and central nervous system (CNS) tumors, neuroblastoma, and non-Hodgkin lymphoma (NHL). Malignant CNS tumors represent the second most prevalent cancers in the pediatric population making up 21% of cases (Ward et al., 2014).

Medulloblastoma (MB) is a highly aggressive embryonal tumor that develops in the cerebellum, accounting for 20% of pediatric central nervous system tumors. It is a heterogeneous tumor characterized by anomalies in genes that are fundamental for healthy cerebellum development.

Medulloblastoma can early invade the cerebellar cortex and white matter and diffuse, through the cerebrospinal fluid, to the leptomeningeal membranes that cover the CNS and the spinal cord (Lau et al., 2012). Disseminations into leptomeningeal membranes are the most common form of metastasis for MB, occurring 30% of cases at diagnosis and predicting poor prognosis (Hoff et al., 2009; Zeltzer et al., 1999). Patients who fail therapy or who relapse with metastasis have the same universally dismal prognosis, with almost all patients succumbing to their recidivist disease. Relapsed tumors from patients with MB have a higher frequency of mutational burden and SVs (Hill et al., 2015; V. Ramaswamy et al., 2013). In general, MB is considered a childhood cancer: 21% of cases are diagnosed in infants, 44% occur in children (4-9 years), 23% occur in older children (10-16 years), while only 12% in adults (>16 years)) (Kool et al., 2012). Age distribution and male:female ratios have different compartments respect to their molecular subgroup makeup (Hovestadt et al., 2019). Thanks to the 2016 World Health Organization (WHO), medulloblastoma divides into four histological variants: classic, desmoplastic/nodular, large-cell/anaplastic, and medulloblastoma with extensive nodularity (MBEN). All these histological subtypes distribute among the different molecular subgroups of MB. The classic phenotype represents the standard-risk tumor, while MBEN phenotype is enriched in very young children and correlates with a good prognosis. The large cell and anaplastic histology is a characteristic of the most clinically aggressive form of the tumor (Louis et al., 2016).

Cancer diagnosis in children and infants is a life-altering fact for them and all the family. The hardship of MB stands into its heterogeneous characteristics. Depending on which type of gene mutations, neoplasms, and currency of metastasis, patients should receive specific different treatments. The problem is that there is not a truthful molecular stratification available for medulloblastoma patients, which is every day under implementation.

Current therapies include a combination of surgery, craniospinal radiotherapy, and chemotherapy, reaching 70-80% of overall survival (OS) rate (Northcott, Jones, et al., 2012). All these therapies are invasive and not specific approaches. Actual therapies have origin in the 1920s when Cushing and Bailey highlight that after surgical resection, relapse was inevitable (Bailey & Cushing, 1925). By 1953 was observed that 3-year survival had reached 50% of patients treated with craniospinal irradiation of 30 Gy and posterior fossa irradiation of 50 Gy (Paterson & Farr, 1953).

Nowadays, Medulloblastomas in children (3-5 years) stratify into standard-risk and high-risk groups. The high-risk group is defined by metastatic dissemination, residual disease >1.5 cm^2, and large-cell-anaplastic histology. 80% of standard-risk patients reach 5-years outcomes, no meter which protocol is using. High-risk patients (older than 3-5 years) are treated with craniospinal irradiation of 36-39 Gy, with a consequent boost to 55 Gy to the posterior fossa-tumor bed, added with cisplatin-cyclophosphamide-based chemotherapy. This protocol treatment results in 5-year survival of 60-65% patients analyzed across studies (Vijay Ramaswamy & Taylor, 2017). The irradiation of the entire nervous system is a technique focused on reducing the future leptomeningeal relapse on treated survivors. Unfortunately, this approach is the primary cause of neurocognitive morbidity in MB survivors. For this reason, new studies are pushing to delay radiation therapy until the age of 3 years, decreasing the devasting long-term sequelae to the entire neuroaxis.

The second adjuvant cancer treatment is chemotherapy. Medulloblastoma can be defined as sensitive to different chemotherapy agents, such as vincristine, etoposide, carboplatin, and cyclophosphamide. Unfortunately, it is still unclear the real contribution of chemotherapy to the overall survivors (Ivanov, Coyle, Walker, & Grabowska, 2016), (R. E. Taylor et al., 2003). Despite the intensification of therapies, survival has been stationary for almost 30 years (Vijay Ramaswamy & Taylor, 2017). Since today's treatments are invasive and not subgroup-specific, most of the survivors suffer from long-term side effects like neurological, developmental, neuroendocrine and psychosocial deficits (Mabbott, Penkman, Witol, Strother, & Bouffet, 2008; Mabbott et al., 2005; Spiegler, Bouffet, Greenberg, Rutka, & Mabbott, 2004). Depending on the type of treatment received, children have lifelong cognitive and motor functions, as mutism, defects in the speed of processing, or reduced coordination and balance.

Through an increased understanding of genetic and molecular basis under MB tumor development, it will be possible to improve patient prognostication, to maximize the choice of the right therapy and to improve the quality of patients' life, decreasing side effects.

1.1.2 Molecular subgroups of medulloblastoma

Among CNS tumors, medulloblastoma is the most common malignant one, and fewer than 40% of MB patients have an adequate diagnosis (Ward et al., 2014).

To have a specific and efficient treatment for each patient is fundamental to have a precise diagnosis, understanding and characterizing the type of MB of the patient. The problem is that a reliable molecular stratification for MB is every day under implementation. Indeed, to increase the biological and clinical characterization of this heterogeneous disease, medulloblastoma has been the focus of intensive molecular profiling efforts. During the past two decades, epigenomic, genomic, transcriptomic, and proteomic prospects have been mapped on a high number of human patient samples to disentangle the molecular basis of medulloblastoma. In 2012 were reported the first next-generation sequencing (NGS) studies run on primary MB samples. Now the molecular stratification results in the generation of a wealth of multidimensional-omics data (Hovestadt et al., 2019).

Four molecular subgroups are now widely recognized: WNT, Sonic hedgehog (SHH), Group 3, and Group 4 (M. D. Taylor et al., 2012). Distinct-omic and clinical features characterize each group.

Thanks to the characterization of increasingly larger cohorts of samples, this molecular stratification can be additionally subdivided into subtypes, necessary for an accurate assignment of patients in the specific protocol treatment. WNT and SHH MB, represent 10% and 30%, respectively, of all patients of MB. WNT subtype has the best prognosis, while SHH MB is the subgroup with an intermediate prognosis. Group 3 and Group 4, that share some molecular and biological features, represent 25% and 35%, respectively, of all patients with MB. The first one is a highly metastatic tumor with the worst prognosis. Group 4 is the most common and less understood MB.

In clinical practice, different expression analyses implement the MB stratification, such as NanoString gene expression assay and panel-based gene expression assays. On the other hand, DNA methylation arrays, which can analyze thousands of methylation sites across the genome, nowadays are the most common platform of choice for MB patient's classification. With this approach, it is easy to analyze different clinical samples of archival tumor material coming from different institutions, limiting the technical variations between different laboratories (Hovestadt et al., 2019).

1.1.2.1 WNT subtype

WNT MB is the subgroup with the best prognosis (>95% of patients survive their disease). Among the four subgroups, it is the less common and rarely metastasizes. WNT tumors occur in children over the age of three, have a longer prediagnostic-interval (11 is the median age of diagnosis) and exhibit a balanced male:female ratio (Northcott, Jones, et al., 2012; Vijay Ramaswamy & Taylor, 2017), (Hovestadt et al., 2019). The somatic mutation in CTNNB1 (which promotes stabilization and nuclear localization of β-catenin) is a characteristic mutation of the WNT subtype, occurring for 85% of patients, whereas the monosomy 6 is present in 70-80% of patients (Vijay Ramaswamy & Taylor, 2017; Waszak et al., 2018). WNT medulloblastoma has been described as a homogeneous tumor, but it can be divided into two more molecular subtypes: WNT-α and WNT-β. These two subtypes differ in frequency of monosomy 6 and age distribution at diagnosis (Hovestadt et al., 2019). Other genes found mutated less frequently in this type of tumor are TP53, DDX3X, SMARCA4, and MLL2. DDX3X is a DEAD-box RNA helicase, fundamental for chromosomal segregation, cell cycle regulation, transcription, and translation. TP53 encodes for p53, SMARC4 is a chromatin-modifier gene and MLL2 is a histone lysine methyltransferase, found mutated in almost, respectively, 12.5%, 25% and 12.5% of cases (Northcott, Dubuc, Pfister, & Taylor, 2012; Northcott, Jones, et al., 2012) Patients that have a favorable outcome with 5-years survival rates of >95% are patients under 16 years (Vijay Ramaswamy & Taylor, 2017).

1.1.2.2 SHH subtype

SHH MB is the most common molecular subgroup in infants (<3 years old) and adults, with a 2:1 male:female ratio. It represents an intermediate prognosis group, with 60-80% overall survival rates. SHH tumor is exclusively characterized by a desmoplastic (or nodular) histology, but there are also classic and large-cell or anaplastic (LCA) cases occurring not only in the SHH subgroup (Northcott, Jones, et al., 2012), (Hovestadt et al., 2019). Genetic events occurring in SHH MB are age-dependent. The most common genetic events in SHH MB are mutations and focal somatic copy number alterations (SCNAs) in genes fundamental for the SHH signaling pathway. Some frequent mutations are the inactivating germline or somatic mutations, deletions in PTCH1 and SUFU (suppressor of used homolog), the amplification in GLI2, and the activating mutations in SMO (smoothened homolog) (Kool et al., 2014; Northcott et al., 2017). Specific infants with germline PTCH1 mutations develop the Gorlin syndrome, a nevoid basal-cell carcinoma syndrome. Between the age of 3-16 years, children can be characterized by exclusive somatic mutations in PTCH1 or germline and/or-somatic

TP53 mutations, which, during the growth of the children, co-occur with amplification of GLI2 and MYCN (Kool et al., 2014),(Manam, Oliphant, Henderson, Husain, & Rajan, 2018),(Rausch et al., 2012). TP53 mutations represent a poor prognosis, presenting 30% of childhood SHH. In pediatric SHH MB, there is an enrichment of gene sets related to extracellular matrix function (Northcott, Dubuc, et al., 2012; Northcott, Jones, et al., 2012).

In adults, SHH tumors mostly present somatic mutation in PTCH1, SMO, TERT promoter, and rarely IDH1 (Vijay Ramaswamy & Taylor, 2017). Compared with pediatric SHH MB, adult tumors are characterized by a higher prevalence of mutations in genes that are SHH pathway-associated (such as PTCH1, SMO), a higher prevalence of chromatin modifier mutations (such as BRPF1 and CREBBP) and also present telomerase reverse transcriptase (TERT) promoter mutation (Kool et al., 2014; Remke et al., 2013)(Koelsche et al., 2013). Moreover, adult SHH medulloblastomas express high level of HOXA family genes (such as HOXA5, HOXA9, and HOXA2) and genes involved in tissue development tissue. The most common chromosomal alterations in SHH subtype include loss of chromosomes 9q, 10q, 14q, and 17q, as well as gain of chromosomes 2 and 9p (Northcott et al., 2017). In addition to SCNA on prominent SHH pathway genes, there is a multitude of genes associated with RTK-PI3K signaling. For example, amplification of insulin-like growth factor 1 receptor (IGF1R), yes-associated protein 1 (YAP1), and deletions of PTEN on chromosome 10q23.31 (Northcott, Jones, et al., 2012). In Humans, PTEN is a significant inhibitor of signaling through the phosphatidylinositol 3-kinase (PI-3 kinase) pathway. Castellito Lab hypothesized that increased signaling of PI-3 kinase might influence MB development in mouse models (Castellino et al., 2010). Indeed, it is known that PI-3 kinase signaling is a significant driving force in several human neoplasms, like brain tumors (Castellino & Durden, 2007).

Recently in Cavalli's work were defined four molecular subtypes of SHH MB: SHH-α and SHH-δ, representing the childhood/adolescent and adult subtypes, respectively, whereas SHH-β and SHH-γ, corresponding to infant subtypes (Cavalli et al., 2017). Patients with TP53 mutations can be localized in the SHH-α subtype, which is associated with inferior outcomes compared to SHH-δ one. SHH-γ infants showed a higher 5-year survival than SHH-β.

Nowadays, new preclinical therapeutic protocols for the high-risk group of SHH patients focus on agents targeting downstream genes of SHH pathway, such as bromodomain inhibitors, PI3K inhibitors, itraconazole, arsenic trioxide and GLI antagonists (Gustafson et al., 2014; Tang et al., 2014),(J. Kim et al., 2013).

1.1.2.3 Group3 and Group 4

Before starting to describe these two types of medulloblastomas, it is essential to highlight that Group 3 and Group 4 MBs are similar, and lots of efforts have been made to find biological/molecular peculiarity useful to distinguish them. Indeed, being able to define the biological and clinical heterogeneity between MB subgroups is the crucial point for the development of specific target therapies. We will start to describe the two groups looking at the common and different features, undergoing throw the several stratifications to which they have been subjected, from the past to the present stratification, described into Cavalli's study (Cavalli et al., 2017).

Among all patients, Group 3 and Group 4 represent the subtypes with the highest frequency of metastatic cases at diagnosis, harboring the 30 and 31%, respectively, and 47 and 36% in infant groups (Kool et al., 2012). Talking about age distribution, Group 3 occurs during infancy and childhood, being rare in patients with >18 years of age. On the other hand, Group 4 patients can have all age groups. The male:female ratios are the same for both groups, being 2:1.

Patients with Group 3 MB represent the worst outcome of the four subgroups. This tumor is frequently of the LCA subtype (Kool et al., 2012). Group 4 is the most common subgroup of medulloblastoma, accounting for 35% of patients. Childhood patients of Group 4 MB have an intermediate prognosis similar to the SHH subgroup (~75% OS), whereas adults may do significantly worse. Group 4 presents mainly classic histology, but the LCA phenotype can also rarely be observed (Northcott, Jones, et al., 2012).

Analysis of genomes of Group 3 and Group4 MB samples revealed that either group is characterized by a preponderance of SCNAs and structural variants (SVs) mapping to 9q34 chromosome (Northcott et al., 2014; Northcott, Shih, Peacock, et al., 2012).

Multidimensional molecular analysis demonstrated that in Group 3 tumors 9% of cases will have SMARCA4 mutations, which in Group 4 will be only 4% of cases, and that, in either subgroup, somatic in-frame insertions that affect KBTBD4 represent the 6% of patients (Canning et al., 2013).

One difference between the two subgroups is the gene expression level related to MYC, expressed at a high level in Group 3 and lower level in Group 4. Amplification of MYC is the most common cytogenic aberration in Group 3 MB. Losses and focal copy number gains of chromosomes 1 and 9, which activates GFi1 family oncogenes, are present in 30% of Group 3 tumors. Besides, patients of this group have arm-level copy number gains and losses, counting the 40% of cases in Group 3 with isochromosome 17q (i17q). I17q, metastasis, and MYC amplification determine a poor prognosis for Group 3 patients, but the role of MYC amplification in nonmetastatic Group 3 tumors is unknown.

To highlight how much the Group 3 and 4 tumors are similar, just think that another member of MYC

family, MYCN, is frequently amplified in Group 4 MB, being also found in Group3 (Northcott, Jones, et al., 2012).

PRDM6, which maps to chromosome 5q23, is a novel and exclusive target for tandem duplications in patients with Group 4 diagnosis. PRDM6 is a transcriptional repressor that mediates gene silencing through histone modification and represents the most frequent somatically altered gene in Group 4 tumors (Davis et al., 2006; Northcott et al., 2017; Wu et al., 2008). Additionally, chromatin remodeling genes such as ZMYM3, MLL2, MLL3, KDM6A, CHD7, and EZH2 are recurrently mutated in Group 4 tumors (Northcott, Jones, et al., 2012). The connection between KDM6A, ZYMYM3, and CHD7 mutations and EZH2 activity was described by Robinson *et al.* work (G. Robinson et al., 2012). Robinson reported that EZH2 gene is overexpressed in Group 3 and Group 4 tumors. EZH2 is a methyltransferase that maintains the undifferentiated state of stem cells by repressing the expression of lineage-specific genes, opposing the H3K27 activity of KDM6A that promotes differentiation (Greer & Shi, 2012; Margueron & Reinberg, 2011). EZH2 role in Group 3 MB will be discussed in depth later (see discussion).

In proteomic analyses, Group 3 and 4 exhibit the lowest mRNA-protein expression correlation. This characteristic highlights the possible role of post-transcriptional mechanisms in tumor development. In Group 3 MBs, there is an elevated expression of eukaryotic initiation factors (such as eIF like EIF2s, EIF3s, EIF4Gs, and EIF4As). Indeed, the inhibition of eIE4F complex formation can reduce *in vitro* the viability of Group 3 cell lines (Forget et al., 2018; Rivero-Hinojosa et al., 2018). In Group 4, the proteomic approach revealed activation of RTK signaling through the aberrant expression of ERBB4 and the phosphorylated tyrosine-protein kinase SRC. Electroporation of this last protein in dominant-negative p53 mouse cerebellum induces Group 4-like tumors (Forget et al., 2018).

As we were saying at the beginning, Group 3 and Group 4 MB harbor many genetic and molecular common features, having radically different prognosis and clinical outcome. Indeed, the stratification and definition of Group 3 and Group 4 have been a topic of discussion since their initial discovery (Cho et al., 2011; Northcott et al., 2011). Old nomenclature described Group 3 and 4 as a mixed subgroup of patients defined ‘non-WNT/non-SHH’s MB (Ellison et al., 2011). Around 2012, four commercial antibodies specific for four markers were used to stratify patient samples: DKK1(for WNT MB), SFRP1 (for SHH MB), NPR3 (for Group 3 MB) and KCNA1 (for Group 4 MB). Despite the specificity of these markers, antibodies could not be seen as a reliable tool for patient’s stratification due to the heterogeneity of MB tumors, the differences in sample preparation and fixation techniques used in different laboratories (Northcott, Dubuc, et al., 2012). In 2018 some groups defined the clinical and genetic similar features, between these two groups, in a separate subgroup called ‘Intermediate ¾ Group (Łastowska et al., 2018). We can say that the classification

and recognition of Group 3 and Group 4 are continuously in evolution, knowing that their definition and distinction as discrete molecular entities is fundamental for specific diagnosis and therapies (Vijay Ramaswamy et al., 2016; Vijay Ramaswamy & Taylor, 2017; J. Wang, Garancher, Ramaswamy, & Wechsler-Reya, 2018). A broad spectrum of molecular classification algorithms using mutational, epigenomic, genomic, or transcriptional profiling was implemented during these years to distinguish Group 3 and 4 MB. Recently, thanks to an integrative multi-omics approach, three different studies classified a varying number of subtypes within Group 3 and Group 4. From Schwalbe et al. study, we can stratify four molecular subtypes in Group 3 and Group 4MB, splitting each subgroup into high- and low-risk subtype (Schwalbe et al., 2017). Cavalli et al. study divided each subgroup into three molecular subtypes: Group 3α, β and γ, and Group 4α, β, and γ (Cavalli et al., 2017). On the other hand, Northcott et al. study identified eight molecular subtypes (form I to VIII) (Northcott et al., 2017). Putting together all data analysis of 1,501 Group 3 and Group 4 MBs from all three mentioned studies, Northcott demonstrated that all the different substructures could be unified into the same eight subtypes (see Fig.1). Subtype I is the least common subtype and is composed of a mixture of Group 3 and Group 4 tumors. It enriches for amplification of OTX2 (orthodenticle homeobox 2) oncogene and activation of GFI1 and GFI1B (see Fig.2). GFI1 and GFI1B are MB oncogenes that cooperate with MYC to promote a highly aggressive Group 3-like mouse model (Northcott et al., 2014). Subtype II and III are associated with poor prognosis, having a frequent amplification of MYC oncogene. Subtype IV is enriched for young patients (age of diagnosis is 3 years) and has a favorable outcome in non-infants. The survival rate of this group is dependent on treatment with craniospinal axis irradiation (CSI) (G. W. Robinson et al., 2018). Subtype II, III, IV are authentic Group 3 subtypes. Going through subtype V, VI, VII are looking mostly at Group 4 MB, with a little presence of Group 3 tumors. In subtype V are present amplification of MYC and MYCN, associated with modest outcomes. Subtype VIII displays a balanced genome, except for the high presence of i17q. This subtype is the most common and only authentic Group 4 subtype, characterized by a favorable 5-year survival. It mostly occurs in children between the age of 10 years, and, unfortunately, patients are affected by late relapse and death (Sharma et al., 2019).

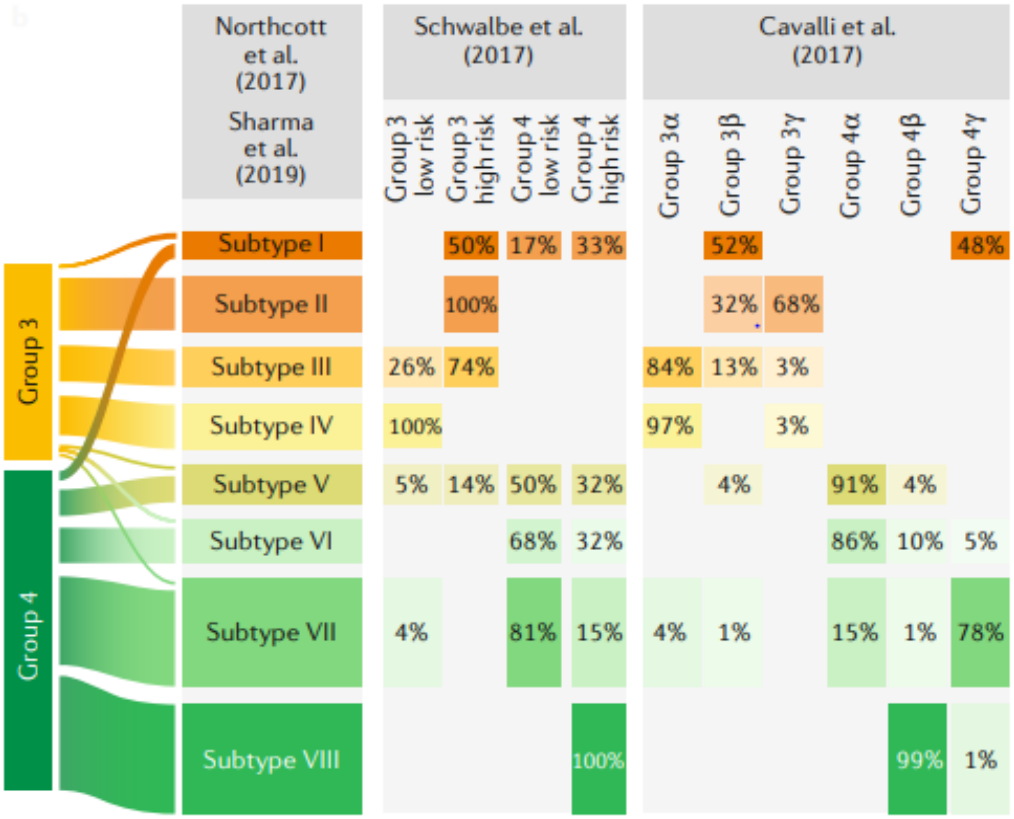

Figure 1: Comparison of MB DNA methylation-derived subtypes described across studies.
Comparison of the eight molecular subtypes of Group 3 and Group 4 MB described by Northcott et al. and Sharma et al. (Northcott et al., 2017; Sharma et al., 2019)(n=1,370 samples; subtype: I=4%, II=13%, III=9%, IV=10%, V=8%, VI=9%, VII=22%, VIII=25%) and the subtypes described in other two additional studies (Schwalbe et al., n=273 samples; Cavalli et al., n=470 samples)(Cavalli et al., 2017; Schwalbe et al., 2017). The line widths between the two consensus subgroups (Group 3 and Group 4) and the eight DNA methylation subtypes indicate the fraction of samples per subtype that were initially classified as Group 3 or Group 4 MB. Reported from (Hovestadt et al., 2019).

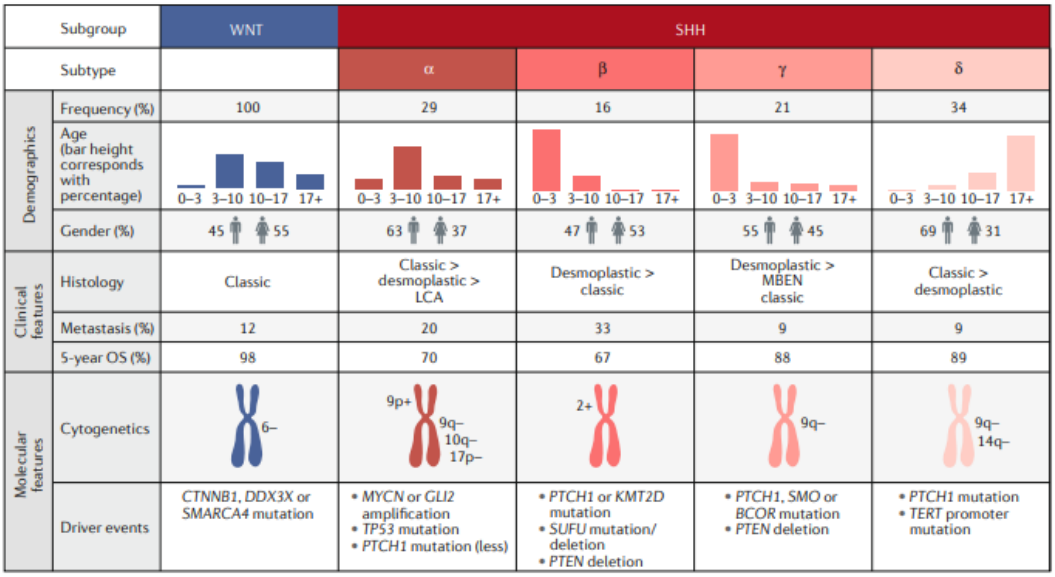

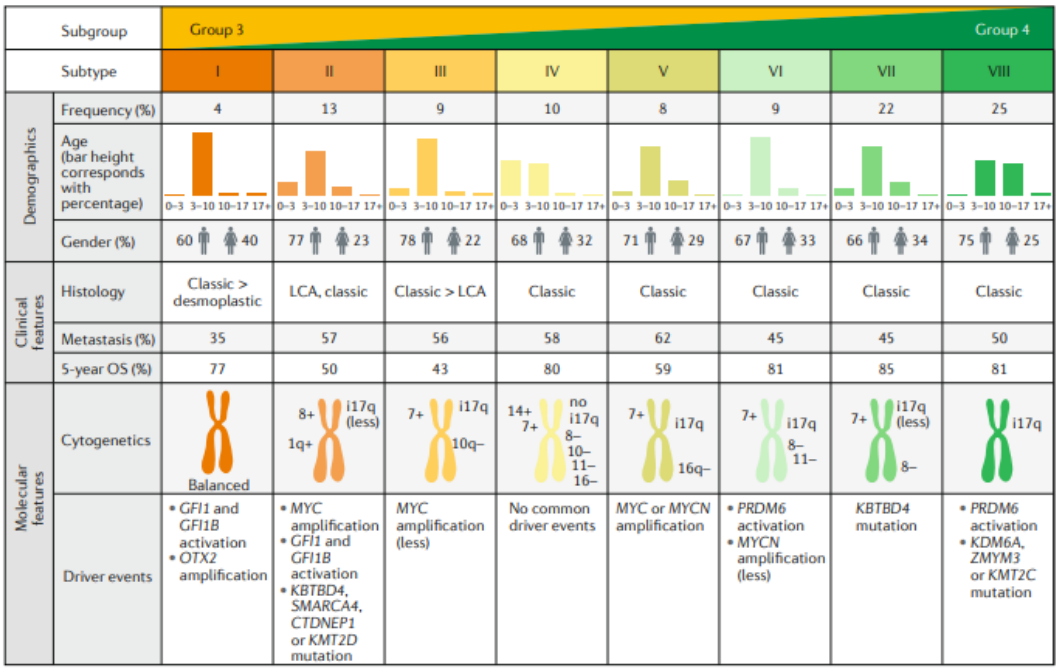

Figure 2: Summary of molecular, clinical and demographic features of MB subtypes: all data come from the Cavalli et al., the Kool et al. and Robinson et al. and Sharma et al. study (Cavalli et al., 2017; Kool et al., 2014; G. W. Robinson et al., 2018; Sharma et al., 2019). BCOR, BCL-6 co-repressor; CTDNEP1, CTD nuclear envelope phosphatase 1; CTNNB1, β-catenin; DDX3X, DEAD-box helicase 3X-linked; GFI1, growth factor independent 1 transcriptional repressor; i17q, isochromosome 17q; KBTBD4, Kelch repeat, and BTB domain-containing 4; KDM6A, lysine demethylase 6A; KMT2C, lysine methyltransferase 2C; LCA, large-cell/ anaplastic; MBEN, MB with extensive nodularity; OTX2, orthodenticle homeobox 2; PRDM6, PR/SET domain 6; PTCH1, patched homolog 1; SMARCA4, SWI/SNF-related matrix-associated actin-dependent regulator of chromatin subfamily A member 4; SMO, smoothened homolog; SUFU, suppressor of fused homolog; TERT, telomerase reverse transcriptase; ZMYM3, zinc finger MYM-type containing 3. Reported from (Hovestadt et al., 2019)

Most of *in vitro* cell lines and *in vivo* models of medulloblastoma do not represent the intertumoral heterogeneity of this particular tumor. Indeed, most Group 3 models represent only the subgroup gamma, characterized by MYC-amplification or activation, denying all the other molecular subtypes. The heterogeneity unrevealed by Cavalli's study highlights the need to design a reliable preclinical model that resembles the different molecular subtypes in Group 3 MB, and within each subgroup.
In this work, we will demonstrate that human cerebellar organoids could be the new reliable 3D model that will mimic this heterogeneous human pathology. We are positive that our novel MB model will be useful for the identification of reliable markers to specify patient stratification and will allow, in the future, the development of effective therapies across each MB subtype.

1.1.3 Group3 Medulloblastoma potential therapies

Group 3 MB therapies world is a complex and knotted research field. With Group 4, Group 3 is one of the less understood subtypes of medulloblastoma. Due to the mixed molecular, genomic, epigenomic, proteomic complexity of Group 3 and Group 4 subtypes do not have a real distinction. Besides, the absence of a reliable model, that resembles the features of Group 3 cancer type, brings to the development of unspecific and inefficient therapy approaches.

Most Group 3 MBs develop in the fourth ventricle as small primary tumors with early dissemination. Group 3 is composed of multiple subcategories, out of which MYC-amplified tumors (Menyhárt, Giangaspero, & Gyorffy, 2019). MYC family genes encode transcription factors that activate or repress downstream signaling. MYC could be studied for therapeutic goals but is a weak target of small molecule inhibition. For this reason, researchers are trying to develop different potential therapies. Group 3 MB lacks spontaneous animal models. Roussel's lab designed novel MYC-driven medulloblastoma models with conditional expression of MYC and loss of TRP53 (D. Kawauchi et al., 2017). These models developed several tumor types in situ from various multipotent embryonic cerebella progenitor cells. In 2012, also Pei's Lab tried to design an MYC-driven model. They demonstrated that cerebellar stem cells expressing Myc and mutant Trp53 develop aggressive tumors following orthotopic transplantation. They showed that these tumors had decreased expression of Foxo targets, which are negatively regulated by the PI3K pathway (Pei et al., 2012). Together, these findings suggest that PI3K/mTOR pathway could be a potential target for the treatment of human MYC-driven MB. For this reason, histone deacetylase inhibitors (HDACIs, such as LBH-589) have been identified in drug screening against these tumors (Pei et al., 2016). The real problem under the design of these mouse models is that TRP53 loss is not a characteristic of primary Group 3 MB

(Northcott et al., 2017). p53 is a well known downstream target of PI-3 kinase signaling. Moreover, PTEN inhibits PI-3 kinase signaling through its interaction with p53 to control cell proliferation (Castellino et al., 2010). It could be a consequence of the absence of p53 expression that MYC-driven MB models (with loss of TRP53) report the activation of PI3K signaling. For this reason, this could be an example of wrong therapy for Group 3, caused by the study of a MYC-driven model and not a specific reliable model for Group 3 MB. Besides, not all Group 3 MB are MYC-amplified tumors. In this respect, proteomic analyses identified a subset of Group 3 MB with increased post-translational activation of MYC, even with the lack of MYC-amplifications. There could be a potential role of the PRKDC kinase in promoting MYC stability, detected in MYC-amplified Group 3 cell lines. PRKDC inhibitor NU7441 sensitizes the MYC-amplified cell line D458 to radiation (Archer et al., 2018).

Other possible therapeutic molecules tested *in vitro* are BET bromodomain inhibitors: they reduce *in vitro* cell proliferation and prolonged survival of MYC-amplified MB xenografts (Bandopadhayay et al., 2014). In gene set enrichment analyses, it was discovered that Group 3 MB increases the folate and purine metabolism pathways. The combination between pemetrexed, a folate synthesis inhibitor, and a nucleoside analog gemcitabine, inhibits cellular growth *in vitro* and increases the survival of mice bearing cortical implants overexpressing MYC-protein. Unfortunately, this approach develops resistance in all cases (Morfouace et al., 2014).

Benzodiazepines function as ligands of $GABA_A$ receptor α5 subunit, which expression is elevated in MYC-driven Group 3 MB. Benzodiazepines have high undesirable toxic side effects, such as respiratory depression in mouse xenograft models (Menyhárt et al., 2019). Currently, *in vitro* and patient-derived xenograft models studies, identified a humanized anti-CD47 antibody with high therapeutic efficacy. This antibody, called Hu5F9-G4, blocks the interaction between CD47 (transmembrane protein, belonging to immunoglobulin superfamily) and the signal regulatory protein-a (SIRPα). CD47 is an anti-phagocyte protein, expressed on the cell surface of malignant paediatric brain tumor, that blocks macrophages from destroying tumor cells (Gholamin et al., 2017). CD47 binds and activates the inhibitory SIRPα on the cell surface. Treatment with the antibody that blocks this interaction, Hu5F9-G4, increases survival in xenograft models with metastasis, being, unfortunately, ineffective on primary tumors (Gholamin et al., 2017).

To conclude, **most available preclinical *in vitro* and *in vivo* models of Group 3 MB have significant limitations and do not represent the molecular and phenotypic** heterogeneity of this class of tumors. Indeed, all Group 3 MB cell lines are MYC-amplified, whereas this MB subtype in human patients represents only 17% of Group 3 events (Northcott, Shih, Remke, et al., 2012).

The lack of faithful models for Group 3 MB subtypes has hampered the development of efficient and targeted therapeutic approaches for these cerebellar tumors.

1.2 Cerebellum development

To understand the features of Medulloblastoma tumors, the study of cerebellum development is fundamental. Indeed, MB is an embryonal tumor, meaning that driver mutations localize in genes that have a fundamental role in the development of the cerebellum, that happens to start from embryos.
Medulloblastoma's field lacks in humanized models resembling the heterogeneity of these tumors that develop during the development of the cerebellum. For this reason, MB is one of the less understood tumors, and human cerebellum organoids could be the perfect start for the design of a good humanized model. Before describing organoids, we will underline the fundamental steps of the development of the cerebellum, the process during which MB occurs.

The central nervous system derives from the neural ectoderm that gives rise to the neural plate. Neural plate folds and fuses to form the neural tube, an epithelium with apical and basal polarity radially organized around a fluid-filled lumen. Morphogen gradients, such as *Shh-Wnt/BMP* for the ventral-dorsal axis and *Fgf* and retinoic acid for the rostral-caudal axis, are fundamental to establish axes. These axes have a role in the subdivision of the brain in the four main regions: forebrain, midbrain, hindbrain, and the spinal cord (Lancaster & Knoblich, 2014). The cerebellum is located at the anterior end of the hindbrain and plays a significant role in sensorimotor functions and a wide range of cognitive functions, including sensory-motor learning, spatial memory, language, balance control, and emotional behavior (Roussel & Hatten, 2011).
Molecular boundaries, rather than morphological, are crucial in determining cerebellum territory, organization, and segmentation. The mouse cerebellar primordium develops from the region of the neural tube that expresses Gbx2 and lack expression of Otx2 and Hoxa2. Shortly after, the primordium starts to reorganize itself, forming a narrow ring encircling the neural tube that will divide the mesencephalon to the rhombencephalon. This ring is called isthmus and contains the isthmic organizer, which represents the interaction between homeodomain transcription factors OTX2 in the rostral epithelium and GBX2 in the caudal domain. FGF8 is a crucial signaling molecule secreted by the isthmic organizer, inhibiting Otx2 expression in the rhombomere 1. So the equilibrium between gradients of Otx2 and Gbx2 expression is fundamental for the establishment of molecular interactions of FGF8, EN1, EN2, WNT1, PAX2, Iroquas (IRXS), SHH and TGF-β family member expression (Marzban et al., 2015).

The primary embryonic cells, from which the cerebellum will develop, localize within the roof of the metencephalon of the mouse embryo between embryonic days 10 and 11 (E10-11). All cerebellar cells derive from two distinct germinal zones: the rhombic lip (RL) and the ventricular zone (VZ). From the RL (see Fig.3), at E10.5 to E12.5, arise glutamatergic projection neurons of the deep nuclei, migrating then to their final distribution via the transitory nuclear zone, which locates below the pial surface at the rostral end of the cerebellar plate (Fink et al., 2006). From the VZ arise GABAergic neurons (such as those of the deep nuclei, Purkinje cells, and Golgi neurons), from multipotent precursor cells in the roof of the fourth ventricle (Gilbertson & Ellison, 2008). After E12.5, a second germinal zone develops from cells within the RL that comprise granule neuron precursors cells (GNPCs). These types of cells migrate across the surface of the cerebellum anlage to develop the external granule layer (EGL).

In mouse, EGL layer persists until postnatal day 15 (P15), whereas into the second postnatal year in the human. During maturation, the GNPCs migrate inward over the Purkinje cells layer, forming the internal granule layer (IGL), composed by mature granule neurons.

Data demonstrated the presence of a third type of cell population, localized in the white matter of the postnatal cerebellum. These cells, characterized by CD133 and Nestin markers, undergo extensive self-renewal, generating astrocyte, oligodendrocytes, and neurons (Gilbertson & Ellison, 2008).

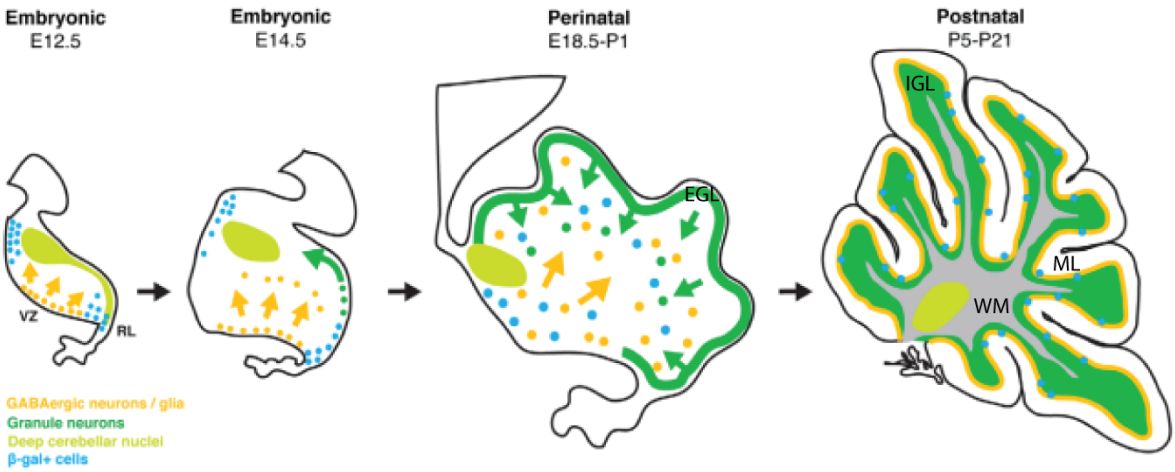

Figure 3: Cerebellum development and principal cerebellum populations stratification.
From rhombic lip (RL) arise glutamatergic projection neurons of the deep nuclei (from E10.5 to E12.5). They will migrate to their final position passing through the nuclear transitory zone. From the ventricular zone (VZ, shown in orange), located in the roof of the fourth ventricle, arise GABAergic neurons (deep nuclei, Purkinje cells, Golgi neurons). In dark green is represented the germinal zone of granule neuron precursors (GNPCs) that will migrate across the anlage to form the external granule layer (EGL). Migrating inward, over the Purkinje cell layer, GNPCs became mature granule neurons forming the internal granule layer (IGL). In light green are represented deep cerebellar nuclei, and in grey is represented the white matter (WM). In blue (b-gal+ cells) are reported Wnt/b-catenin cells, that have a dynamic spatiotemporal pattern during development. Initially, Wnt/b-catenin cells are at the cerebellar rhombic lip and the isthmus. By E18.5, expand into a more widespread pattern with strong expression at the VZ. During postnatal development, it is mostly restricted to the PCL as a subpopulation of Bergmann glia. Adapted from (Selvadurai & Mason, 2011).

Murine cerebellum shares many features of lamination, circuitry, foliation, and neural morphology with humans. However, in humans, the development of the cerebellum is a longer and more complicated process that starts from 30 days after conception to the end of postnatal year 2. Mouse cerebellum development is almost completed already at postnatal day 15. The human cerebellum contains 80% of all brain neurons, with a 750-fold larger surface area, increased neural numbers, and altered neural subtype ratios in comparison to mouse cerebellum (Haldipur et al., 2019). Both humans and mice have two primary zones of neurogenesis, RL and VZ, but they have a different spatiotemporal expansion of progenitor zones. The human embryonic RL is small, but the VZ thickens through 10 postconception weeks (PCW). In humans, the cerebellar plate starts from the dorsal aspect of the rhombencephalon 28 days after fertilization (called stage 13). The cerebellar primordium expands in a thick ventricular layer 32 days after fertilization. The RL is established 40 days after fertilization, and by stage 20 (52 days after fertilization), cells migrate rostromedially from the RL and radially from the VZ. Rudiments of vermis are present around stage 22, and the external granule layer spreads from the RL onto the dorsum of the cerebellar bulge (Marzban et al., 2015). Murine external granule layer can be seen by E12.5, composed by proliferating granule cell progenitors and driving postnatal foliation expansion. Human EGL proliferates during the period between 26-32 PCW (Haldipur et al., 2019). At Carnegie stage 12 (CS12), human VZ resembles E12.5 mouse VZ, and by CS14, an emerging subventricular zone (SVZ) is present in human (mouse cerebellar does not have an SVZ). Basal PH3 positive progenitors are present SVZ around between CS18-23. Cell differentiate in the outer SVZ diminishing SVZ size, until the end of embryogenesis (8 PCW), where it remains only a residual VZ (Haldipur et al., 2019). Also, the human RL, after 10 PCW, can be divided into ventricular (RL^{vz}) and subventricular (RL^{svz}) zone, having a more complex proliferation profile. RL^{vz} represents the Sox2 positive and KI67-rich cells, and RL^{svz} the KI-67, Sox2-sparse cells, that migrate into the external granule layer (Haldipur et al., 2019). Tbr2 is expressed in the RL^{svz} with a few scattered nascent unipolar brush cells, in both the external and internal granule layer. These are only some information about the different developmental timing in humans, but the knowledge regarding cellular and molecular biology of cerebellum development comes from studies done in rodents (Muguruma, 2018). It is essential to keep in mind the value and limitations of mouse genetic models of human neurodevelopmental disorders.

The cerebellar cortex is a laminar structure composed of a monolayer of inhibitory Purkinje cells (see Fig.4), closed by a dense layer of excitatory granule neurons and a sub-pial molecular layer of granule cell axons and Purkinje cell dendritic trees. Granule neurons are the most prevalent neuronal subclass

within the cerebellum, having the role in coordinating afferent input to and motor output from the cerebellum through their connection with the Purkinje cells. Most Purkinje cells, through a diverse set of interneurons, project to a variety of cerebellar nuclei, localized in the white matter. An example of interneuron is the unipolar brush cell population that is fundamental in receiving inputs from the vestibular system nuclei in the hindbrain and project to granule cells. Another essential population that has a role in the maturation of granule cells is Bergmann glial cells. This population is a specific glial population that function as scaffolds to the radial migration of granule cell precursors from EGL to IGL (Butts, Green, & Wingate, 2014).

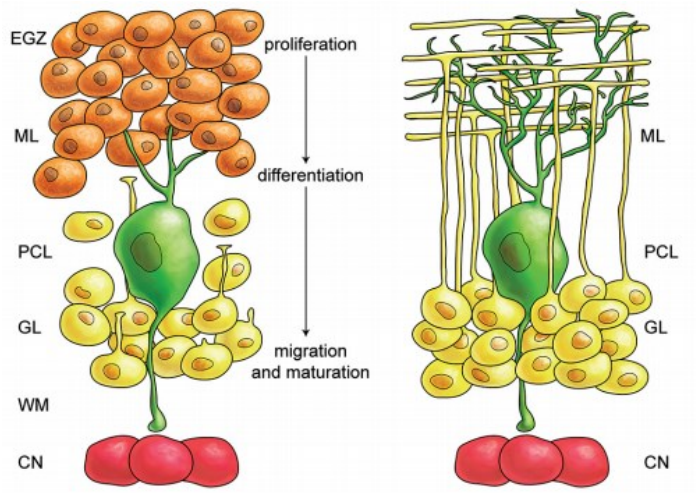

Figure 4: Schematic illustration of germinal zones and organization of the cerebellar cortex.
On the left is represented a P10 cerebellum, on the right, an adult cerebellum. Purkinje cells (green) express SHH that increases the proliferative activity of external germinal zone (EGZ) cells, composed by precursors of granule cells. Granule cells differentiate and migrate cross Purkinje cells layer to the final destination. Maturation completes in this layer. Abbreviations: EGZ: external germinal layer (zone), WM: white matter, CN: cerebellar nuclei, PCL: Purkinje cell layer, ML: molecular layer, GL: granule layer. Adapted from (Marzban et al., 2015).

As illustrated above, the cerebellar cortex is a simple structure, but with a complex intercommunication between all cerebellar populations. At this point, it is evident that it would be fundamental to define the role of somatic genomic alterations in specific human cells of medulloblastoma, better to understand the origin and the mechanism of tumorigenesis. We think, like many other laboratories, that a specific mutation can be tumorigenic in a determined spatial-temporal condition, and the type of cell in which it occurs is the spark that triggers the tumorigenesis. For this reason, it is fundamental to understand the cell of origin of the driver mutation in a faithful human model for MB, avoiding murine models that do not develop the same human cellular precursors.

1.3 Medulloblastoma models

Due to ethical and technical motivations, not every time is possible to study a human disease taking patient samples. Thinking about it, samples from children with medulloblastoma implies surgical resection of part of the cerebellum, which is risky, invasive, not replicable in all patients and will have secondary effects on children's life.

For these reasons, to study the molecular, genomic, cellular features of a disease, science is based on studies effectuated on reliable models that resemble the human pathology. Unfortunately, MB is a real heterogeneous type of tumor that gives a real hard time to the realization of a good model. This tumor is challenging to design because it is a mix of types of tumors, each having their specific molecular and genomic features that define, in humans, the different diagnoses and overall survival. We can say that the development of reliable cancer models is still an Achille's heel of researchers.

Until now, medulloblastoma is one of the diseases that remain without a reliable model that can recreate all features present in MB patients, for any of the subgroups. Until now, many attempts approached a possible MB model, and we will report here some of the most famous examples.

1.3.1 State of the art of *in vitro* models of medulloblastoma

Primary tissues and established cell lines represent the *in vitro* laboratory experiments used to test molecular, biological hypothesis and treatment strategies. *In vitro* experiments allow the employment of human patient-derived tissue to be expanded and used in a broad range of experiments that are reproducible, inexpensive, and yield rapid results. One disadvantage of this type of method is the departure from the physiological micro-environment in which the tumor develops in human patients. Primary cultures are the initial *in vitro* culture that represents the highest resemblance to the *in vivo* state, but they increase variability, making this type of model hard to reproduce and standardize.

Until the first passage, primary cultures can be compared to the original tissue. As time passes, cells can stop dividing, or they continue to divide, growing cells that are adapted to *in vitro* growth conditions and are characteristically distant from the patient (Ivanov et al., 2016). In the beginning, researchers thought that the *in vitro* selection could be avoided by culturing and passaging these cells in immunocompromised mice in the original anatomical location. However, systematic genotyping and gene expression studies show that subsequent passaging *in vivo* introduces genetic drift (almost 30 gene differences from passage 1 to 3) and possible loss of heterozygosity (Shu et al., 2008).

Less variability, compared to primary cultures, can be found in long-established continuous cell-lines. They have the advantages of being easy to expand, relatively uniform, and highly reproducible in different laboratories with different roles. Selection bias, phenotypic and genetic drift are the main disadvantages in the usage of this type of cells (Ivanov et al., 2016).

Looking at medulloblastoma's characterization methods, it is difficult to have a clear picture of the medulloblastoma cell line landscape. However, there are around 44 established continuous medulloblastoma cell-lines representing the four MB subgroups. For example, UW-228 and DAOY are SHH cell lines that have mutations in TP53; MED5R are WNT cell lines, with β-catenin mutation; the D238 cell line, characterized by MYC and OTX2 overexpression, have been placed in an intermediate group between Group 3 and 4 (Ivanov et al., 2016). All Group 3 MB cell-lines harbor MYC amplification, representing only the characteristics of high-risk aggressive medulloblastoma. We know that Group 3 MB has many other genomic and molecular features, meaning that maybe the more aggressive subtypes of MB are better suited to grow *in vitro*.

Regarding Group 4, there is only one pair of cell-lines called CHLA-01-MED and CHLA-01R-MED, derived from the same patient (Ivanov et al., 2016). There are many other cell lines available in research, but they have not been characterized and stratified to the standard of molecular MB era. We can conclude that the state of the art of cell lines is not able to cover all the subgroup features of this type of tumor.

Another approach used to recapitulate MB tumor development is the use of genetically engineered mouse models (GEMMs). GEMMs can be seen as a mix of *in vivo* and *in vitro* modeling because they are used for *in vivo* phenomena study, but also cells derived from mice in which the tumor develops *de novo* can be used for high-throughput screens and drug testing *in vitro* (Morfouace et al., 2014). These models are engineered by retroviral or chemically induced mutations. It can be possible to control the spatial and temporal expression of genes through the use of systems like Cre-LoxP or Tet-off/on. Many MB GEMMs were generated for SHH subgroup, modifying SHH signaling genes, such as Ptch, Smo, Sufu, with deletion of Trp53 or cyclin-dependent kinases. WNT MB GEMM reported the overexpression of Ctnnb1 and a Pik3ca mutation in combination with Trp53 knock-out. Until now, no specific group 4 MB GEMMs are available, and, compared to WNT and SHH, few models are present for Group 3.

Human neural stem cells are another *in vitro* model. They can be obtained from human umbilical cord blood stem cells, human embryonic stem cells, and fetal brain tissue. These types of cells are difficult to be cultured and follow many long steps protocol to reach neural stem state, also highlighting gene expression differences between the three sources. On the other hand, there are also ethical issues that make this model tricky to be used. To avoid these problems, it is possible to use human induced

pluripotent stem cells (hiPSCs). Human iPSCs are similar to human embryonic stem (ES) cells in morphology, proliferation, surface antigens, epigenetic status of pluripotent cell-specific genes, gene expression, and telomerase activity. These cells can *in vitro* differentiate into cell types of the three germ layers and teratomas obtained by subcutaneous transplantation into nude mice (Takahashi et al., 2007). Because of their differentiation potential, hiPSCs can generate any cell type, and they can be used not only as a 2D model but a three-dimensional (3D) model to resemble the development of several human organs.

Here comes the last and most recent model: organoids derived from pluripotent stem cells or isolated organ progenitors. The path that led to the development of 3D models has been tortuous, and researchers used different approaches over the years. The *in vivo* growth of the majority of healthy cells and tumors, seen as three-dimensional tissues, is surrounded by a microenvironment composed by extracellular matrix, nutrients, cell-cell communication, gradient oxygen levels depending on their proximity to blood vessels. Multicellular spheroids, recapitulate the physiological features of normal or tumor tissues, considering that they synthesize their own extracellular matrix and mimicking cell-cell interactions. Ivanov et al. demonstrated that, compared to monolayers, gene expression profiles in spheroids are closer to those of tumor patients (Ivanov et al., 2016). However, this model has some limitations. Just think that in the context of medulloblastoma, a realistic model should develop a complex network of differentiated neurons and glia along with progenitors. Regarding this, human neurospheres fulfill most of the populations of the cerebellum, reproducing just a simple mix of progenitors, glial, and neural cells. In this respect, they can be used to assess toxic effects and toxical implications, being a possible model for collateral damage targets in children's brains (Riggs et al., 2014). However, they can be a disadvantage in representing all mature population of child's brain, because they are characterized by poorly-differentiated cells. Muguruma and Sasai protocol is the last and the only complete protocol to develop human cerebellar organoids (Muguruma, 2018; Muguruma, Nishiyama, Kawakami, Hashimoto, & Sasai, 2015), necessary to resemble the healthy cerebellum development. Indeed, our project started developing cerebellum organoids using this Muguruma's protocol, which we will discuss later (see paragraph 1.4.3). When researchers try to model a specific tumor, like medulloblastoma, it is fundamental to include in the study the interaction between normal and tumor tissue. This aspect is vital to understand chemosensitivity, radiosensitivity, angiogenesis, proliferation, cell adhesion, cell spreading, and gene expression. This method of co-colture seems to increase the physiological relevance of the model (Ivanov et al., 2015).

The last *in vitro* model that closely represents the *in vivo* state of the brain outside of the body are organotypic brain slices. This type of model has a mix of differentiated cells in the right spatial organization, the in vivo-like architecture with the native extracellular matrix of the brain. Brain slices

derive from adult human brain (Jung et al., 2002) and rodents pups (Stoppini, Buchs, & Muller, 1991). They are essential for several types of studies, such as drug delivery in medulloblastoma (Meng, Garnett, Walker, & Parker, 2016), tumor invasion, and metastasis in glioma (Aaberg-Jessen et al., 2013). The disadvantages of this model are the low-throughput manual work to derive the cultures, limited life-span, and high variability between slices preparations (Ivanov et al., 2016).
In the end, we can conclude that all present MB *in vitro* models are insufficient to resemble human pathology, having many limitations. Besides, medulloblastoma is an embryonal tumor, but any current *in vitro* models can resemble the development of the tumor during the development of the cerebellum.

1.3.2 State of the art of *in vivo* models of medulloblastoma

Mus musculus is the most commonly used model organism in human disease research, to provide insight into the genetic and molecular mechanisms, to explore the efficacy of candidate drugs, to predict patient responses and possible metastasis relapses. Mice are a model organism to study human pathologies, having genetic and physiological similarities with humans. In respect, we must highlight that mice have evolved in dissimilar environments and respond differently from the human counterpart (Junhee et al., 2013). So, when researchers use mice in biomedical studies, they need to take account of the similarities as well as the evolved differences between mice and humans. Nonetheless, significant steps have been made to decrease the distance between the two parts, knowing that mice remain the closer species to humans in biomedical research (Perlman, 2016).

In order to study the complexity of Medulloblastoma tumors, in the first line, there is the generation of reliable mouse models, that could match genetic alterations and gene expression as in the human pathology. The four MB groups significantly differ from each other on genetic, epigenetic, gene expression, histology, and clinical level, which can vary even within one subgroup. Therefore, the mouse model used to study a specific MB subgroup has to adapt to the advances in human medulloblastoma subgrouping (Pöschl et al., 2014).
Mouse models of brain tumors are engineered by retroviral or targeting expression of oncogenes into neural progenitors or stem cells, fundamental during the healthy development of the brain.
Pöschl *et al.* work highlight that genome sequencing of human and mouse tumors demonstrates that the genetic make-up is not the single driver of medulloblastoma, which determines molecular MB classification. Nonetheless, in this study have been collected 140 gene expression datasets from 20 different known medulloblastoma mouse models and gene expression profiles of 423 human

medulloblastoma specimens on the other (Pöschl et al., 2014). It was done to generate a repository of reliable mouse models for medulloblastoma, to match them to human tumor samples to see how precisely they were mimicking the pathology and to identify good mouse model candidates for preclinical studies in a sub-group specific stratification.

Figure 5 reports the main used MB mouse models, summarized in Pöschl *et al.* work, comparing them with human samples through the AGDEX (agreement of differential expression) analysis and k-means clustering (Pöschl et al., 2014). *Blbp-Cre::Ctnnb1*$^{+/lox(Ex3)}$*; Trp53*$^{flx/flx}$ mouse model appears suitable for the study of WNT medulloblastoma. It is based on a conditional allele of *CTNNB1* that it is expressed in rhombic lip progenitor cells, carrying a deletion of *TRP53.*

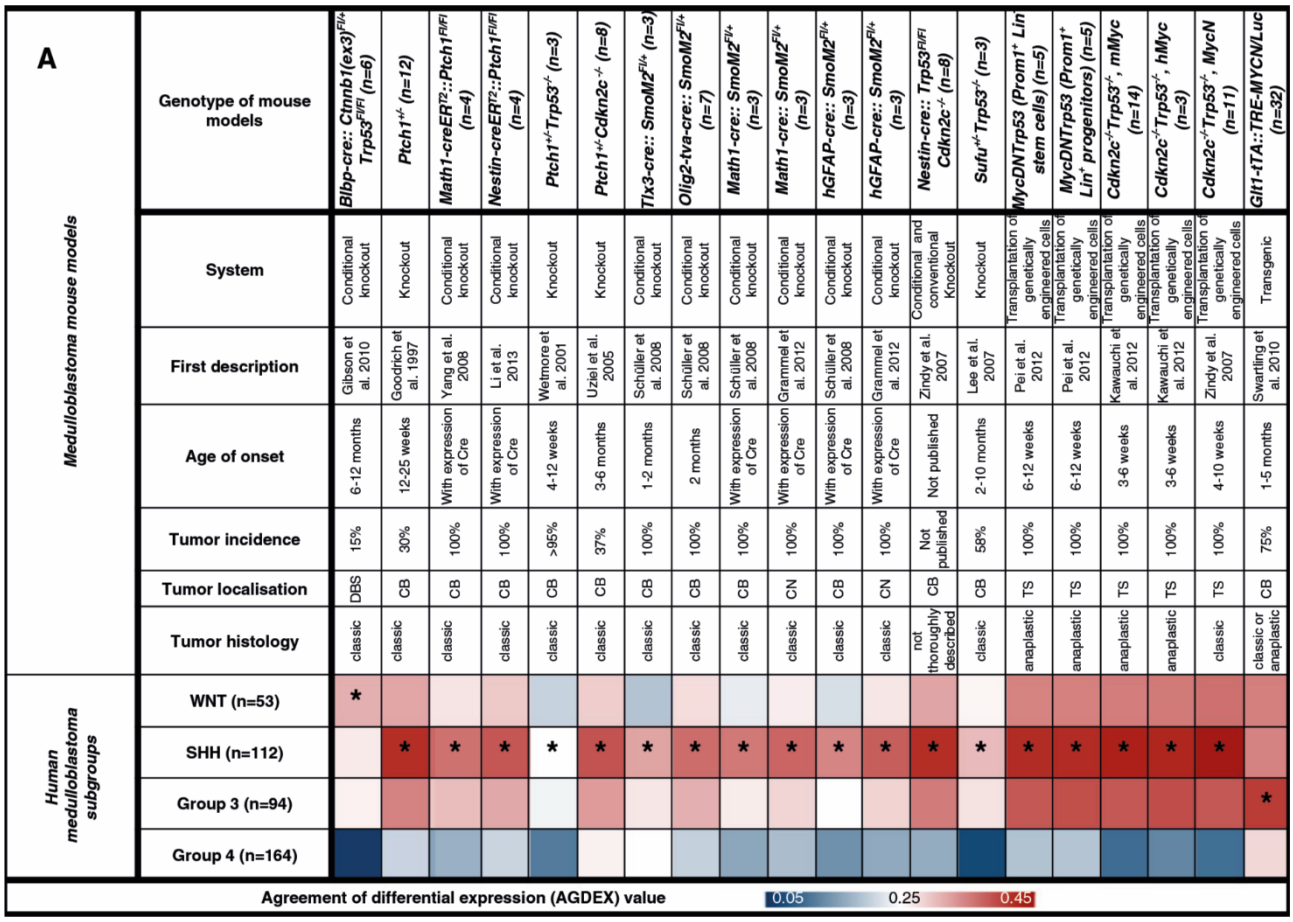

Figure 5: Characterisation of diverse medulloblastoma mouse models.
ADGEX for 20 different MB mouse models (140 tumor samples) compared to the four human MB subgroups (423 tumor samples). Asterisks mark the highest significant AGDEX score per column ($p < 0.05$). Adapted from (Pöschl et al., 2014).

Blbp is the brain lipid-binding protein, and the expression of it correlates spatially and temporally with neuronal differentiation in several parts of the mouse CNS, such as postnatal cerebellum. This WNT mouse model develops, after 10-12 months, classic medulloblastoma with 15% penetrance (Gibson et al., 2010).

More recently, this model has the addition of PI3K catalytic-α polypeptide mutant allele. Pik3caE545K mutant tumors contained more significant AKT pathway activity, which likely activates the AKT pathway to progress, rather than initiates, WNT-medulloblastoma. This type of model has a more aggressive penetrance, harboring 100% by 3 months of age (G. Robinson et al., 2012). Cancer-associated, activating mutations in PIK3CA were detected, also, in a single case of SHH (PIK3CAH1047R) medulloblastoma. Comparing SHH and WNT medulloblastoma, the first one subtype has a higher number of mouse models resembling it.

SHH MB models represent the first models in medulloblastoma *in vivo* research. In 1997 Goodrich laboratory was the one that created the first SHH MB mouse model, called $Ptch1^{+/-}$ mouse, using a germline inactivating mutation of Ptch1. This model develops sporadic medulloblastoma from GNPCs of EGL with a penetrance of 14-20%, arising within 5 months (Goodrich, Milenković, Higgins, & Scott, 1997). Models following this one are improvements of $Ptch1^{+/-}$ mouse, developed by either different mutation addiction or the usage of driver promoters (Larson & Largaespada, 2012). Some examples: $Ptch1^{+/-}Trp53^{-/-}$ mouse (Wetmore, Eberhart, & Curran, 2001), $Ptch1^{+/-}Cdkn2c^{-/-}$ mouse (Uziel et al., 2005), $Ptch1^{+/-}Cdkn2c^{-/-}$, *MycN* mouse (Pöschl et al., 2014), *Nestin-creER*^{T2}*::Ptch1*$^{Fl/Fl}$ mouse(P. Li et al., 2013), *Math1-creER*^{T2}*::Ptch1*$^{Fl/Fl}$ mouse and *GFAP-Cre::Ptch1*$^{flx/flx}$ mouse (Yang et al., 2008).

There is a big part of SHH mouse models that is characterized by mutations in *Smoothened* (SMO) or combined mutated Sufu with Tp53 deficiency. As reported in Figure 5, we will report here models that match significantly with the human counterpart of SHH MB (Pöschl et al., 2014): *Tlx3-Cre::SmoM2*$^{Fl/+}$ mouse, *Olig2-tva-Cre::SmoM2*$^{Fl/+}$ mouse (Schüller et al., 2008), *Math1-Cre::SmoM2*$^{Fl/+}$ mouse, *hGFAP-Cre::SmoM2*$^{Fl/+}$ mouse(Schüller et al., 2008), (Grammel et al., 2012), $Sufu^{+/-}Trp53^{-/-}$ mouse (Lee et al., 2007). To conclude, *Myc* and *MycN*-based mouse models with *Trp53* mutations show an SHH signature to some extent (Pöschl et al., 2014).

With Group 3 and Group 4 mouse models, it is a different story: the lack of knowledge of these two groups is at the basis of the lack of models, and the other way around. Talking about Group 3 MB, the GTML mice is a *Glt1-tTA; TRE-MycN; Luc* model it seems to be the only transgenic Group 3 mouse model (Pöschl et al., 2014). There are also models based on transplantation of MycT58A (stabilized Myc) and DNTrp53 (dominant negative Trp53) transfected cerebellar stem or progenitor cells (Pei et al., 2012), that initially were presented as Group 3 models. These models, as well as

Cdkn2c−/−Trp53−/−, mMyc or hMyc models (Daisuke Kawauchi et al., 2012; Pei et al., 2012), did not match specifically to Group 3 MB, but agreed with human SHH MB in the ADGEX analysis. The similarity to SHH group could be caused by TP53 alterations, that have not been detected in the 72 human Group 3 MB that Pöschl analyzed (Pöschl et al., 2014). An *in vivo* reliable approach for Group 3 MB modeling, is represented by the orthotopic transplantation done by Northcott et al. in 2014. Retrovirus encoding Gfi1 and Gfi1b were transduced with Myc into neural stem cells and then were transplantation into cerebella of immunocompromised mice (Northcott et al., 2014). The combination between Myc and Gfi1, insufficient to generate MB on its own in this system, developed highly aggressive cerebellar tumors in nearly all injected mice. It was a nice *in vivo* work to understand the driving role of a combination of MB oncogenes but is not a transgenic mouse model. Moreover, in 2017 it was developed, by in utero electroporation, a Group 3 mouse model based on the conditional expression of Myc and DNTrp53 in different multipotent embryonic cerebellar progenitors. It is important to highlight that these models are based on p53 loss of function, a molecular feature that does not represent Group 3 tumors, but only relapse (Ramaswamy, Nör, & Taylor, 2016).
Regarding Group 4, proteomic and phosphoproteomic analyses identified aberrant ERBB4-SRC signaling in Group 4 MBs. These results inspired the first *in vivo* study for Group 4 MB. Indeed, in utero-electroporation of SRC and a dominant-negative form of p53 induces murine tumors that resemble Group 4 MB (Forget et al., 2018).

To conclude, Group 3 is the most aggressive MB, but it remains with a few reliable mouse model that resembles the human pathology. The development of a suitable Group 3 and 4 MB model must be one of the main points of medulloblastoma research.

1.4 Organogenesis: the new cancer modeling approach

1.4.1 Overview

Cancer model research is a field that is struggling to recapitulate the heterogeneity of human tumors. It is fundamental to develop a specific, reliable, and precise experimental model, to investigate the basics of cancer biology and advance therapeutic protocols.

Accurate tumor modeling is based on the capture of the complexity of homotypic and heterotypic cellular interactions within the context of a 3D tissue microenvironment.

As reported previously, many different methods are available in the literature for model cancer diseases, but all of them have some significant pitfalls. For example, transformed cell lines can be expanded and experimentally manipulated by genetic and pharmacological approaches. The disadvantages of cell lines are the undefined mutational background, caused by long-term passages, and the lack of three-dimensional tissue cell-organization and tumor heterogeneity (Neal & Kuo, 2016). The *in vivo* cancer modeling makes possible the overcome of some of the 2D limitations of *in vitro* cell lines, allowing initiation of neoplasia into 3D normal tissue context, transgenic or mutagenic manipulation, and breeding strategies. At the same time, these models are expensive to be maintained, can present drawbacks of scalability and throughput. They have many differences from human genomic expression, and they lack on communication between the model and the adjacent human tissue (Neal & Kuo, 2016).

To generate a reliable model that combines the 3D structure of *in vivo* organ with the easy maneuverability of 2D cell lines, researchers designed and developed numerous *ex vivo* 3D organotypic culture methods. These types of cultures start from different sources, such as whole organ explants or tissue slices, spheroids derived from transformed cells, 3D organotypic cultures of healthy and transformed human tissues, the so-called *organoids.* The term organoid, which stands for “form of an organ”, it is a culture system that closely recapitulates the specific features of the organ itself, like multilineage differentiation, stem cells, and 3D architecture in the manner by which the organ develops (Neal & Kuo, 2016). The definition of organoid from Lancaster and Knoblich's work is: “a collection of organ-specific cell types that develops from stem cells or organ progenitors and self-organizes through cell-sorting and spatially restricted lineage commitment like the *in vivo* counterpart” (Lancaster & Knoblich, 2014).

Primary organoid cultures have been established for mammalian organs, like liver, colon, brain, breast, eye, esophagus, kidney, lung, pancreas, and stomach (Neal & Kuo, 2016). For each organ, there is a derivative method, with specific attention in the recapitulation of endogenous developmental processes. Depending on the organ we are considering, organoids have been created both from

patient-specific derived cells or from healthy human stem cells. The most common patient-derived organoid (PDO) cultures are from biopsies or surgical resections of cancers of the colon, pancreas, lung, and prostate (Neal & Kuo, 2016). The most considerable promise of the PDO models is their application to precision medicine. The rapidity in the generation of organoids from a patient's tumor tissue enables personalized drug testing and the development of targeted therapies that have been previously impossible. For example, in Inoue's lab, lung PDOs have been used to recapitulate the sensitivity of EGFR-mutant lung cancers to the erlotinib (a tyrosine kinase inhibitor) and to model crizotinib resistance in lung PDO harboring EML-ALK4 fusion (Endo et al., 2013; Kimura et al., 2015).

If we look at the history, organoids are the methodological evolution of the embryoid bodies (EBs), an in vitro system similar to an early teratoma. They represent 3D aggregates of pluripotent stem cells (PSCs) that go through an initial developmental specification, like a pre-gastrulating embryo, to then differentiate into various organized tissues, much like a teratoma (Lancaster & Knoblich, 2014). It is essential to specify that not all organoids methods have to start from an initial EB stage, whereas the crucial factor is the exogenous tissue patterning by the use of specific factors to form a 3D self-organized structure. This self-organization is one of the advantages of organoids that grow moving away from the 2D culture, even if some of them need support for this purpose, like the laminin-rich extracellular matrix Matrigel or Collagen I (Lancaster & Knoblich, 2014; Neal & Kuo, 2016). Due to the lack of embryonic axis formation, it is possible to say that every organoid is unique: it has a typical tissue architecture, but with high heterogeneity in relative tissue regions positioning. It can be an obstacle for the generation of pure populations of single cells, but in organoids there is always more than one type of cell population, and this feature can be a powerful tool for modeling development and therapeutic cancer perspective (Lancaster & Knoblich, 2014). Current technologies established derived organoids from human iPSCs for gut, kidney, retina, brain (Lancaster & Knoblich, 2014), and cerebellum (Muguruma et al., 2015).

Organoids can be defined as an easily accessible model system, thanks to which we can answer developmental questions that have been difficult to study until now. In particular, this is true for biological principles that are specific for humans and would be different studied in other species. For example, retina organoids have been essential to highlight differences between human and rodent tissue morphologies and developmental timing (Nakano et al., 2012). Another example is brain organoids that are fundamental to study the unique division mode of human neural stem cells (Lancaster et al., 2013). In the next paragraph, we will discuss how organoids can improve cancer patient outcomes, being a reliable platform for drug discovery and precision medicine.

1.4.2 Organoid's therapeutic potential in cancer research

Organoids are a turning point for cancer research: they allow to study the development of the malignancy during the development of the specific tissue, increasing the opportunity to design a target therapeutic approach. Carcinogenesis is a complex process, defined by the hallmarks of Hanahan and Weinberg (Hanahan & Weinberg, 2000): sustenance of proliferative signaling, evasion of growth suppressors, resistance to cell death, genome instability, enabling of replicative immortality, activation of invasion and metastasis, induction of angiogenesis, and tumor-promoting inflammation (Hanahan & Weinberg, 2011). Organoids have been used to mimic a variety of cancer hallmarks, and more are possible with minor modifications in comparison to existing culture cell lines. For example, proliferation can be inferred from longitudinal organoid viability or metabolism-based assays, or by immunostaining for Ki67 (X. Li et al., 2014); invasive phenotype can be tested via 3D transwell invasion assays as performed by Li et al., which used immune-compromised mice; Kwong et al. demonstrated the effect of inflammation on tumorigenesis with the ovarian organoid system (Kwong et al., 2009).

Regarding genomic mutations and instability, one of the most critical improvements in organoid cultures is the ability to alter their genomes, transcriptomes, and epigenomes to study how these alterations may push organoids to cancer (Neal & Kuo, 2016). The simplest example is gain-of-function experiments, whereby organoids are models to study the effects of driving oncogenes or dominant-negative suppressor alleles. In our study, we modified organoids only by a specific buffer (under patent) mixed with Piggy Bac plasmids expressing specific oncogenes, targeting DNA by electroporation (Ballabio et al., 2020). It is one of the easiest, fastest, and low-cost methods to modify organoids. Loss-of-function studies are based on CRISPR/Cas9 gene editing or RNA interference using shRNAs.

An advantage in drug screening approaches is the usage of organoid models that allow the study of compound efficacy and toxicity on normal and tumor cells, with the benefit of 3D architecture. If successful, this approach can decrease the usage of animal testing. At this point, drug screening on liver organoids would be of particular relevance because the human liver metabolizes drugs differently from animal's metabolism (Lancaster & Knoblich, 2014). A future step, in the drug screening field, will be the usage of organoids in coculture studies, mimicking more closely the *in vivo* situation (Neal & Kuo, 2016).

Also, organoids have the potential to be a useful alternative to cell lines or whole-organ in replacement strategies. Human renal failure causes the highest organ demand for transplant, leading to renal organoids an enormous therapeutic potential (Lancaster & Knoblich, 2014). Even if we understood

that organoids are a potent tool for cancer research, it is fundamental to keep in mind that there is always a downside. The characterization of organoid development recapitulation is essential. Fortunately, nowadays, there are reliable protocols. The second common hurdle is the maturation issue: organoids are *in vitro* models that do not develop vascularization and is essential to determine if this can influence their therapeutic and research potential (Lancaster & Knoblich, 2014). Some organoids could use the transplantation to complete the full maturation: liver buds and kidney organoids lead the invasion from host vasculature, fundamental for final maturation (Taguchi et al., 2014). Current organoids methodologies allow the recapitulation of cell population stratification, tumor histology, molecular subtype, and response to treatment. The possibility to convert wild-type organoids into the tumor *in vitro* models represents a powerful tool for the discovery and functional validation of driver gene mutations. We believe that the use of organoid models will aid in the development of new therapies for the benefit of cancer patients.

In our work, we will focus our attention on the usage of cerebellum organoids as our MB model, modified by the delivery and overexpression of specific genes that represent driver oncogenes for medulloblastoma development. For this reason, in the next paragraph, cerebellum organoids will be introduced.

1.4.3 Human cerebellum organoids

The knowledge gained with post mortem human cerebellum tissue and the use of animal models is limited to structural physiological features and cross-species similarities, respectively. The development of human-induced pluripotent stem cells (hiPSCs) to derive 3D organoid methodologies has built up the approach to the *in vitro* study of the human cerebellum. HiPSCs derived organoids present significant potential for disease modeling, drug screening, and regenerative medicine, avoiding ethical problems with post-surgical tissue samples or experimental investigations in living humans.

Cerebellum organoids derived from iPSCs are quite recent, born from a combinatorial and sequential treatment of positioning signals (Muguruma, 2018). Everything started in 2010 (Muguruma et al., 2010) by Muguruma's lab. They started the development of the cerebellum organoid for the ontogeny-recapitulating generation and tissue integration of mouse embryonic stem (ES) cell-derived Purkinje cells. In this work, they demonstrated that Purkinje cells, output neurons of cerebellar cortex, can be generated by recapitulating the self-inductive signaling microenvironment of the mid-hindbrain boundary, called isthmic organizer (Muguruma et al., 2010). The isthmic organizer is the primary

inducer of cerebellar development through the expression of two principal factors: Fgf8 and Wnt1. The next step of this technology is the development of organoids from mouse to human embryonic stem cells (hESCs), and the addition of specific factors fundamental for the desired tissue identity, such as fibroblast growth factor 2 (Fgf2), insulin, mesenchymal differentiation inhibitors, like TGFβ-inhibitor and ROCK-inhibitor for the promotion of cell survival (Muguruma et al., 2015).

Fgf2 and insulin are implicated in the isthmic organizer formation, promoting the expression of Fgf8 and Wnt1 (Muguruma, 2018). A fundamental step within the formation of embryonic stem cells in 3D culture, is the induction of the isthmic organizer formation, in a way that this secondarily self-induces cerebellar cells populations. In this protocol, cell self-organize a polarized neuroepithelial structure, from which develop cerebellar-like neuroepithelium organized as the early cerebellar plate. Muguruma's lab demonstrates to be able to develop cerebellum cell populations: Purkinje cells progenitors (*LHX5*$^{+}$, *KIRREL2*$^{+}$, *PTF1A*$^{+,}$ and *SKOR2*$^{+}$ cells), mature Purkinje cells (*L7*, Calbindin, *GABA* and Aldolase C positive cells) granule cells, GABAergic interneurons and glutamatergic CN neurons (Muguruma, 2018; Muguruma et al., 2015).

Mimic the *in vivo* structure of the tissue is a fundamental feature for a 3D model. In this respect, Fgf19 and Sdf1 are two factors applied to the culture to promote the self-formation of polarized cerebellar tissue that represents at the edge of the sheet RL-like regions and cerebellum proper-like region in the center of the organoid. Thanks to these factors, cerebellar organoid has an apical-basal

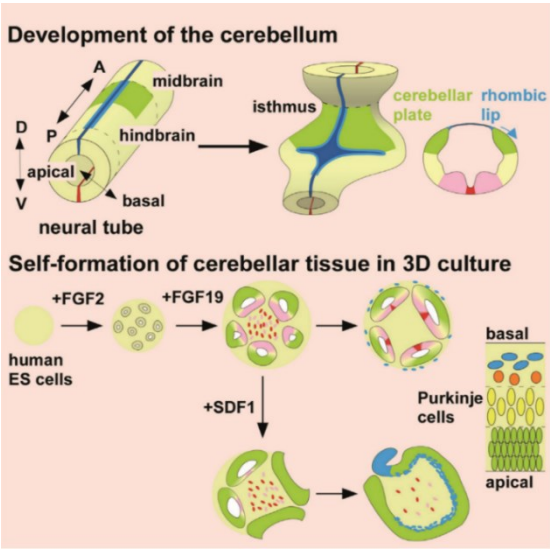

Figure 6: Schematic representation of cerebellum development and self-formation of cerebellar tissue in 3D culture.
On the upper left part is represented the neural tube, which has axes though the action of morphogen gradients and divides in the forebrain, midbrain, hindbrain, and spinal cord. The isthmic organizer induces the cerebellar plate formation in the dorsal region of rhombomere 1. On the bottom part is reported the self-formation schematic principle to generate human cerebellar tissue in 3D culture: use of specific factors, such as FGF2, FGF19, and SDF1, induce an ordered cerebellar plate-like tissue, with a basal and apical organization. Adapted from (Muguruma et al., 2015).

layered arrangement: the ventricular zone is an inner layer (composed by progenitors with $SOX2^+$, $KIRREL2^+$, $PTF1A^+$ markers); Purkinje cell precursor layer that is an intermediate layer (composed by $OLIG2^+$, $LHX5^+$, $SKOR2^+$, GAD^+ cells); the rhombic lip, represented by an outer layer of granule cell precursors ($ATOH1^+$, $BARHL1^+$ cells) (Muguruma et al., 2015). In 2016, Ishida et al. applied the Muguruma and Sasai protocol, changing the starting source: human induced pluripotent stem cells (hiPSCs) derived from a healthy and patient donor (Ishida et al., 2016). Ishida's work confirmed the possibility of using this protocol for the derivation of human 3D organoids, starting from different sources of stem cells. Besides, it was a starting point for the demonstration of a reliable model resembling the features of human pathology.

To conclude, the Muguruma and Sasai/Ishida protocol enables the development of human cerebellar organoids starting from different human sources, with the best potential to be a useful tool to design a medulloblastoma model that resembles the characteristic of MB development. From this point we started our work.

1.5 Pipeline and Aim of the project

In this paragraph, I will connect all the information that took us to consider human iPSCs-derived cerebellum organoids as the best tool to design a reliable model for Group 3 MB.

1.5.1 Organoids and driver oncogenes of Group 3 MB

I focused my attention only on Group 3 because it is the most malignant subtype, and it needs reliable models. To design a consistent human *in vitro* model that resembles Group 3 medulloblastoma, we decided to modify human cerebellar organoids derived from hiPSCs genetically.
With this approach, we were confident to combine important critical points discussed until now: the easy manageability of *in vitro* cultures, the low cost of electroporation approaches, the correct 3D cell structure obtained within organoids, the possibility to study an embryonal tumor during the development of the same "organ", and the possibility to specify which type of Group 3 subtype we are mimicking by methylation analysis, currently the most reliable tool to stratify patient MBs.
AIM 1: The first important step is the accurate fine-tuning of the protocol realized by Muguruma (Muguruma, 2018; Muguruma et al., 2015), **to develop cerebellar organoids from hiPSCs**. The second step is the **implementation of a method for the genetic modification of human cerebellum organoids**. It is a tricky point because cerebellar organoids cannot be disrupted and divided into single cells like many other types of organoids. The modification of our organoids focuses on the insertion and stable expression of *PiggyBac* donor plasmids, encoding driver genes involved in medulloblastoma Group 3 development. To select driver genes that have a role in Group 3 MB development, we took advantage of the whole-genome landscape studies of Northcott *et al.* (Northcott et al., 2017). In this work, they create a comprehensive spectrum of driver genes and molecular processes that have a role in medulloblastoma subgroups, reporting the epigenetic heterogeneity and the somatic landscape of a massive number of human patient samples. In Figure 7, there is some of this information. Oncogenes used to modify cerebellar organoids were selected from earlier *in vivo* screening done by members of our laboratory (Ballabio et al., 2020), pursued injecting in CD1 mice *PiggyBac* donor plasmids expressing Group 3 genes selected from Northcott's work.

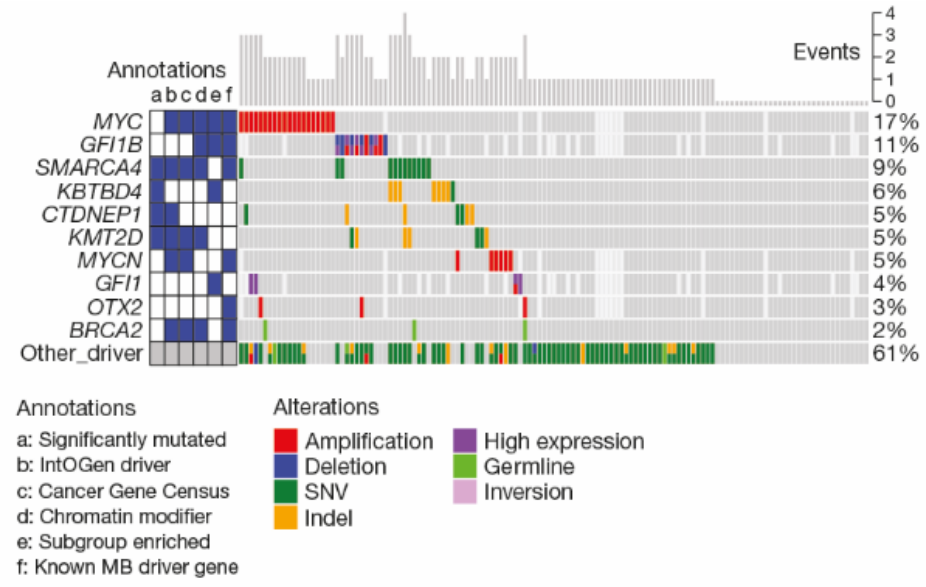

Figure 7: Schematic representation of the mutational landscape of Group 3 medulloblastoma.
Here are reported recurrently mutated genes, overexpression, structural variants, and somatic copy number variants (CNVs) found in a consistent cohort of Group 3 MB human patients. Adapted from (Northcott et al., 2017).

In the end, the two combinations of oncogenes that were selected to modify our organoids were: **cMyc/Gfi1** and **cMyc/Otx2**. The first one was already reported in the literature to promote, by overexpression, the development of Group 3 MB *in vivo* (Northcott et al., 2014).

The second combination of oncogenes was recently reported in the literature (Stromecki et al., 2018), (Lu et al., 2017), and there is not an *in vitro* or *in vivo* model representing this type of driver oncogenes' combination.

In specific, Northcott's work established that GFI1 and GFI1B are novel and highly prevalent MB oncogenes activated in Group 3 and Group4 (Northcott et al., 2014). By transcriptional analysis, Northcott reported that the activation of GFI1 was tightly restricted to group 3 MBs, observed in 25% of Group 3 and only 5% of Group 4 MBs. Pathway analysis on Group 3 MB expression data, confirmed a significant up-regulation of MYC in GFI1/GFI1B-activated cases. To confirm that GFI1/GFI1B is driving MB oncogenes, they utilized an orthotopic transplantation model: retrovirus encoding Gfi1 or Gfi1b were transduced with Myc into neural stem cells followed by their transplantation into immunocompromised mice cerebella. Only in combination, these two oncogenes were capable of producing aggressive cerebellar tumors, being an optimum candidate for molecularly targeted therapy (Northcott et al., 2014).

In this respect, I took cMYC/GFI1 oncogenes driver combination as my control combination to demonstrate that our modified organoids could be a reliable 3D MB model. After demonstrating this, here comes the **AIM 2:** modify cerebellar organoids with new oncogenes combination, selected from

whole-genome sequencing data, and, as we said before**, I selected to test in organoids cMYC/OTX2 combination, as an oncogene combination that drives Group 3 MB *in vivo*.**

It is known that in non-WNT/non-SHH MB there is an elevated expression of OTX2, a target of TGFβ signaling (Menyhárt et al., 2019). OTX2 has a role in MB development, regulating cell cycle, driving proliferation, and inhibiting cellular differentiation. Knockdown and overexpression of OTX2 are associated with altered expression levels of genes encoding H3K27 demethylases, such as KDM6A, KDM6B, JARID2, and KDM7A (Bunt et al., 2013). Indeed, the maintenance of stem-like state achieved by sustaining H3K27 trimethylation, leads to the inhibition of differentiation, by the repression of lineage-specific genes in stem cells. OTX2-bound promoters increased H3K27-me3 activation markers, and silencing OTX2 reduces H3K27 levels. We can say that OTX2 locus is amplified in Group 3 and 4, also found independent of mutations in H3K27 demethylases, showing that OTX2 and H3K27 demethylases play essential roles in this tumors (Lu et al., 2017). In this respect, some OTX2 targets are EZH2 (a component of PRC2 complex), NRL and CRX. These two last genes are fundamental for tumor maintenance, while the protein BCL-XL, the target of NRL, has a role in tumor cell survival (Garancher et al., 2018). EZH2 could be a potential target, interesting for Group 3 therapies (McCabe & Creasy, 2014) because its alteration could disrupt chromatin marking of genes, including OTX2, MYC, and MYCN in medulloblastomas. We will discuss EZH2 in the next paragraph.

1.5.2 Aberrant epigenetic programming as a new target therapy

Group 3 medulloblastoma is the most aggressive of four brain tumors, and it urgently needs new therapies. Targeting aberrant epigenetic programming in this type of tumor holds high promise for new therapies. Indeed, genomic studies highlight a high rate of alterations in epigenetic regulators in MB, occurring group-specific clustering of aberrations (Northcott et al., 2017). EZH2 is the enzymatic subunit of Polycomb repressive complex 2 (PRC2), a complex that has a role in the methylation of lysine 27 of histone H3 (H3K27), promoting transcriptional silencing (K. H. Kim & Roberts, 2016). PRC2 has an essential role during tissue development in establishing cell identity, and it is deregulated in several cancers (Comet, Riising, Leblanc, & Helin, 2016; K. H. Kim & Roberts, 2016). In WNT and SHH MBs, at the transcriptional level, EZH2 expression is increased (Smits et al., 2012), and loss-of-function mutations in the CREBBP gene (encoding CBP acetyltransferase that acetylases H3K27) are found in some WNT-MBs.

EZH2 is overexpressed in Group 3 and Group 4 MB and promotes transcriptional silencing, being a marker of suppressive chromatin (Zhang et al., 2019). In general, high levels of and gain-of-function mutations in EZH2 are associated with several aggressive cancers for which potent competitive inhibitors of EZH2 catalytic activity have revealed a therapeutic activity in pre-clinical and phase I/II clinical stage (K. H. Kim & Roberts, 2016). Contrary, Vo et al. work demonstrated that in mouse model Group 3 MB induced by Gfi1 and cMyc, the inactivation of EZH2 accelerates tumor development, suggesting a specific role for EZH2 in a specific subset of MB (Vo et al., 2017).

Demonstrated that EZH2 enzymatic gain of function is a critical cancer driver in specific subsets of MB, the development of EZH2-specific inhibitors started spontaneously as an active research area of biotech and pharmaceutical companies. The first compound that was widely used in research was 3-deazaneplanocin A (DZNep). It is a cyclopentenyl analog of 3-deazaadenosine, so represses the activity of *S*-adenosyl-L-methionine–dependent histone lysine methyltransferase (Glazer et al., 1986). Therefore, the histone methylation inhibition done by DZNep is not specific to EZH2. Nonetheless, DZNep treatments induce significant antitumor activity in several tumor types, consistent with inhibition of PCR2 and removal of H3K27me3 marks(Tan et al., 2007). For this antitumoral activity, we tried DZNep treatment on our Group 3 MB organoids, to initiate and set up a possible drug screening on our cMyc/Otx2 model. On the other hand, we knew that this compound had some disadvantages, such as very short plasma half-life, conferring nonspecific inhibition of histone methylation, and toxicity in animal models (Miranda et al., 2009). Indeed, the effectiveness of targeting EZH2 in MB groups with clinically approved drugs has not been established, and the critical target genes suppressed by H3K27me3 in MB remain to be identified. In this respect, we also tried other compounds, such as Tazemetostat.

Zhang et al. demonstrated that the treatment with EPZ-6438 (also called Tazemetostat) blocks *in vitro* and *in vivo* MB cell growth (Zhang et al., 2019). Tazemetostat is a highly selective EZH2 inhibitor that was approved, with also GSK2816126 and CPI-1205, for clinical trials on lymphomas and advanced solid cancers (Yan, Herman, & Guo, 2016). They investigated the therapeutic impact of targeting H3K27me3 with Tazemetostat in cultured MB cells and orthotopic MB xenografts, showing that this treatment increases survival in both SHH and Group 3 MB xenograft models, increasing apoptosis and reducing tumor cell proliferation (Zhang et al., 2019). In general, Tazemetostat has antitumor activity *in vitro* in SMARCA4-negative malignant rhabdoid tumor of the ovary(Knutson et al., 2014). A recent phase 2 clinical trial is defining the therapeutic effects of Tazemetostat in patients with non-Hodgkin lymphoma and solid tumors that have EZH2, SMARCB1, or SMARCA4 gene mutations (Italiano et al., 2018).

Recent results showed that Tazemetostat treatment is dependent upon p53: deletion of EZH2 accelerates tumor growth in MYC-driven Group-3 MB model with TP53 deletion (Vo et al., 2017). For this reason, we can conclude that epigenetic targeting of EZH2 is therapeutic in MB with wild-type p53, predicting that MB with overexpression of Mdm2 or mutated p53 will develop therapeutic resistance.

The evaluation of EZH2 as a possible target therapy in cancer is mutually ongoing, but the exact critical points in epigenetic reprogramming are still unknown. The discovery of these effectors would be life-changer: it will be possible to understand the treatment patient's response, tumor recurrence, and which genes can lead to resistance. For all we discussed in this paragraph, my **AIM3** is **to test Tazemetostat on our Group 3 MB organoids.**

Organoids could be a good MB model in cancer therapy to determine the extent of therapy-induced reprogramming, the essential genes that drive response, defining which tumors will respond and how resistance could develop.

1.5.2.1 Smarca4: a putative oncosuppressor

Talking about the druggable signaling pathways, we wanted to discover a possible new therapeutic alternative to block Group 3 MB. Therefore, we analyzed human sequencing data harboring Otx2 and c-Myc overexpression, focusing our attention on oncosuppressors. We identified a possible role in SMARCA4 gene, being the most frequently mutated oncosuppressor in Group3 MB (missense mutations in helicase domains). Indeed, exon sequencing studies of human tumors have defined that the 20% of all human malignancies harbor mutated subunits of SWI/SNF (BAF) complexes. BAF complexes are polymorphic ensembles of approximately 15 subunits, that use ATP hydrolysis to control chromatin structure and the placement of Polycomb (PcG) across genome (Dykhuizen et al., 2013). This complex is a chromatin modifier, a significant regulator of gene expression, and plays an important role in human tumors (Kadoch & Crabtree, 2015), but the mechanisms are unclear. Several proteins compose this complex, such as SMARCA4 (BRG1) and BAF250A (ARID1A). In specific, BRG1 represents the ATPase core of the complex, and it is mutated in 5-10 % of childhood MB. It's known that the deletion or point mutations of SMARC4 lead to anaphase bridge formation, blocking the G2/M cellular phase, which is a fundamental step in the replication of sister chromatids (Dykhuizen et al., 2013).

It is essential to know that the SWI/SNF complex role has a functional relationship with EZH2-containing PRC2 complex in oncogenic transformation (Wilson et al., 2010). Proteins from the

Polycomb group (PcG) have a role in the epigenetically based gene silencing during development and tumorigenesis (Bracken & Helin, 2009), and EZH2 (the catalytic subunit in the PRC2 polycomb repressor complex) is highly expressed in a range of cancer types. Accumulating information suggested that the SWI/SNF complex has a different role in epigenetic silencing by PcG proteins. For example, Wilson laboratory demonstrated an antagonistic relationship between SNF5, a core subunit of the SWI/SNF complex, and EZH2, describing the role of EZH2 as a driver of SNF5-deficient tumors (Wilson et al., 2010). Given this type of relationship, Chan-Penebre demonstrated that Tazemetostat, the phase II clinical trial compound, blocks tumor proliferation in SCCOHT (small-cell carcinoma of the ovary hypercalcemic type) cell lines and xenografts deficient in SMARC4 and SMARCA2 (Chan-Penebre et al., 2017).

We can conclude that **the relationship between the SWI/SNF complex and EZH2 represents a novel link between epigenetic regulation and tumor suppression.**

SMARCA4 gene in Group 3 MB patients has several missense mutations, and the most common is T910M (3 out of 12). This mutation has been characterized in human cell lines, mouse fibroblasts and SMARCA4 deficient cell lines (Dykhuizen et al., 2013; Husain et al., 2016; Pan et al., 2019). When SMARC4 T910M is incorporated into the BAF complex, ATPase activity is highly compromised, and the expression of this mutation is present in heterozygosity. Since the presence of both SMARC4 wt and SMARCA4 T910M in human Group 3 MB, we wanted to analyse the co-overexpression of both wildtype and mutated form in human cerebellar organoids, studying if the mutated form acts as a dominant-negative.

Starting from all this information taken from literature, **AIM 4** is **to test the effect of SMARCA4, or T910 mutant, in human cerebellar organoids modified to express either cMyc/Otx2 or cMyc/Gfi1. We hypothesize that SMARCA4 could act as an oncosuppressor in Group 3 MB by countering cell proliferation induced by the two combinations of oncogenes**.

1.5.3 Aim of the Project

In this paragraph, I will highlight the aims of my project:

- AIM1: To accurately fine-tune the protocol realized by Muguruma (Muguruma et al., 2015), and develop cerebellar organoids from hiPSCs, implementing a method for their genetic modification.
- AIM2: To select new Group 3 MB oncogenes' combinations from whole-genome sequencing data to modify human cerebellar organoids, demonstrating that cMyc/Gfi1 and cMyc/Otx2 drive Group 3 MB *in vivo*. Analyze the methylation profile of the two combinations, reporting, if it is possible, stratification differences.
- AIM3: To test Tazemetostat on our new cMyc/Otx2 Group 3 model.
- AIM4: To test SMARCA4 and SMARCA4 T910M in our modified human cerebellar organoids, demonstrating the reduction of cMyc/Otx2 proliferation. Demonstrate if SMARCA4 could have an oncosuppressor role in reducing a type of Group 3 MB.

To conclude, we want to **create a specific MB subgroup model through the development of human cerebellar organoids**, demonstrating how this system **can resemble different molecular stratification inside the same Group 3 MB subtype.** In the current absence of reliable human models for Group 3, we want to demonstrate the **usefulness of human cerebellar organoids for future clinical trials and target therapies.**

Methods

2.1 Identification of genes differentially expressed

Genes that show differential expression (higher than 16 folds) compared to normal cerebellum have been identified using the online tool:
https://hgserver1.amc.nl/cgi-bin/r2/main.cgi?&dscope=MB500&option=about_dscope#

2.1.1 Plasmids

The plasmid encoding a hyperactive form of the piggyBac transposase (pCMV HAhyPBase, pPBase) was a gift from https://www.sanger.ac.uk/form/Sanger_CloneRequests (Yusa, Zhou, Li, Bradley, & Craig, 2011). The piggyBac donor plasmid pPB CAG cMyc was a gift from https://www.sanger.ac.uk/form/Sanger_CloneRequests (W. Wang et al., 2011). This plasmid was used as a piggyBac donor backbone to clone by PCR other coding sequences, replacing cMyc coding sequence. Venus was amplified from pSCV2 (Tiberi et al., 2014), to generate pPB CAG Venus plasmid (pPBVenus). The Firefly Luciferase coding sequence was cloned from pGL3 (Promega) into pPB CAG. Murine Gfi1 cDNA was amplified by PCR from Gfi1 NGFR (Addgene Plasmid #44630) and tagged by inserting in frame the FLAG-tag sequence at the 3' end of the coding sequence. FLAG-tagged Gfi1 cDNA (Addgene #44630) was subcloned into the piggyBac donor backbone together with an IRES-GFP cassette, generating the plasmid pPB CAG Gfi1:FLAG-IRES-GFP. The piggyBac donor plasmid pPB CAG Otx2-IRES-GFP and pPB CAG SMARCA4-IRES-GFP were generated by substituting Gfi1:FLAG with murine Otx2 or human SMARCA4 cDNAs, which were amplified by PCR from pcDNA3.1mouse cdk6 R31C (Addgene Plasmid #75171) and pBS hBRG1(Smarca4) (a gift from Anthony Imbalzano), respectively. A single nucleotide mutation (C2729T) was introduced in the human SMARCA4 sequence to generate the missense mutation T910M using a one-step PCR method. The pPBNL-CAG-mPRDM6:FLAG-P2A-Venus plasmid was created amplifying by PCR the mPRDM6:FLAG-P2A-Venus sequence from the original plasmid pPB-CAG-LSLmPRDM6:FLAG-P2A-Venus-IRES-Luciferase (provided by Cyagen Biosciences Inc.) and cloning it into the pPBNL donor backbone. The Jackson Laboratory gently provided pPBNL-CAG-Gfi1B-P2A-Venus, and pPB-CAG-MycN was gently provided by Marco Kramer (Kramer, Ribeiro, Arsenian-Henriksson, Deller, & Rohrer, 2016).

2.2 Organoids maintenance, modification, injection and analysis

Human iPS cells (iPSCs, ATCC-DYS0100) were maintained in self-renewal on a layer of geltrex (Gibco, A14133-01), in E8 Basal Medium (Gibco, A15169-01) supplemented with E8 Supplement (50X). iPSCs were dissociated with EDTA (Invitrogen) 0.5mM, pH 8.0, for 3 minutes incubation, to maintain cell clusters. Cerebellar organoids were cultured as described in Muguruma and Ishida's work (Ishida et al., 2016; Muguruma, 2018; Muguruma et al., 2015). After 21 days of differentiation, organoids were collected by cut tips to maintain 3D structure intact. Organoids were transferred into Spinning flask (Celstir, 734-3006), in Neurobasal Medium (Thermo Fisher, 21103049), supplemented with Glutamax 100X (Thermo Fisher, 35050038) and N2 supplement (Thermo Fisher, 17502048). The medium was changed every 6-7 days. We decided to electroporate organoids at 35 days of differentiation because, at this stage, precursors of all cerebellar populations are present in the organoid (Muguruma et al., 2015). Organoids were electroporated with 16,6 µg pCAG PiggyBac (PBase), 83,4 µg of pPB-YFP (Venus) and 16,6 µg pCAG PiggyBac (PBase), 16,6 µg of pPB-YFP and either pPB CAG c-Myc (33,2µg)+ pPB CAG Gfi1 (33,2µg)(GM) or pPB CAG c-Myc (33,2µg)+pPB CAG Otx2 (33,2µg)(OM) resuspended in Buffer 5 (under patent). Regarding Smarca4 experiment, organoids were electroporated with 16,6 µg pCAG PiggyBac (PBase), 16,6 µg of pPB-YFP, PB CAG c-Myc (22,2µg), pPB CAG Gfi1 (22,2µg)(GM) and pPB CAG SMARCA4-IRES-GFP ((22,2µg) WT or mutant) or pPB CAG c-Myc (22,2µg), pPB CAG Otx2 (2,2µg)(OM) and pPB CAG SMARCA4-IRES-GFP ((22,2µg) WT or mutant), or GM/OM with pPB CAG SMARCA4-IRES-GFP WT and mutant (11,1µg). Organoids were transferred inside the electroporation cuvettes (VWR, ECN 732-1136, 2mm), and electroporation was performed with the Gene Pulser XcellTM. The electroporation buffer (under patent) and the voltage settings were set to maintain intact and alive the organoids.

About the drug screening, organoids were treated from day 37 to day 57 of differentiation, with 2 doses of 5 µM 3-deazaneplanocin A (DZNep, Selleckchem) or DMSO. Organoids were treated from day 36 to day 41 of differentiation, with 1 dose of either 5 µM Tazemetostat (EPZ-6438) or 5 µM GSK126 or DMSO. After the drug treatment, organoids were fixed in PFA 4%, cryoprotected in 20% sucrose, and embedded in Frozen Section Compound (Leica, 3801480). Frozen section compound embedded organoids were cryosectioned at 40 µm with Leica CM 1850 UV Cryostat.

2.2.1 Gene expression data and Functional Analysis of electroporated organoids

Two biological replicates for each group (Untreated or Electroporated) were used. Total Organoids RNAs were extracted using Trizol reagent (Invitrogen), subjected to DNase-I (Ambion) treatment, and RNAs were depleted of ribosomal RNA. Sequencing libraries for whole transcriptome analysis were prepared using Stranded mRNA-Seq Library Preparation Kit. RNA-seq was performed on an Illumina HiSeq 2500 Sequencer using standard conditions at the Next Generation Sequence Facility of the University of Trento (CIBIO). The obtained reads were 75bp long, paired ends, and 30 Million on average for each sample. Quality control analysis was performed using FastQC (www.bioinformatics.babraham.ac.uk/projects/fastqc/). All the sample sequence reads were mapped with STAR aligner (v2.5.3) using recommend parameters. To provide an estimate of gene expression and compute differential gene expression, the reads were proportionally assigned to the human gene transcripts (ENSEMBL HG38), based on the mappings using HT-SEQ count (http://www-huber.embl.de/users/anders/HTSeq). Differential gene expression analysis was performed using the gene raw counts, within the R/Bioconductor edgeR package. The differential gene expression pipeline within the edgeR package was customized to estimate the dispersion parameter for each library using the biological group dispersion and identify DE genes between treated versus the control samples. log2(fold-change) ≥ 1 and baseMean > 3 CPM were considered for differentially regulated genes, and the P-value was adjusted for multiple testing using the Benjamini–Hochberg correction with a false discovery rate (FDR) ≤ 0.05. Differentially expressed gene lists obtained from low-level procedures were analyzed for functional associations. Data were analyzed through DAVID Bioinformatics Resources v6.8 using the suggested standard parameters.

2.2.2 Organoid quantitative analysis

Data are presented as mean + s.e.m., for each condition 5-11 organoids were examined, and at least 110-200 cells were quantified. Organoids electroporated with pPBase + pPBVenus (encoding for Venus) were considered as the positive control and were used to set the parameters for cells count on ImageJ software. Data were compared using a paired Student t-test, two tails.

2.2.3 Organoid injection into nude mice

24-120 days after electroporation, OM and GM organoids were separately collected and dissociated into Neurobasal Medium (Gibco, cat.21103049) until they became clumps of cells. For each experiment (either Venus, OM, or GM), 5 to 8 organoids were mixed together. The mixture of clumps was injected intracranially into nude mice (P04-P08) with a 30-gauge Hamilton Syringe, placed on a stage in a stereotactic apparatus (medially injected at lambda: -3.6 D/V: -1.6 with 4 µl of transfection). The mice were sacrificed at the experimental endpoint (loss of weight, ataxia phenotype, suffering phenotype, kyphoscoliosis) and intraventricularly perfused with 4% PFA. After 2 days in PFA at 4°C, the brains were cryoprotected in 30% sucrose in water and left at 4°C for 2 days. After the incubation, brains were embedded in Frozen Section Compound (Leica, 3801480). Frozen section compound embedded brains were cryosectioned at 20-40 µm with Leica CM 1850 UV Cryostat. Control mice (nude mice injected with Venus organoids) were sacrificed at the experimental endpoint of OM or GM mice. All experiments were done with all relevant ethical regulations for animal testing and research. The Italian Ministry approved the experiments of Health as conforming to the relevant regulatory standards. For DNA methylation profiling, we used carbon dioxide euthanasia for mice at the experimental endpoint, and pieces of tumors were collected and stored at -80°C. Frozen tissues were smashed by cold mortar and pestle, and from the powder, DNA was extracted as described in paragraph 2.2.6. DNA samples were analysed by Evelina Miele (paragraph 2.2.4).

2.2.4 DNA methylation profiling

DNA methylation profiling was performed according to protocols approved by the institutional review board with written consent obtained from the patients' parents. Tumor areas with the highest tumor cell content (≥70%) were selected for DNA extraction. Samples were analyzed using Illumina Infinium HumanMethylationEPIC BeadChip (EPIC) arrays according to the manufacturer's instructions, on Illumina iScan Platform. In detail, 250 ng or 500 ng DNA was used as input material for fresh-frozen or formalin-fixed paraffin-embedded tissues, respectively. Generated methylation data were compared with the Heidelberg brain tumor classifier (Capper et al. Nature 2018) (http://molecularneuropathology.org) to assign a subgroup score for the tumor compared to 91 different brain tumor entities. All tumors had a score of at least 0.8 in the reported methylation class. EPIC BeadChip data were analyzed by means of R (V .3.4.3), using different packages: ChAMP pipeline (V.2.9.9, (Morris et al., 2014)) for quality checks and filters, to calculate methylation levels

and functionally annotate probes at the gene-level. Multidimensional scaling (MDS) on the cohort samples was performed using cmdscale function, with Euclidean distance. Heatmap depicting normalized beta values was created by means of pheatmap function, using Ward's minimum variance method (Murtagh & Legendre, 2014) and Euclidean distance to cluster samples and probes. Low-quality CpG islands among the 48 ones identified from Hovestadt and colleagues(Hovestadt et al., 2013) were removed from the analysis. Finally, bootstrap analyses were carried out using pvclust package (Suzuki & Shimodaira, 2006).

DNA Methylation Raw Data and classifier Results:

https://www.dropbox.com/s/qdcklj82vy4e2gi/Tiberi_methylation_OM-GM-MB_GEO.zip?dl=0

2.2.5 Imaging: Immunofluorescence and immunohistochemistry

Immunofluorescence stainings were performed on glass slides. Antibody solution consisted of PBS supplemented with 3% goat serum, 0.3% Triton X-100 (Sigma). Primary antibodies were incubated overnight at 4°C. After incubation, 45 min of washing was done in PBS 1X supplemented by 0.3% Triton X-100. Secondary antibodies for 1 hour at room temperature. After incubation, 45 min of washing was done. Nuclei were stained with 1 µg/ml DAPI (Sigma) or 1 µM DRAQ5 (ThermoFisher). After 3 min of incubation at RT, 3 min of washing was done. Sections and coverslips were mounted with Permanent Mounting Medium.

Immunohistochemistry stainings were performed on rehydrated paraffin sections. Antigen retrieval was performed by incubating slices for 30 min in retrieval solution (10 mM Sodium Citrate, 0.5% Tween-20 (v/v), pH 6.0) at 98°C. Primary antibodies were incubated overnight at 4°C and secondary antibodies for 1 hour at room temperature in the Antibody solution. ABC solution was used 2 hours at room temperature (Vectastain Elite ABC Kit Standard PK-6100). The sections were incubated with the substrate at room temperature until suitable staining was observed (DAB Peroxidase Substrate Kit, SK-4100). Nuclei were counterstained with Hematoxylin.

The used antibodies are listed below:

Primary antibodies	Host species	Dilution	Company	Reference
BARHL1	Rabbit	1:1000 (organoids) 1:500 (tissues)	Atlas Antibodies	HPA004809
β3tubulin	Mouse	1:2000	Thermofisher Scientific	MA1-118
Calbindin-D-28K	Rabbit	1:500	Sigma Aldrich	C9848
c-MYC (Y69)	Rabbit	1:200	Abcam	ab32072
GFAP	Rabbit	1:200	Sigma Aldrich	G9269
GFP	Chicken	1:2000	Abcam	ab13970
Kirrel2	Rabbit	1:1000	Invitrogen	PA5-72823
NPR3	Rabbit	1:100	Abcam	ab37617
Nestin	Mouse	1:500	Abcam	ab22035
OLIG2	Rabbit	1:200	Abcam	ab33427
OTX2	Mouse	1:100	Santa Cruz Biotechnology	sc-514195
PCNA	Mouse	1:2000 (organoids) 1:500 (tissues)	EMD Millipore Corporation	MAB424
PH3	Rat	1:500	Abcam	ab10543
SOX2	Rabbit	1:1000 (organoids) 1:500 (tissues)	Abcam	ab97959
SOX9	Rabbit	1:4000 (organoids) 1:2000 (tissues)	EMD Millipore Corporation	ab5535
Tbr2	Rabbit	1:200	Abcam	ab 23345
Pax6	mouse	1:100	Santa Cruz	Sc-53108

Secondary antibodies	Dilution	Company	Reference
Alexa Fluor 488 goat anti-chicken IgY	1:500	Thermofisher Scientific	A11039
Alexa Fluor 546 goat anti-mouse IgG	1:500	Thermofisher Scientific	A11030
Alexa Fluor 647 goat anti-mouse IgG	1:500	Thermofisher Scientific	A21235
Alexa Fluor 546 goat anti-rabbit IgG	1:500	Thermofisher Scientific	A11035 A11010
Alexa Fluor 647 goat anti-rabbit IgG	1:500	Thermofisher Scientific	A21245
Alexa Fluor 647 goat anti-rat IgG	1:500	Thermofisher Scientific	A21247
Goat anti-Rabbit IgG-heavy and light chain Biotinylated	1:250	Bethyl Laboratories Inc.	A120-101B
Goat anti-Mouse IgG-heavy and light chain Biotinylated	1:250	Bethyl Laboratories Inc.	A90-116B

Images were acquired with a Zeiss Axio Imager M2 (Axiocam MRc, Axiocam MRm), and for confocal imaging with either Leica TCS Sp5 or X-Light V2 confocal Imager optical. Images were processed using ImageJ software. Figures were prepared using Illustrator.

2.2.6 Genomic DNA extraction

Organoids were lysed in lysis buffer (20 mM EDTA, 10 mM Tris 8.0, 200 mM NaCl, 0.2% Triton X-100, 100 µg/ml Proteinase K) for 1 hour at 37°C. Genomic DNA was extracted with phenol-chloroform and precipitated with isopropanol.

Results

3.1 Modeling of Group 3 MB in human cerebellar organoids

3.1.1 Characterization

I developed hiPSC-derived organoids using Muguruma and colleagues protocol (Ishida et al., 2016; Muguruma, 2018; Muguruma et al., 2015). Muguruma demonstrated that hESC/iPSC cells could differentiate into cerebellar progenitors, neurons (interneurons, Purkinje cells, and granule neurons) and glial cells. The protocol is based on the induction of progenitors to self-form neuro-epithelial structures that resemble early cerebellar plate. The first step was the characterization of our cerebellar organoids. By immunostaining on cryosections of cerebellar organoids fixed at different time points during their development, I looked at different cellular populations of cerebellum that we expected to find in Muguruma's organoids (Fig.8, 9). At the beginning of cerebellum development (25 days of differentiation), we showed the presence of positive cells for SOX2, which is a stem cell marker, present in progenitor cells of ventricular zone in the cerebellum, from which GABAergic neurons differentiate (Ahlfeld et al., 2017). SOX2 positive cells, at 25 days differentiation, display near the lumen of initial hollow rosettes that will resemble the neuroepithelium with an apical-basal polarity (Figure 8A). At 60 days of differentiation, SOX2 positive cells can be organized in a rhombic lip-similar structure (Muguruma et al., 2015)(Haldipur et al., 2019)(Figure 8C). These observations agree with what reports in Muguruma's work (Muguruma, 2018), which described the formation of structures that should resemble the cerebellum morphology. I demonstrated the presence of Calbindin positive cells (at 41 days), that represent Purkinje cell progenitors, and SOX9 positive cells (Figure 8B, D). SOX9 is a marker expressed by astrocytes in the adult brain, except ependymal cells and in neurogenic regions in which neural progenitor cells express it (Sun et al., 2017). Indeed, VZ precursors express SOX9 during cerebellum development (Vong, Leung, Behringer, & Kwan, 2015). I also demonstrated, at 60 days, the presence of Nestin positive cells that represent neural stem cells or radial, Bergmann glia (P. Li et al., 2013), and the presence of Tbr2 positive cells (Figure 8E). A subset of unipolar brush cells (UBCs), excitatory interneurons with their soma located in the granular layer (Haldipur et al., 2019), express Tbr2 marker. In Figure 9, we reported immunostaining on organoids that represent the differentiation point at which we decided to electroporate (35-40 days). I observed the presence of Barlh1 and Pax6 positive cells (Figure 9A), markers of the granule cells precursors of the rhombic lip, and granule cells. Figure 9A shows that Barhl1 cells organize in rosettes that will resemble the neuroepithelium with an apical-basal polarity (Muguruma et al., 2015). I

demonstrated the presence of Kirrel2 positive cells, GABAergic progenitor-selective cell surface marker, that can represent GABAergic Purkinje precursors (Mizuhara et al., 2010). In Figure 9D, we show the presence of β3-tubulin positive cells, a marker for differentiated neuronal cell types (Salero & Hatten, 2007). It is possible to observe that these cells are organized around the rosette structure, and not inside as neural stem cells.

We can conclude that we replied at best the Muguruma's protocol, being able to develop human cerebellar cell populations organized in organoids.

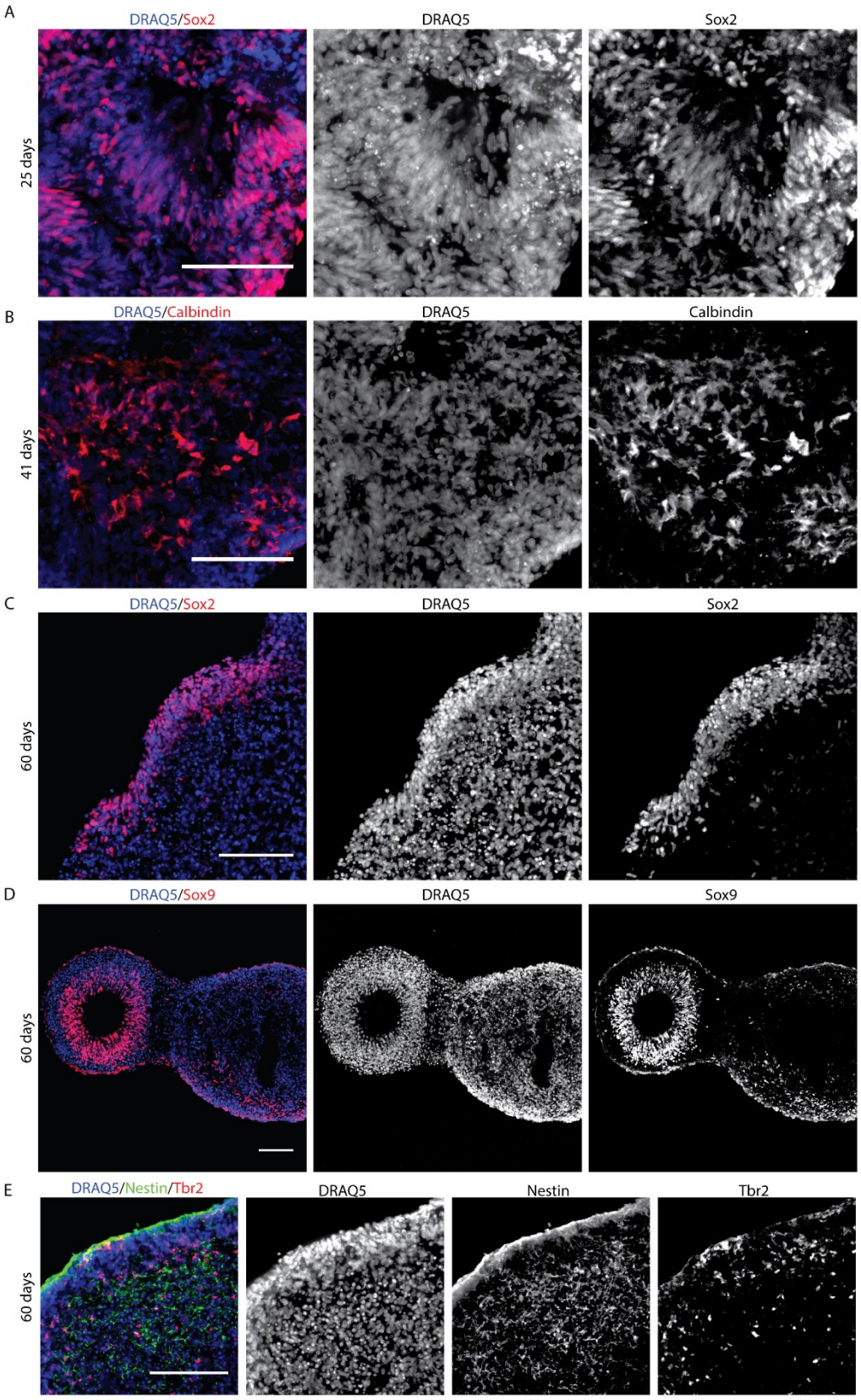

Figure 8: **Immunostaining of human cerebellar organoids at 25, 41, and 60 days of differentiation.**
(**A**) Confocal images of DRAQ5 and Sox2 (red) immunofluorescence of cerebellar organoids at 25 days. (**B**) Confocal images of DRAQ5 and Calbindin (red) immunofluorescence of cerebellar organoids at 41 days. (**C**) Confocal images of DRAQ5 and Sox2 (red) immunofluorescence of cerebellar organoids at day 60. (**D**) Confocal images of DRAQ5 and Sox9 (red) immunofluorescence of cerebellar organoids at day 60. (**E**) Confocal images of DRAQ5, Nestin (green), and Tbr2 (red) immunofluorescence of cerebellar organoids at day 60. Scale bars are 100µm.

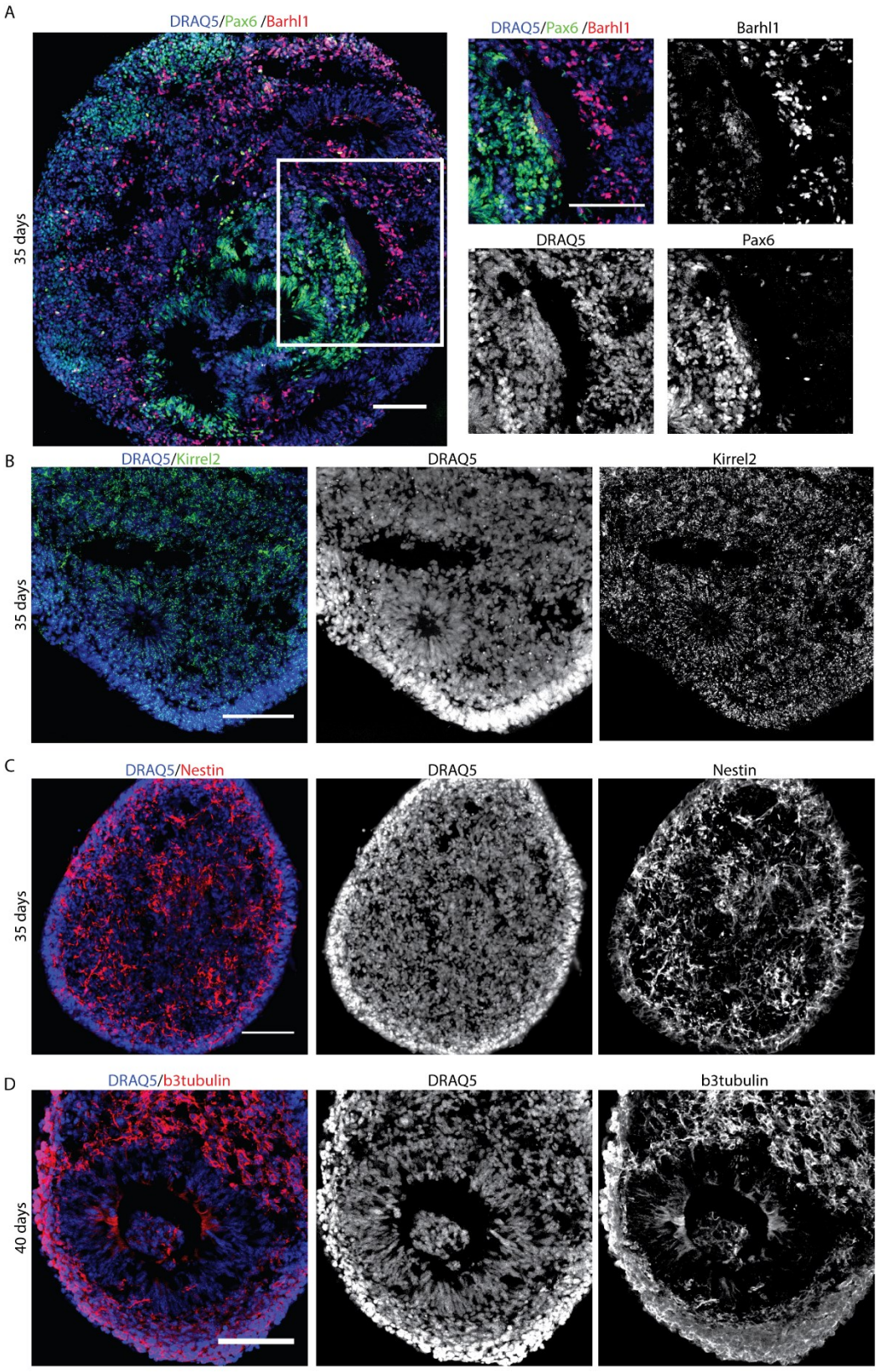

Figure 9: Immunostaining of human cerebellar organoids at 35, 40 days of differentiation.
(**A**) Confocal images of DRAQ5, Pax6 (green), and Barhl1 (red) immunofluorescence of cerebellar organoids at 35 days. The white squares in (**A**) mark the region shown at higher magnification on the right. (**B**) Confocal images of DRAQ5 and Kirrel2 (green) immunofluorescence of cerebellar organoids at 35 days. (**C**) Confocal images of DRAQ5 and Nestin (red) immunofluorescence of cerebellar organoids at 35 days. (**D**) Confocal images of DRAQ5 and b3tubulin (red) immunofluorescence of cerebellar organoids at day 40. Scale bars are 100µm.

After the characterization, we developed an electroporation protocol to deliver PiggyBac vectors expressing Venus into human cerebellar organoids (Figure10A). We invented the electroporation buffer trying different compositions and different voltage settings. We set the electroporation buffer, which is under patent, and the voltage settings to decrease the level of impact of the electric shock on cell populations and to maintain intact and alive the organoids. With this method, we were able to deliver DNA inside intact 3D human cerebellar organoids (Figure 10B, D), not only on the surface as it happens with other approaches (such as virus and lipofection). We decided to electroporate these organoids at 35 days of differentiation, when almost all cerebellar progenitors are present (Muguruma et al., 2015). We performed an analysis of the differentially expressed genes (DEGs) to be sure that the electroporation did not induce any change in the transcriptome of the cerebellar organoids. We demonstrated that the number of DEGs is minimal (done by Silvano Piazza in Ballabio and Anderle et al. 2020, for details see Supplementary Data 1). Defined that the electroporation is not invasive, we started to design our possible MB model. I proceed to test our patient-specific screen results in human organoids by electroporating them at 35 days of differentiation, with Gfi1-cMyc (GM) and Otx2-cMyc (OM) oncogenes. Looking at Figure 11, we can observe the formation of small buds of Venus positive cells in GM and OM modified organoids, after 25 days. The control organoids, the one electroporated with only Venus, expressed a few Venus positive cell, but not organized buds.

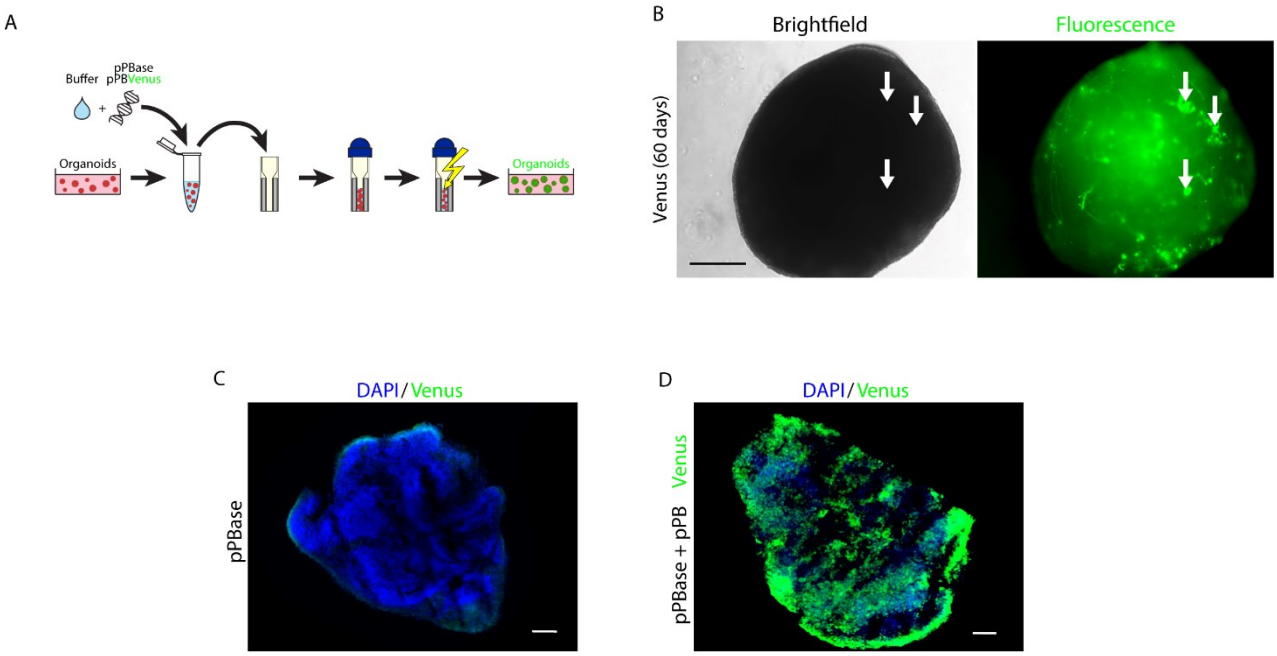

Figure 10: Cerebellar organoids electroporation with Venus.
(**A**) Schematic representation of organoids electroporation. (**B**) Brightfield and Fluorescence images of cerebellar organoids at day 60 electroporated at 35 days with pPBVenus. White arrows indicate cells expressing Venus. (**C**) Confocal images of DAPI staining and GFP (Venus) immunofluorescence of cerebellar organoids at day 60, electroporated with pPBase, or (**D**) electroporated at day 35 with pPBase + pPBVenus. Scale bars are 250µm.

Comparing GM and OM with control organoids (electroporated only with Venus), it is possible to see a high number of PCNA positive cells within the Venus positive cells in GM and OM organoids (Figure 11A-E). Besides, we performed immunostaining on OM organoid against the b3tubulin marker. Compared to control, OM organoids (within the Venus-positive cells) had less b3tubulin positive cells (Figure 11F). We think that GM and OM oncogene combinations induce overproliferation of human cerebellar progenitors, impairing their differentiation process, highlight by the low b3tubulin expression. After these qualitative analyses, we quantify PCNA, b3tubulin, SOX9, SKOR2 (Figure 12). In GM and OM organoids, we also observed an increase of Sox9 positive cells, which could represent an increase in glial cells or early cerebellar progenitors. Changes in the number of Skor2-positive Purkinje cell precursors were not significant. To understand how the two oncogenes' combinations modify the proliferation, we quantified the positive marker cells at an earlier time point (40 days of differentiation). Five days after electroporation, we confirmed an increase in PCNA positive cells (Figure 12E).

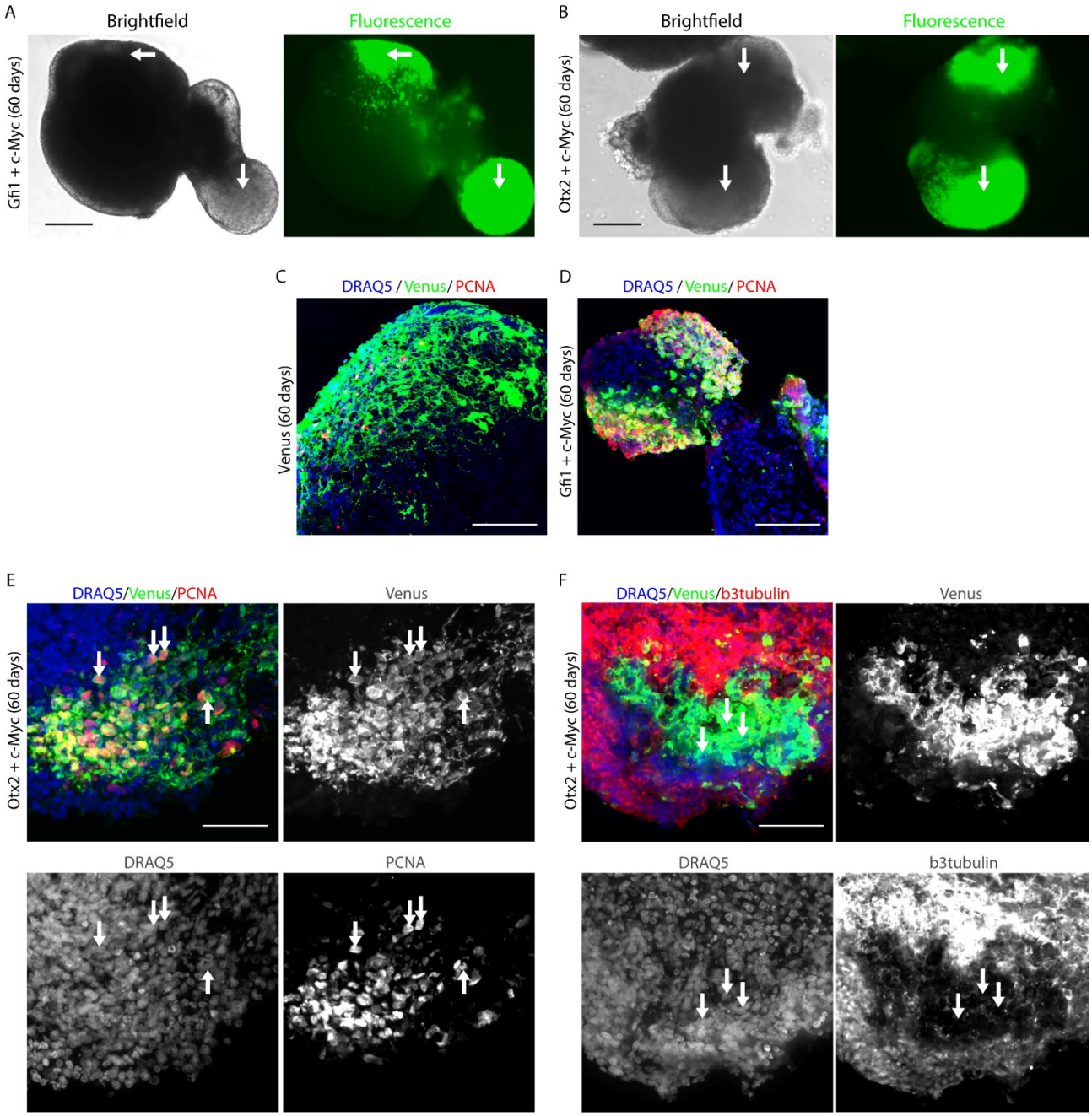

Figure 11: **Immunostaining of cerebellar organoids electroporated with Venus, Gfi1/c-Myc, and Otx2/c-Myc.**
(**A**) Brightfield and Fluorescence images of cerebellar organoids at day 60 electroporated at day 35 with pPBase + pPBMyc + pPBGfi1 + pPBVenus. (**B**) Brightfield and Fluorescence images of cerebellar organoids at day 60 electroporated at day 35 with pPBase + pPBMyc + pPBOtx2 + pPBVenus. In A-B, white arrows indicate the organized bud of cells expressing Venus and in overproliferation. (**C**) Confocal images of GFP (Venus) and PCNA immunofluorescence of cerebellar organoids at day 60, electroporated at day 35 with pPBase + pPBVenus. (**D**) Confocal images of GFP (Venus) and PCNA immunofluorescence of cerebellar organoids at day 60, electroporated at day 35 with pPBase + pPBMyc + pPBGfi1 + pPBVenus. (**E**) Confocal images of GFP (Venus) and PCNA immunofluorescence of cerebellar organoids at day 60 electroporated at day 35 with pPBVenus + pPBMyc and pPBOtx2. Arrows indicate double-positive cells. (**F**) Confocal images of GFP (Venus) and b3tubulin immunofluorescence of cerebellar organoids at day 60 electroporated at day 35 with pPBase + pPBMyc + pPBOtx2 + pPBVenus. Arrows indicate b3tubulin negative cells. Scale bars 250 µm in (**A, B**) and 100 µm in (**C, D**).

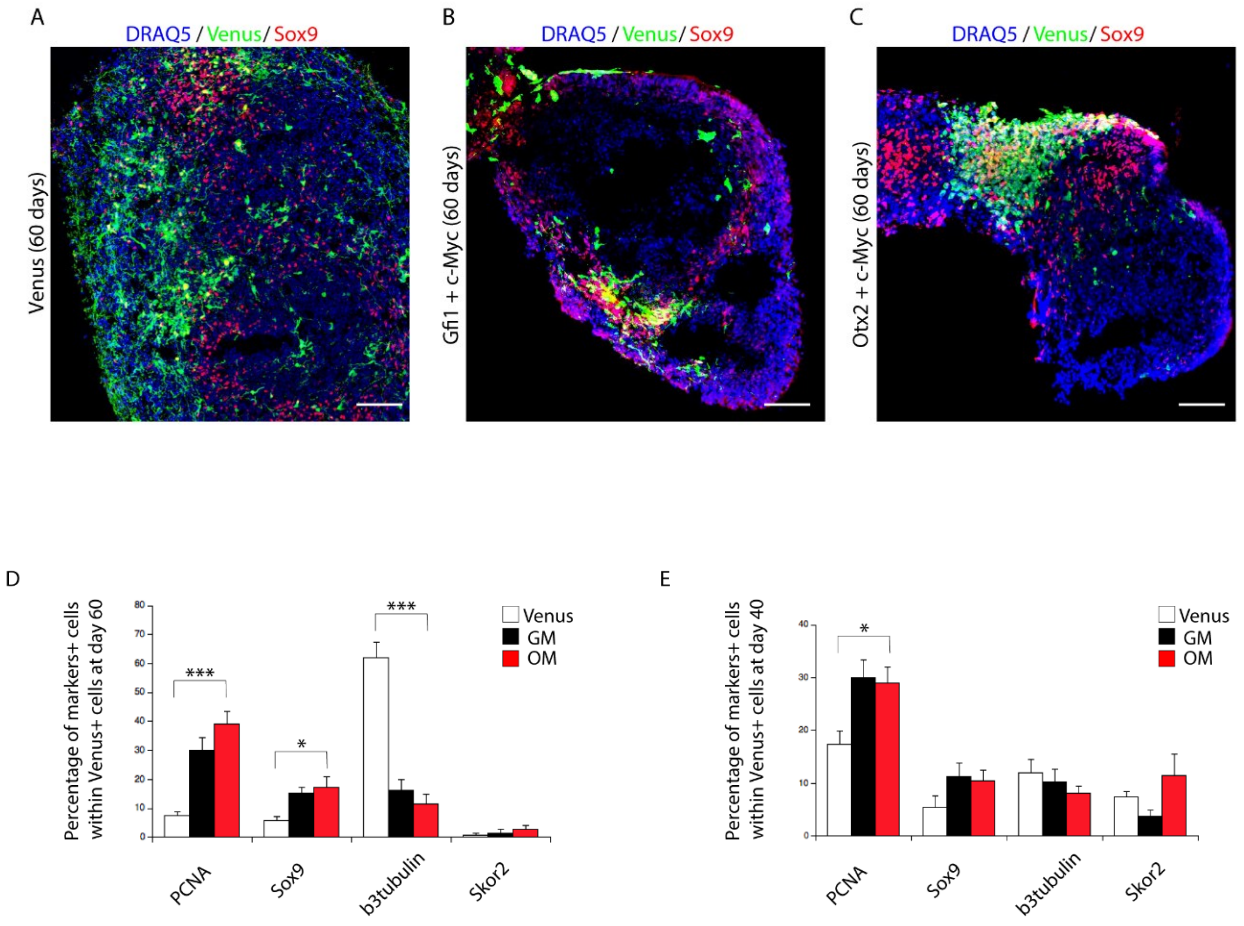

Figure 12 | Immunostaining and quantification of cerebellar organoids electroporated with Venus, Gfi1/c-Myc and Otx2/c-Myc. (**A**) Confocal images of GFP (Venus) and Sox9 immunofluorescence of cerebellar organoids at day 60, electroporated at day 35 with pPBase + pPBVenus. (**B**) Confocal images of GFP (Venus) and Sox9 immunofluorescence of cerebellar organoids at day 60, electroporated at day 35 with pPBase + pPBMyc + pPBGfi1 + pPBVenus. (**C**) Confocal images of GFP (Venus) and Sox9 immunofluorescence of cerebellar organoids at day 60, electroporated at day 35 with pPBase + pPBMyc + pPBOtx2 + pPBVenus. Scale bars are 100µm in (A-C). (**D**) Quantification of cerebellar organoids at day 60, electroporated at day 35 with either pPBase + pPBVenus or pPBase + pPBMyc + pPBOtx2 + pPBVenus (OM) or pPBase + pPBMyc + pPBGfi1 + pPBVenus (GM). n=6 biologically independent organoids. (**E**) Quantification of cerebellar organoids at day 40, electroporated at day 35 with either pPBVenus or pPBase + pPBMyc + pPBOtx2 + pPBVenus (OM) or pPBase + pPBMyc + pPBGfi1 + pPBVenus (GM) n=6 biologically independent organoids. Error bars in (**D, E**) represent standard error of the mean. Paired Student t-test, two tails. *p value < 0.05, **p value<0.01. ***p value<0.001.

3.1.2 Smarca4 function in GM and OM human cerebellar organoids

Starting from the literature and our previous data in mice, we wanted to test if SMARCA4 has a role in the reduction of GM and OM organoid's proliferation. We decided to electroporate 35days organoids with Gfi1-cMyc-Smarca4 or Otx2-cMyc-Smarca4 and analyze them after five days. SMARCA4 it is a chromatin modifier, and its action implies the activation or repression of many other genes. For this reason, we decided to look at organoids proliferation in a short time, because we wanted to see the direct SMARCA4 function and not secondary effects. At 60 days, it might not be possible to see the direct action of SMARCA4. As shown in Figure 13A, B, Smarca4 overexpression reduces proliferation in OM human organoids, demonstrating that Smarca4 could have a role in reducing tumorigenicity in OM-induced Group 3 MB. On the other hand, Smarca4 overexpression did not reduce GM organoid proliferation (Figure 13C), data also found in our *in vivo* findings. Our work (Ballabio et al., 2020) analyses the mechanism underlying Smarca4 in MB development, overexpressing OM and Smarca4 not only in human organoids, but also in human cerebella progenitors (AFF cells). Checking the expression of downstream genes of Otx2, c-Myc, and Smarca4, we found that Otx2-cMyc affects CDKN2B and CRABP1 expression, whereas Smarca4 can rescue these effects.

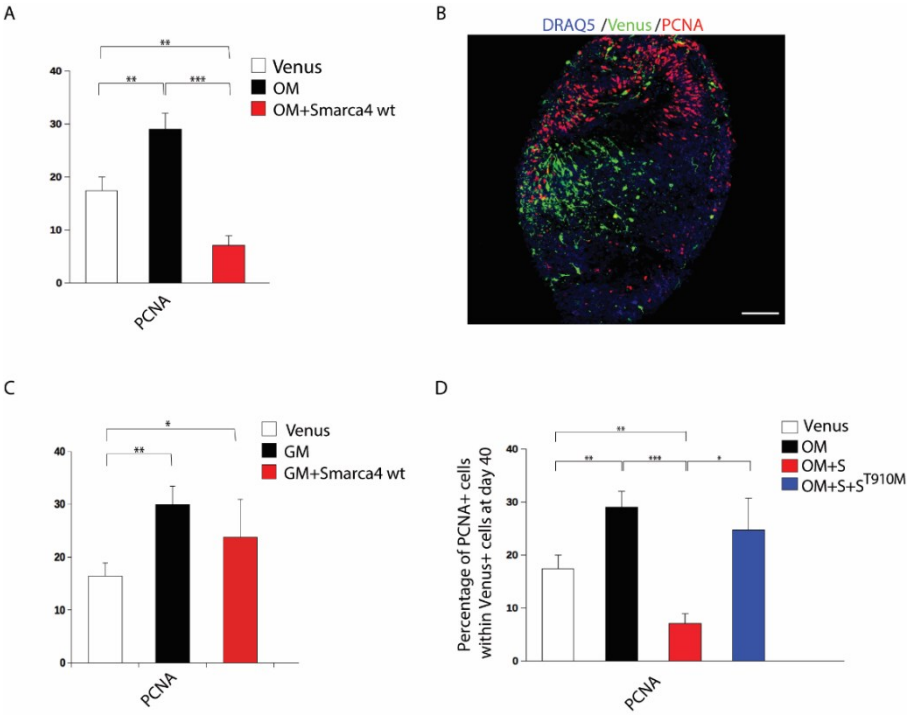

Figure 13: Smarca4 reduces proliferative cells in Gfi1/c-Myc and Otx2/c-Myc.
(A) Quantification of cerebellar organoids GFP+/PCNA+ cells at day 40 electroporated at day 35 with either pPBase + pPBVenus (Venus) or pPBase + pPBMyc + pPBOtx2 + pPBVenus (OM) or pPBase + pPBMyc + pPBOtx2 + pPBVenus + pPBSmarca4 (OM+Smarca4 wt). (B) Confocal images of GFP (Venus) and PCNA immunofluorescence of cerebellar organoids at day 40, electroporated at day 35 with pPBase + pPBMyc + pPBOtx2 + pPBSmarca4. (C) Quantification of cerebellar organoids GFP+/PCNA+ cells at day 40 electroporated at day 35 with either pPBase + pPBVenus (Venus) or pPBase + pPBMyc + pPBGfi1 + pPBVenus (GM) or pPBase+pPBMyc+pPBGfi1+pPBVenus+pPBSmarca4 (GM+Smarca4 wt). Scale bars 100µm in (B). Error bars in (A, C) represent standard error of the mean. Paired Student t-test, two tails. *p value<0.05, **p value<0.01. ***p value<0.001.

We also tried to analyze the loss of function of Smarc4, which did not influence CDKN2B and CRABP1 modulation by OM (Ballabio et al., 2020). CRABP1 is a protein essential in the transportation of retinoic acid inside cells. The expression of this protein is associated with poor patient prognosis and high tumor grade in breast cancer (Liu et al., 2015). In literature has already been described that the protein encoded by CDKN2B gene ($p15^{INK4b}$ protein) is an oncosuppressor, that can be modulated by c-Myc and Smarca4 in cell lines (Hendricks, Shanahan, & Lees, 2004; Kia, Gorski, Giannakopoulos, & Verrijzer, 2008; Seoane et al., 2001).

The most common mutation in Smarca4 in Group 3 MB patients is Smarca4 mutation T910M, which has been characterized in human cell lines, Smarca4 deficient cell lines, and mouse fibroblast. No one characterized this mutation and its role in MB and cerebellar progenitors. With T910M mutation, Smarca4 typically incorporates into the BAF complex, and it has the ATPase activity highly compromised (Dykhuizen et al., 2013; Husain et al., 2016; Pan et al., 2019). To study the function of Smarca4 in our model, we took into account that T910M is mainly present in heterozygosity. For this reason, we co-expressed in MO human cerebellar organoids Smarca4 wild-type (wt) and T910M. We showed that Smarca4 T910M could block the Smarca4 wt function (Figure 13D). From this data, we can conclude that in patients with Smarca4 missense mutations, Smarca4 T910M represses the function of Smarca4 wt, acting as a dominant-negative.

3.1.3 *In vivo* injection of OM/GM organoids induces Group 3 MB

Until now, we demonstrated that the two selected oncogene combinations induce proliferation in human cerebellar organoids. Besides, we were interested to understand whether GM and OM organoids were able to induce and develop cancer *in vivo*: we injected Venus, GM and OM organoids into the cerebellum of Foxn1nu mice, called nude mice (Figure 14). 24-120 days after electroporation, for each experiment (either Venus, OM, or GM), 5 to 8 organoids were mixed together and dissociated into Neurobasal Medium, until they became clumps of cells. 4ul of this mixture were injected intracranially into nude mice at P04-P08.

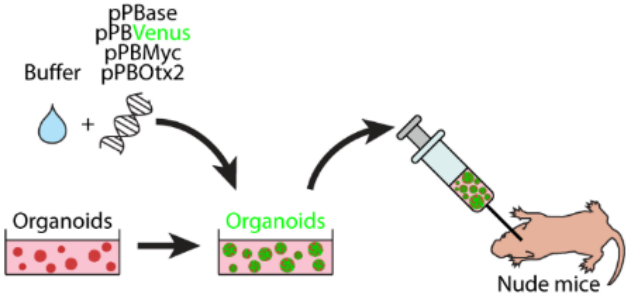

Figure 14: Schematic representation of *in vivo* injection of modified cerebellar organoids.

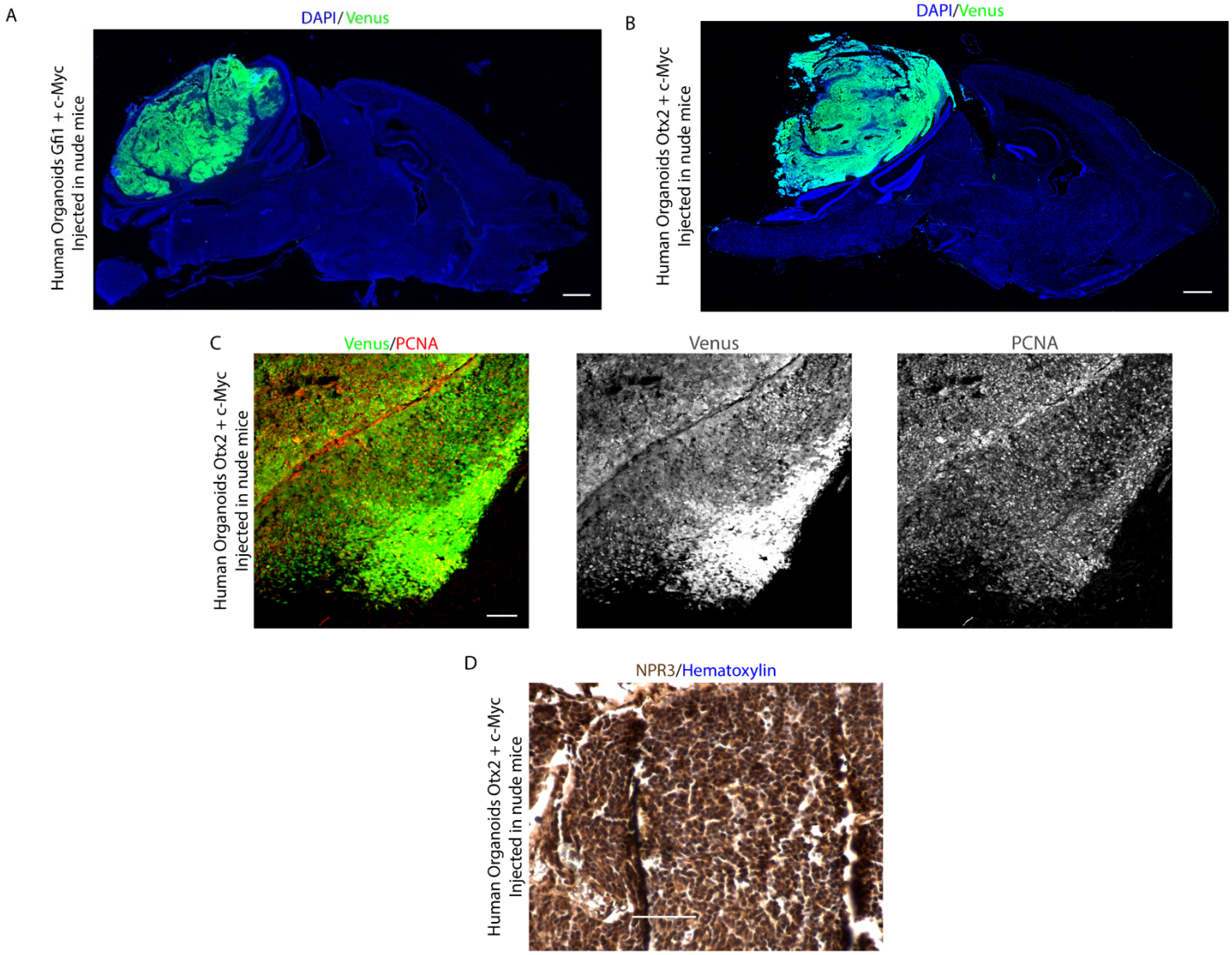

Figure 15: Cerebellar organoids electroporation with Gfi1/c-Myc and Otx2/c-Myc induces Group3 MB *in vivo.*
(**A**) DAPI staining and GFP (Venus) immunofluorescence of sagittal brain section of a nude mouse after injection of GM organoids. (**B**) DAPI staining and GFP immunofluorescence of brain section of a nude mouse one month after injection of OM organoids. (**C**) Confocal images of GFP and PCNA immunofluorescence of tumors in nude mice one month after injection of OM organoids. (**D**) NPR3 immunohistochemistry and Hematoxylin staining of tumor in nude mouse one month after injection of OM organoids. Scale bars 1 mm in (**A**, **B**), 100 µm in (**C**, **D**).

We decided to sacrificed mice at the experimental endpoint (loss of weight, ataxia phenotype, suffering phenotype, kyphoscoliosis) and sacrifice control experiments (Venus organoid injected mice) at the endpoint of OM/GM injected mice. We injected 6 mice with Venus organoids, and none of them developed tumors (Figure 16 A, B). We obtained the formation of tumors in nude mice cerebellum injected with GM (11/11) and OM (7/7) modified organoids (Figure 15 A, B, 16 C-F). The fastest experimental endpoint, and our earliest brain collection, was 30 days after injection (reached with both types of organoids).

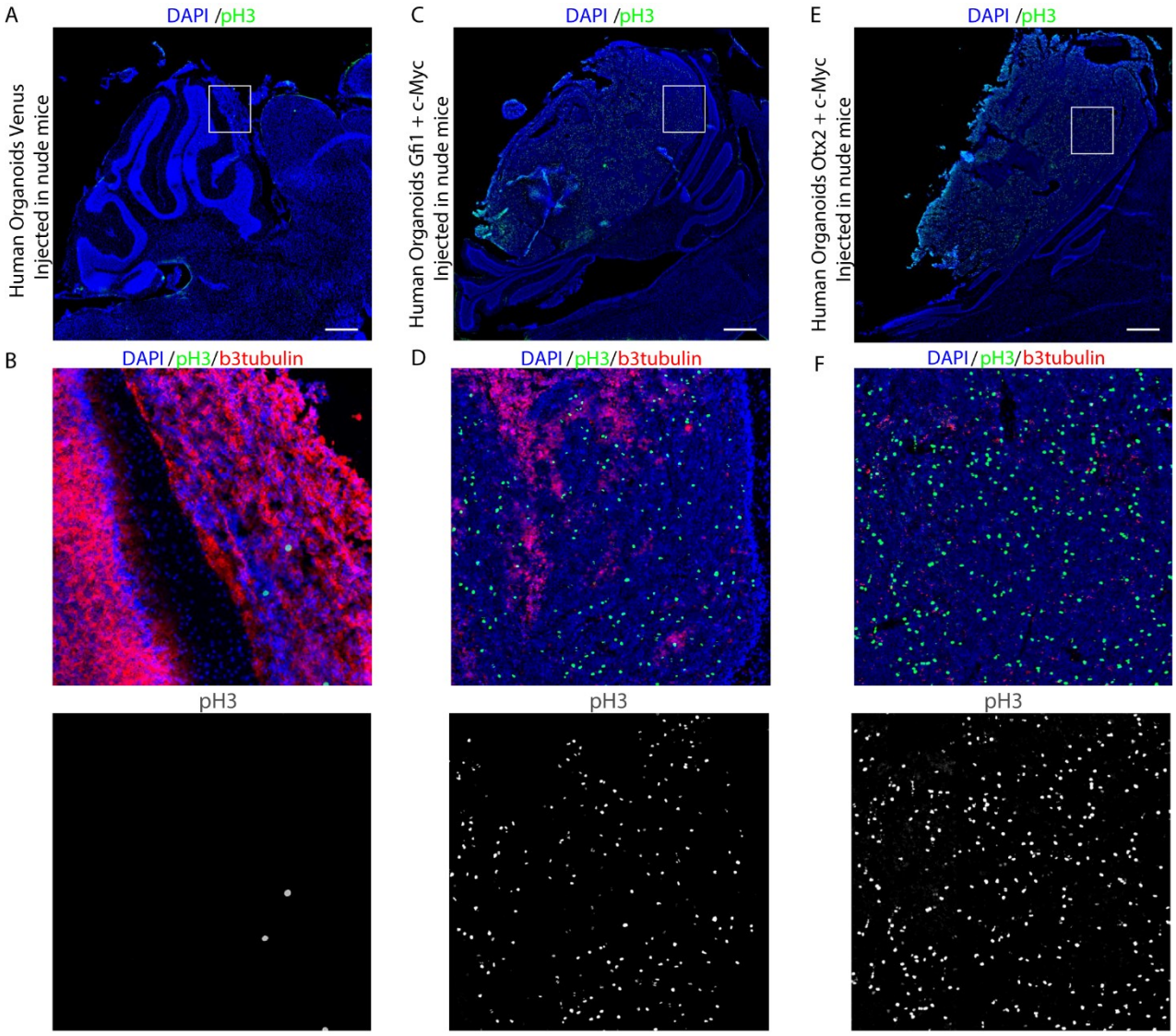

Figure 16: **GM and OM cerebellar organoids induce *in vivo* brain tumors.**
(**A-C**) DAPI staining and pH3 immunofluorescence of sagittal brain sections of nude mice after injection of human cerebellar organoids electroporated with pPBase + pPBVenus (**A**, 72 days), pPBase + pPBMyc + pPBGfi1 + pPBVenus (**B**, 72 days), pPBase + pPBMyc + pPBOtx2 + pPBVenus (**C**,30 days). (**B,D,F**) DAPI staining and pH3 and b3tubulin immunofluorescence of sagittal brain sections of nude mice after injection of human cerebellar organoids (Venus, GM, and OM). The white squares in (**A, C, E**) mark the region shown at higher magnification in (**B, D, F**). Scale bars 1 mm in (**A, C, E**).

By PCNA and pH3 immunostaining (Figure 15C and 16C-F), we demonstrated that the tumor was still growing several days after injection: 72 days for GM and 30 days for OM modified organoids injected into mice. We characterized the tumor developed from OM injected organoids by NPR3 histochemistry, and Otx2, GFAP, Olig2, and Bahrl1 immunostaining (Figure 15 D and 17). We are confident to show that OM injected organoids tumors are NPR3, Otx2 positive and GFAP, Olig2, Bahrl1 negative, such as tumors induced by OM injection into CD1 mice (see paper Figure 2D, F, H, Supplementary Figure 7A-D) and to human Group 3 MBs (Northcott et al., 2011; Sandén et al., 2017). We can conclude that Gfi1/cMyc and Otx2/cMyc are two oncogene combinations that induce MB into human cerebellar organoids, which develop tumor also *in vivo* if injected into nude mice.

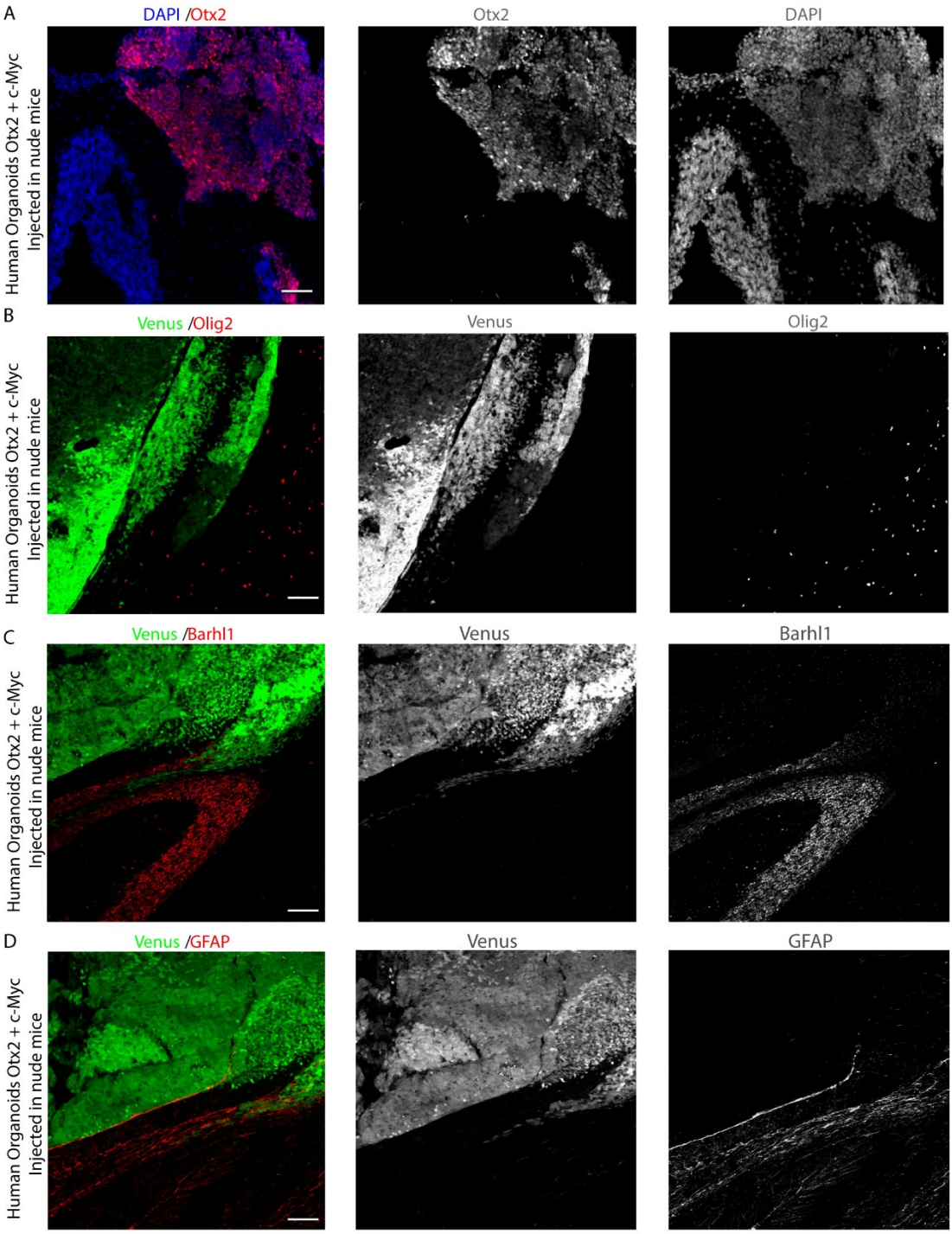

Figure 17: Characterization of brain tumor derived from the *in vivo* injection of OM cerebellar organoids.
(A) Confocal images of DAPI staining and Otx2 immunofluorescence of tumor in nude mouse one month after injection of human cerebellar organoids electroporated with pPBase + pPBMyc + pPBOtx2 + pPBVenus. (B) Confocal images of GFP (Venus) and Olig2 immunofluorescence of tumors in nude mouse one month after injection of human cerebellar organoids electroporated with pPBase + pPBMyc + pPBOtx2 + pPBVenus. (C,D) Confocal images of GFP (Venus), Barhl1 (C), and GFAP (D) immunofluorescence of tumors in nude mouse one month after injection of human cerebellar organoids electroporated with pPBase + pPBMyc + pPBOtx2 + pPBVenus. Scale bars 100 μm in (A-D).

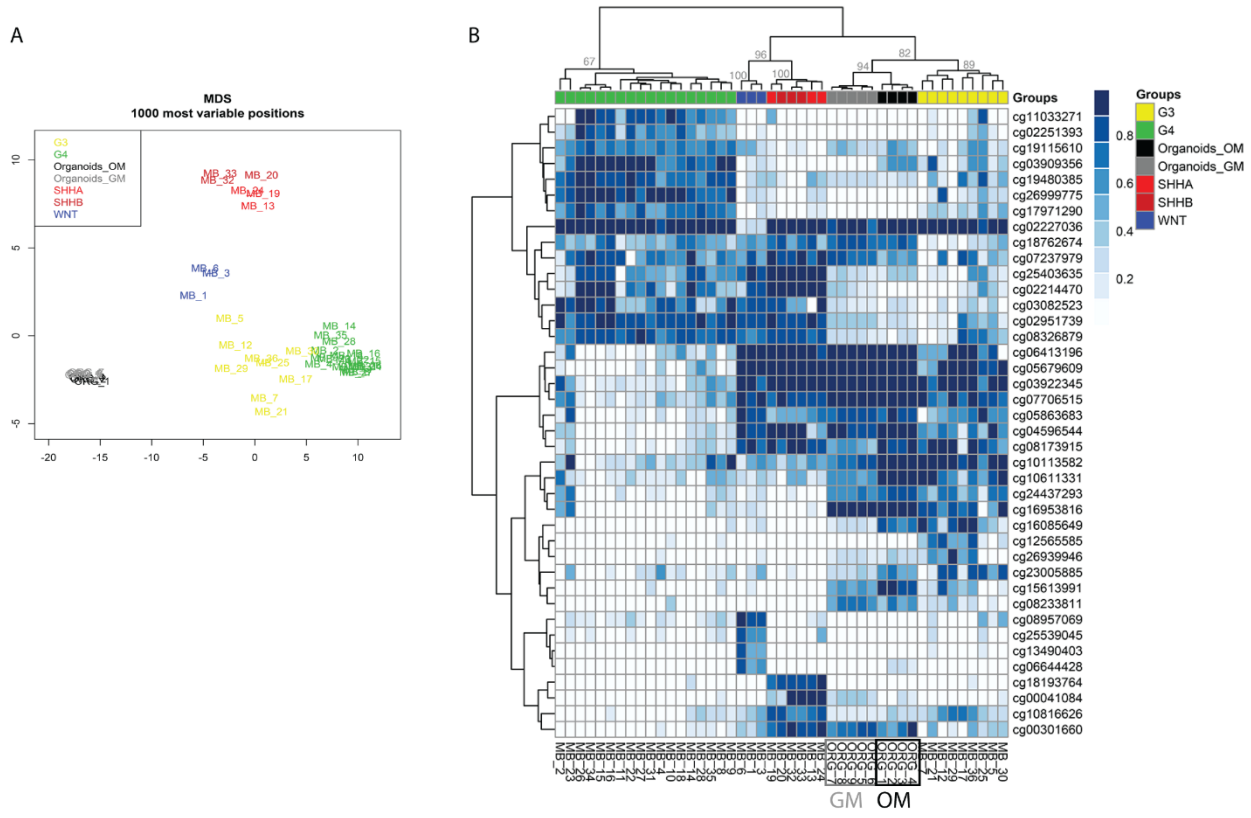

Figure 18: The methylation profile of human cerebellar organoids electroporated with Gfi1/cMyc and Otx2/cMyc is similar to Group3 patient samples.
(A) MDS analysis performed on the 1000 most variable probes of the whole-genome DNA methylation data shows a close similarity between organoids and Group 3 MBs. **(B)** Hierarchical clustering and heatmap show normalized methylation levels in organoid samples and MB samples. Color legend of the MDS plot as follows: Organoids_OM, black; Organoids_GM, grey; WNT MB (blue); SHH-A MB- adulthood and childhood (red); SHH-B MB infant (dark red); G3, Group 3 MB (yellow); G4, Group 4 MB (green). Clusters were obtained by means of Ward's minimum variance method, using the Euclidean distance.

Currently, the DNA methylation profile is a clinical decision-making approach to stratify human patient MB and decide which therapy can be applied (Capper et al., 2018; Hovestadt et al., 2013). To demonstrate that our modified organoids can stratify into Group 3 MB subtype, we analyzed the DNA methylation profile of both tumor tissues derived from OM and GM injected organoids, comparing them with 36 human tissues derived from human primary MB patients (diagnosed and treated at the Ospedale Pediatrico Bambino Gesù OPBG, in Rome). Injected organoid tumor samples showed a methylation profile close to Group 3 MBs, demonstrated by multidimensional scaling analysis performed on the 1000 most variable islands in the cohort (Figure 18A) and the hierarchical clustering analysis (Figure 18B), run on only 48 CpG islands that better characterize MB subgroups (Hovestadt et al., 2013). We know that the stratification of patient samples is one of the most critical points in target therapy, that has to evolve in MB models. For this reason, to be more precise, we run a methylation data analysis of OM and GM injected organoid-derived tumors through the brain tumor classifier (Capper et al., 2018). Both samples were classified in the methylation class family MB

Group 3 and Group 4 (and specifically subgroup 3), with a score >0.3 (data are in Supplementary Data 3 of Ballabio and Anderle et al. 2020). Knowing that with the classifier group 3/4 v1.0 we could take into account the second-generation molecular subgrouping of medulloblastoma (Sharma et al., 2019), we wanted to go deep into the classification of our OM and GM organoid-derived tumors. We were satisfied to see the results: GM samples were classified as Subtype II, representing high-risk Group 3 MBs, and OM samples as Subtype IV, which stands for standard-risk Group 3 MBs.
In the end, we demonstrated that our 3D organoid model not only can develop Group 3 MBs, but also defines differences between the subclasses within the Group 3 subtype, only by manipulating distinct genes combinations. These results are an important starting point for the development of precise target therapies that are specific for each subclass of medulloblastoma.

3.1.4 Histone methyltransferase inhibition reduces Group 3 MB growth

After demonstrating that our modified organoids are the first human Group 3 MB model, we wanted to find a possible treatment for OM MB based on novel molecules. Knowing that Smarca4 has an antagonistic relationship with histone methyltransferase EZH2, we decided to treat MB organoids with histone methylation inhibitor DZNep (3-deazaneplanocin A). It is known that DZNep treatment reduces tumor development in various cancer types, inhibiting PRC2 and removing H3K27me3 marks (Alimova et al., 2012; K. H. Kim & Roberts, 2016; Miele et al., 2017). In the beginning, we tested DZNep on ex-vivo culture of cancer cells from mouse OM tumors (see Ballabio and Anderle et al. Supplementary Figure 9A-C). We demonstrated that DZNep blocked OM-induced tumor growth, reducing the size of ex-vivo cultures of OM-derived tumor spheroids. Starting from this data, I further wanted to analyze DZNep function in human OM organoids. I demonstrated that DZNep blocks the growth of OM tumor, decreasing the number of GFP+/PCNA+ cells comparing to the control (Figure 19).
Nowadays, it is known that DZNep is not a specific inhibitor for EZH2. It has a short plasma half-life and is toxic in animal models (Miranda et al., 2009). For these reasons, we decided to test the other two specific inhibitors that are currently in clinical trials: Tazemetostat and GSK-126 (Knutson et al., 2014; McCabe et al., 2012). Tazemetostat is a selective EZH2 inhibitor that has potent antitumor activity *in vitro* and in SMARCA4-negative malignant rhabdoid ovary tumors (Chan-Penebre et al., 2017; Knutson et al., 2014). For all this information, we decided to test Tazemetostat and GSK-126 on our human OM-derived MB cerebellar organoids. We treated the OM organoids for five days, demonstrating an increased number of Cleaved-Caspase3 and decreased number of PCNA positive

cells compared to the control (Figure 19 D, E). While both treatments were effective at inhibiting tumor growth in MB organoids, Tazemetostat was more efficient as it resulted in enhanced apoptosis (cleaved-caspase3-positive cells) compared to GSK126. We can conclude that the treatment with Tazemetostat performed on our MB organoid model highlights its potential therapeutic strategy for Group 3 MB patients with high level of Otx2-cMyc.

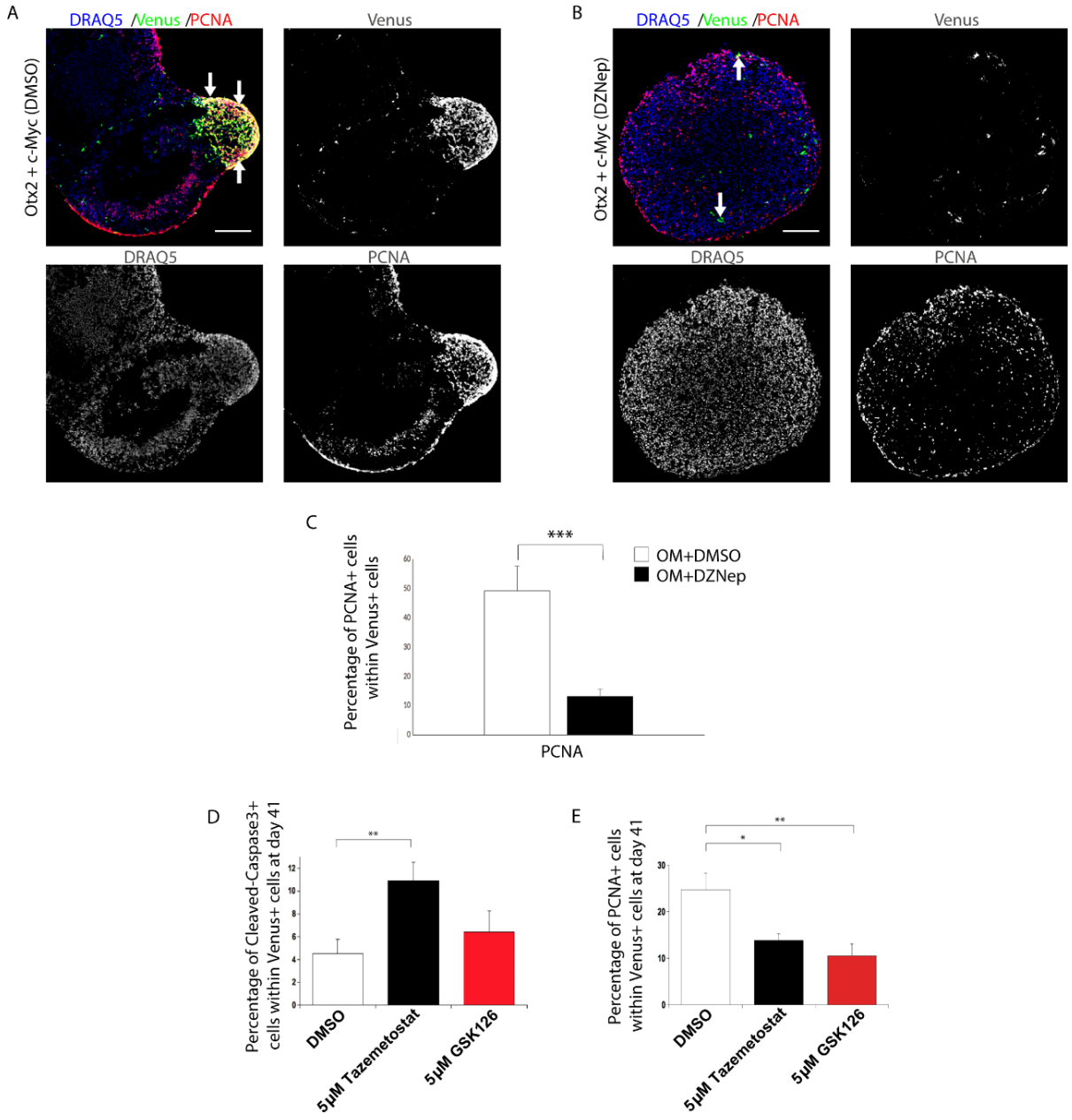

Figure 19: Immunostaining and quantification of OM cerebellar organoids treated with DZNep, GSK126 or Tazemetostat. (**A-B**) Confocal images of GFP (Venus) and PCNA immunofluorescence of OM cerebellar organoids at day 57 electroporated at day 35 and treated with DMSO (**A**) and 5 µM DZNep (**B**) from day 37 to day 57. Arrows in (**A**) indicate Venus positive cells in an organized bud. Arrows in (**B**) indicate venus positive cells. (**C**) Quantification of OM cerebellar organoids GFP+/PCNA+ cells at day 57 electroporated at day 35 and treated with either DMSO or 5 µM DZNep. (**D**) Quantification of OM cerebellar organoids at day 41 and treated for 5 days with either DMSO or Tazemetostat or GSK-126. Percentage of active caspase3 positive cells between Venus positive cells. (**E**) Quantification of OM cerebellar organoids cells at day 41 and treated for 5 days with either DMSO or Tazemetostat or GSK-126. Percentage of PCNA positive cells between Venus positive cells. Error bars represent standard error of the mean. Paired Student t-test, two tails for organoids quantification. ***p value<0.001. Scale bars 100 µm in (**A, B**).

3.2 Modeling of Group 4 MB in human cerebellar organoids

After demonstrating that our organoid model is a reliable model that mimics Group 3 human pathology also at the methylation profile, I decided to start the design of a Group 4 MB model. This MB subtype is the most common one, but the less understood. For this reason, it would be essential to develop a reliable human model also for Group 4 MB. I followed the same pipeline as the Group 3 modeling project. In the beginning, we selected driver genes that have a role in Group 4 MB development, taking advantage of the whole-genome landscape studies of Northcott *et al.* (Northcott et al., 2017). Mainly, I focused my attention on genes like Gfi1, Gfi1B, and Otx2, already described before for their importance, and Prdm6 that represents a novelty found only recently dysregulated in Group 4 medulloblastoma (Northcott et al., 2017). The combinations that I electroporated are Otx2/MycN, Gfi1/MycN, Gfi1b/MycN, and Prdm6/MycN.

I electroporated hiPSC-derived organoids at 35 days of differentiation, and I analyzed them with immunostainings, relative quantifications, injection into nude mice (Figure 20A), and methylation profiles. Until now, I was able to analyze that some combinations that we selected increased the overproliferation of cerebellar organoids (Figure 20B-E) and decreased b3tubulin expression (Figure 20F, H), as I saw in Group 3 OM and GM organoids (Figure 11). To test if our modified organoid were tumorigenic, I injected them into nude mice. Now I am waiting to see if the modified organoids can develop *in vivo* tumors and to see if the methylation profile is similar to Group 4 MB patients' samples. Until now, we can conclude that we found some genes combinations, selected from whole-genome sequencing of Group 4 MB patients, that induce overproliferation in human cerebellar organoids. We might have a starting point to design a Group 4 MB human model, if the methylation profile will be similar to human patients' samples.

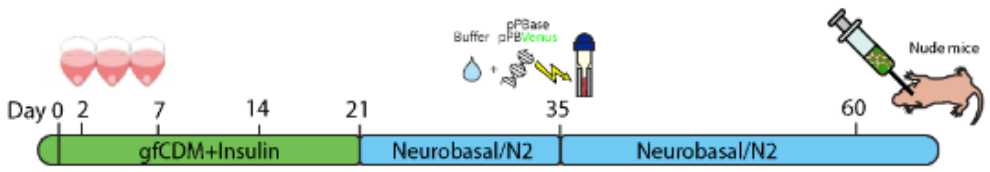

Figure 20 A: Pipeline from hiPSC differentiation to *in vivo* injection of modified cerebellar organoids.
Until now, we are characterizing and injecting into nude mice organoids electroporated with different combinations of Group 4 oncogenes.

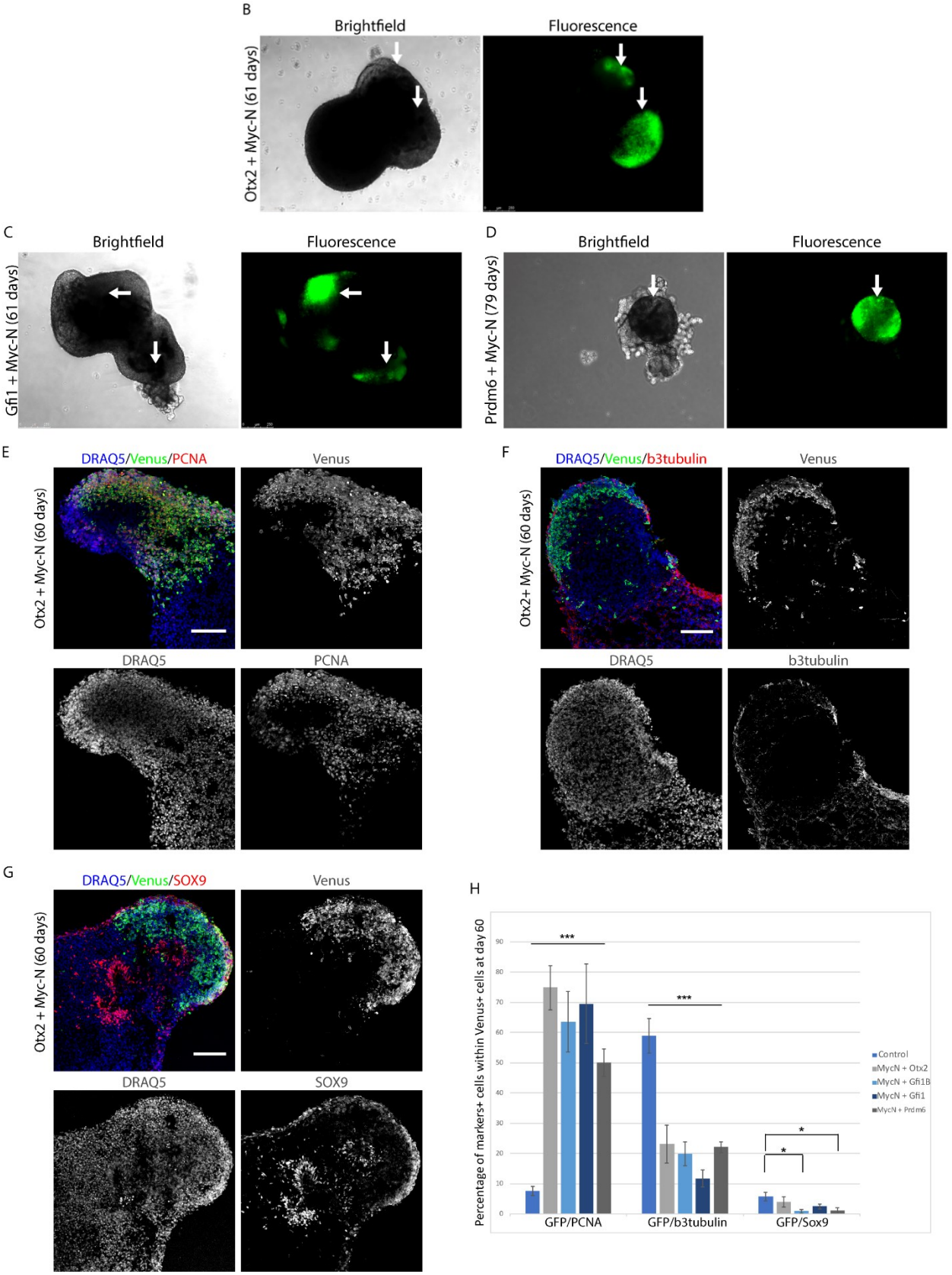

Figure 20 B-H: Immunostaining and quantification of cerebellar organoids electroporated with Group 4 oncogenes' combinations. (B-D) Brightfield and fluorescence images of organoids modified with three different Group 4 combinations. Arrows indicate organized buds of cells expressing Venus and in overproliferation. **(E-G)** Confocal images of GFP (Venus), PCNA, or b3tubulin or Sox9 immunofluorescence of cerebellar organoids at day 60. (**H**) Quantification of cerebellar organoids at day 60, electroporated at day 35 with four different Group 4 combinations, n=6 biologically independent organoids. Scale bars are 100µm. Error bars represent standard error of the mean. Paired Student t-test, two tails. *p-value < 0.05, **p value<0.01. ***p value<0.001.

Discussion

Our work started from an *in vivo* screening to find new combinations of driver oncogenes, taken from genome-wide analyses of human MB patients. From *in vivo* results, we found two combinations that caused tumor development (Gfi1/cMyc and Otx2/cMyc), and we decided to focus our attention on Otx2/cMyc (OM) oncogene combination because it is a new MB model. It is known that Otx2 has a role in human MB cell lines growth, and it is highly expressed or amplified in a subset of Group 3 and Group 4 MB. Interestingly, Otx2 downstream genes NRL and CRX are fundamental to this type of Group 3 MB development (Garancher et al., 2018). These are two genes that are not involved in Gfi1-driven MB development. This observation highlights intra-subgroups heterogeneity in MB (Cavalli et al., 2017; Northcott et al., 2017), supporting that Group 3 MBs are comprised of molecularly distinct subtypes.

We modified human iPSC-derived cerebellar organoids with both selected combinations, Gfi1-cMyc and Otx2-cMyc overexpression, starting from Gfi1/cMyc combination, to see whether our model could resemble the features of an already validated Group 3 model. On the other side, our OM model characterization gives knowledge to the field, since there was not a model demonstrating the *in vivo* tumorigenic role of Otx2-cMyc in human cerebellar cells. Indeed, in our work, we demonstrated that **Gfi1/cMyc** and **Otx2-cMyc oncogene combinations are necessary to develop *in vivo* Group 3 tumors in human cerebellar organoids**. Besides, by DNA methylation profile analyses (Capper et al., 2018), we were excited to prove that our humanized organoid-based model can resemble intertumoral heterogeneity that defines Group 3 MB. Indeed, the GM cancer organoids were defined, by the MB classifier Group ¾ (Sharma et al., 2019) as Subtype II, high-risk G3 tumors, and OM cancer organoids as Subtype IV, called standard-risk G3 tumors. These results demonstrate that our model is the first humanized Group 3 MB able to resemble the subtype differences, by manipulating distinct genes.

Trying to study the molecular mechanism that drives Group 3 MB, **we showed that SMARCA4 can decrease proliferation in OM organoids**. SMARCA4 is a core subunit of the SWI/SNF chromatin remodeling complex and contains an ATPase domain that provides the enzymatic activity for chromatin modeling and transcription regulation (Hodges, Kirkland, & Crabtree, 2016). SMARCA4 is essential for cerebellum development, and it is mutated in Group 3 and SHH MBs (Moreno et al., 2014; Shi, Wang, Gu, Xuan, & Wu, 2016). In our case, SMARCA4 did not inhibit GM organoid-derived tumor proliferation. This result highlights the fact that patients with Group 3 tumors must

receive different therapeutic treatments depending on their type of mutations, and subtype of Group 3 MB.

Mutations on SWI/SNF complex are present in 20% of human cancers and T910M is the most common missense mutation present in Group 3 MB. This mutation compromises the ATPase activity of SMARCA4 (Dykhuizen et al., 2013; Husain et al., 2016) and induces chromosome aneuploidy, which is common in MB (Jones et al., 2012). We decided to co-overexpress SMARCA4 wt with SMARCA4 T910M, because the mutated form is present in heterozygosity in human Group 3 MB. We speculate that Smarca4 T910M has a dominant-negative role, blocking the wt form functions. From these results, we can conclude that SMARCA4, required in SHH and Otx2-cMyc Group 3 MB development, has different roles depending on which genetic alterations are involved.

After demonstrating that our organoids recapitulate some Group 3 MB features, we wanted to study a possible druggable target to block the development of Group 3 tumors. Knowing that SWI/SNF complex has an antagonistic relationship with PRC2 in several tumors (K. H. Kim et al., 2015; Pierre & Kadoch, 2017), we tried to understand the implications of EZH2 inactivation in OM Group3 MB organoids. The polycomb repressive complex 2 (PRC2) is composed of the catalytic histone-lysine methyltransferases, EZH2, together with other accessory proteins (Margueron & Reinberg, 2011).

It has been already found that EZH2 and Polycomb genes are highly upregulated in Group 3 and Group 4 MB (Bunt et al., 2013; G. Robinson et al., 2012). However, which is the role of EZH2 in a broad spectrum of tumors is an active debate. High levels of EZH2 are associated with several aggressive and advanced cancers, for which specific competitive inhibitors of EZH2 catalytic activity have preclinical and phase I/II clinical activity (K. H. Kim & Roberts, 2016). In direct contrast, EZH2 can act as a tumor suppressor in cancers characterized by loss of function mutations on EZH2 (Comet et al., 2016). In 2017 Roussel's laboratory tried to investigate the dependency of Group 3 MB on EZH2 (Vo et al., 2017). They used gene-editing systems to explore EZH2 functional relationship with cMyc and Gfi1, genes implicated in MB formation. In Myc+; Trp53-/-; Cdkn2c-/- GNPs or established derived Myc+ Group 3 MB tumorsphere lines, they showed that the inactivation of EZH2 and disruption of PRC2 histone methylase function accelerates Group 3 MB formation. From these data, they speculate that EZH2 has an oncosuppressor role in their MB model. This information highlights the unclear relationship between oncogenes that drive Group 3 MB.

In literature, studies demonstrate that Gfi1 is implied in chromatin modification. Indeed, it is known that Gfi1 binds to promoter-proximal sequences (Zhijun Duan & Horwitz, 2003), and generates repressive H3K27me3 chromatin modifications recruiting histone deacetylase and EZH2 (Z. Duan, Zarebski, Montoya-Durango, Grimes, & Horwitz, 2005; Saleque, Kim, Rooke, & Orkin, 2007). Moreover, the inactivation of EZH2 decreases GFi1 H3K27me3 modification and increases GFi1

expression (Vo et al., 2017). Despite the effort, the exact functional relationship between Gfi1, Myc, and EZH2 remains unclear. Only Roussel's group speculates that loss of EZH2 derepresses expression of Gfi1, which cooperates with Myc to promote Group 3 medulloblastoma development (Vo et al., 2017). In this respect, it is fundamental to underline that Roussel's data come from a Trp53-/- model. It is known that primary human Group 3 MB lack TP53 mutations, although these can happen during relapse (Ramaswamy et al., 2016). For this reason, we think that studies on the relationship between Gfi1, Myc, and EZH2 have to be done on a reliable Group 3 model. It would be interesting to reproduce the same analysis on our GM organoids.

These studies on EZH2-Gfi1 relationship point to future efforts directed to develop an understanding of how and with which specificity oncogenes contributes to Group 3 MB subgroup stratification. With this perspective, we wanted to amplify the knowledge of OTX2 contribution on Group 3 MB development, understanding also the implications of EZH2 inactivation in OM Group3 MB organoids. OTX2 is a homeobox transcription factor, highly expressed in proliferating progenitor cells of healthy cerebellum development. During cerebellum development, OTX2 is silenced in differentiated neurons and absent in the postnatal cerebellum (Bunt et al., 2013; De Haas et al., 2006). The mechanism underlying OTX2-mediated maintenance of pluripotency and self-renewal in tumor cells remains under investigation, focusing the attention on the regulatory role of OTX2 in the epigenome (Lu et al., 2017). OTX2 locus is amplified in Group 3 and 4 MB (Adamson et al., 2010; G. Robinson et al., 2012). Bunt *et al.* reported that also some polycomb genes, required for H3K27 methylation, are upregulated in Group 3 and 4 MBs. They explained that OTX2 expression might favour increased levels of H3K27me3, regulating the expression of H3K27 modifiers in medulloblastoma (Bunt et al., 2013). They demonstrated that silencing of OTX2 in D425 MB cells results both in a decrease in polycomb gene expression (such as EZH2) and increase in expression of H3K27 demethylases (such as KDM6A, KDM6B), as well as a drop of H3K27me3 levels (Bunt et al., 2013). From these data, they assume the presence of a relationship in promoters between the binding of OTX2 and H3K27 trimethylation. Even though there is not any proof of evidence, direct interaction of bound OTX2 with polycomb proteins could be a possible explanation.

Based on the assumed relationship between OTX2 and EZH2 (or PRC2 complex), we decided to test at first DZNep on OM organoids. DZNep is the most widely used non-specific EZH2 inhibitor. It has significant antitumor activity in several cancer types, inhibiting PRC2, and removing H3K27me3 marks (Tan et al., 2007). DZNep was able to reduce Otx2/cMyc cancer cell growth in human cerebellar organoids, demonstrating that the inhibition of EZH2 can be a druggable pathway to target in human therapy. We also tested other two molecules, called Tazemetostat and GSK-126, because it is known that DZNep is toxic in animal models, it has short plasma half-life, and it is not specific for

EZH2 (Miranda et al., 2009). Tazemetostat is currently in a Phase 2 Clinical Trial in patients with solid tumors and Non-Hodgkin lymphoma that have EZH2, SMARCA4, or SMARCB1 gene mutations and do not respond to standard treatments (Italiano et al., 2018). We showed that Tazemetostat was able to reduce proliferating cells and increase apoptotic cells in OM human organoids. GSK-126 was only able to increase the number of apoptotic cells. We can conclude that Tazemetostat might be a specific treatment for Group 3 patients with high levels of Otx2/cMyc.
From this data, we can speculate that **human MB organoids will be also useful for drug screening to select a specific molecule for each different type of MB subgroups**.

With this work, **we wanted to highlight the importance of human organoids as a new reliable model to study medulloblastoma**. Organoids **mimic the structure of a developmental cerebellum**, important to **resemble the molecular mechanisms underlying an embryonic** tumor as MB. They can be modified with a smooth, low cost and fast approach as electroporation. **They resemble the Group 3 MB features and molecular stratification** dictated by different oncogene combinations. They can be a **reliable tool to generate novel patient-specific cancer models** and **to design a drug screening specific for each MB stratification**.
The creation of an organoid-based model in medulloblastoma's field might be the best approach to develop efficient target therapy.

Future perspectives

The design of new humanized MB models raised many interesting questions. First, it will be important to understand the relationship between EZH2 and the two oncogenes, Gfi1 and Otx2. One approach could be to perform a Chipseq analysis for Gfi1 and Otx2 upon modulation of EZH2 expression. These experiments could give answers about the role of EZH2 and the different implications of oncogenes in different MB subgroups.

Second, to test the effect of Tazemetostat on GM organoids. This experiment can be done to study the different roles of Tazemetostat in Group 3 MB subgroups. We demonstrated that Smarca4 blocks proliferation only in OM organoids. It would be interesting to see that Tazemetostat has a different effect on GM than OM organoids.

Talking about the drugs that we tested in this work, it would be interesting to analyze the mechanism of function of Tazemetostat. Indeed, in our *in vivo* experiments, the mechanism of action of Tazemetostat was not clear. We observed an effect on apoptosis and cell cycle. It would be interesting to perform cell cycle analysis after the treatment of Tazemetostat in our organoid-derived model.

Another point could be to test Tazemetostat function *in vivo*. We could inject OM organoids in nude mice and treat mice at two different time points, a few days after the injection and after the development of the tumor. In this way, we could test the efficiency of Tazemetostat in blocking the initiation of the tumor and tumor development.

Another aspect of MB is the lack of early tests to detect the tumor. It would be essential to find MB markers in the blood of patients. In this way, the diagnosis could be a straightforward blood test. We could try to analyze, by Mass Spectrometry, proteins specifically expressed or overexpressed in the blood of mice injected with OM or GM organoids.

Talking about drug screening, we can say that our Group 3 MB organoids opened new possibilities in this field. We are setting up an automized drug screening to test more than 10 drugs on 3 different organoid conditions (Venus, GMV, and MOV).

After the optimization of the drug screen and the selection of efficient drugs, we could run the **drug screening on patient-derived organoids**, **to develop target therapies** for specific patients, being able to design different treatments for the specific patient stratification. **Nowadays, there is not an efficient therapy, either a specific cure for each MB stratification**. So, this will be a huge step forward in the target therapy field.

As the last point, we are thrilled to use our human cerebellar organoids **to design Group 4 MB model**. The knowledge of this type of medulloblastoma is low due to the absence of mouse or human models. It is known that in **human cerebellum develops some neural precursors that are absent in mice**.

Maybe it is for this reason that no one has been able to develop a murine Group 4 model: mouse does not develop the same neural precursors that are present in humans, and **some of the human precursors could be the cell of origin of Group 4 MB** (Haldipur et al., 2019).

We are facing the problem using the same workflow we developed in this Group 3 project: we selected several combinations of Group 4 oncogenes to electroporate human cerebellum organoids. As we described in 3.2 paragraph, we obtained proliferative buds with different Group 4 combinations, and, injecting them into nude mice, we are waiting for an *in vivo* tumorigenic behaviour. Then we have to wait for the methylation profile analysis to confirm that we potentially developed a human Group 4 MB model. To conclude, we think that our **organoids will be an essential approach to trigger and study tumorigenesis in specific and exclusive human cells.**

Bibliography

Aaberg-Jessen, C., Nørregaard, A., Christensen, K., Pedersen, C. B., Andersen, C., & Kristensen, B. W. (2013). Invasion of primary glioma- and cell line-derived spheroids implanted into corticostriatal slice cultures. *International Journal of Clinical and Experimental Pathology*.

Adamson, D. C., Shi, Q., Wortham, M., Northcott, P. A., Di, C., Duncan, C. G., … Yan, H. (2010). OTX2 is critical for the maintenance and progression of Shh-independent medulloblastomas. *Cancer Research*. https://doi.org/10.1158/0008-5472.CAN-09-2331

Ahlfeld, J., Filser, S., Schmidt, F., Wefers, A. K., Merk, D. J., Glaß, R., … Schüller, U. (2017). Neurogenesis from Sox2 expressing cells in the adult cerebellar cortex. *Scientific Reports*, *7*(1), 1–7. https://doi.org/10.1038/s41598-017-06150-x

Alimova, I., Venkataraman, S., Harris, P., Marquez, V. E., Northcott, P. A., Dubuc, A., … Vibhakar, R. (2012). Targeting the enhancer of zeste homologue 2 in medulloblastoma. *International Journal of Cancer*. https://doi.org/10.1002/ijc.27455

Archer, T. C., Ehrenberger, T., Mundt, F., Gold, M. P., Krug, K., Mah, C. K., … Fraenkel, E. (2018). Proteomics, Post-translational Modifications, and Integrative Analyses Reveal Molecular Heterogeneity within Medulloblastoma Subgroups. *Cancer Cell*. https://doi.org/10.1016/j.ccell.2018.08.004

Bailey, P., & Cushing, H. (1925). Medulloblastoma cerebelli: A common type of midcerebellar glioma of childhood. *Archives of Neurology And Psychiatry*. https://doi.org/10.1001/archneurpsyc.1925.02200140055002

Ballabio, C., Anderle, M., Gianesello, M., Chiara, L., Miele, E., Cardano, M., … Tiberi, L. (2020). Modeling medulloblastoma in vivo and with human cerebellar organoids. *Nature Communications*. Retrieved from https://www.ncbi.nlm.nih.gov/pmc/articles/PMC6989674/pdf/41467_2019_Article_13989.pdf

Bandopadhayay, P., Bergthold, G., Nguyen, B., Schubert, S., Gholamin, S., Tang, Y., … R., B. (2014). BET bromodomain inhibition of MYC-amplified medulloblastoma. *Clinical Cancer Research*.

Bracken, A. P., & Helin, K. (2009). Polycomb group proteins: Navigators of lineage pathways led astray in cancer. *Nature Reviews Cancer*. https://doi.org/10.1038/nrc2736

Bunt, J., Hasselt, N. A., Zwijnenburg, D. A., Koster, J., Versteeg, R., & Kool, M. (2013). OTX2 sustains a bivalent-like state of OTX2-bound promoters in medulloblastoma by maintaining their H3K27me3 levels. *Acta Neuropathologica*.

Butts, T., Green, M. J., & Wingate, R. J. T. (2014). Development of the cerebellum: Simple steps to

make a ‘little brain.’ *Development (Cambridge)*. https://doi.org/10.1242/dev.106559

Canning, P., Cooper, C. D. O., Krojer, T., Murray, J. W., Pike, A. C. W., Chaikuad, A., … Bullock, A. N. (2013). Structural basis for Cul3 protein assembly with the BTB-Kelch family of E3 ubiquitin ligases. *Journal of Biological Chemistry*. https://doi.org/10.1074/jbc.M112.437996

Capper, D., Jones, D. T. W., Sill, M., Hovestadt, V., Schrimpf, D., Sturm, D., … Pfister, S. M. (2018). DNA methylation-based classification of central nervous system tumours. *Nature*. https://doi.org/10.1038/nature26000

Castellino, R. C., Barwick, B. G., Schniederjan, M., Buss, M. C., Becher, O., Hambardzumyan, D., … Durden, D. L. (2010). Heterozygosity for Ptenpromotes Tumorigenesis in a Mouse Model of Medulloblastoma. *PLoS ONE*. https://doi.org/10.1371/journal.pone.0010849

Castellino, R. C., & Durden, D. L. (2007). Mechanisms of Disease: The PI3K-Akt-PTEN signaling node - An intercept point for the control of angiogenesis in brain tumors. *Nature Clinical Practice Neurology*. https://doi.org/10.1038/ncpneuro0661

Cavalli, F. M. G., Remke, M., Rampasek, L., Peacock, J., Shih, D. J. H., Luu, B., … Taylor, M. D. (2017). Intertumoral Heterogeneity within Medulloblastoma Subgroups. *Cancer Cell*. https://doi.org/10.1016/j.ccell.2017.05.005

Chan-Penebre, E., Armstrong, K., Drew, A., Grassian, A. R., Feldman, I., Knutson, S. K., … Ribich, S. A. (2017). Selective killing of SMARCA2- and SMARCA4-deficient small cell carcinoma of the ovary, hypercalcemic type cells by inhibition of EZH2: In vitro and in vivo preclinical models. *Molecular Cancer Therapeutics*. https://doi.org/10.1158/1535-7163.MCT-16-0678

Cho, Y. J., Tsherniak, A., Tamayo, P., Santagata, S., Ligon, A., Greulich, H., … Pomeroy, S. L. (2011). Integrative genomic analysis of medulloblastoma identifies a molecular subgroup that drives poor clinical outcome. *Journal of Clinical Oncology*, *29*(11), 1424–1430. https://doi.org/10.1200/JCO.2010.28.5148

Comet, I., Riising, E. M., Leblanc, B., & Helin, K. (2016). Maintaining cell identity: PRC2-mediated regulation of transcription and cancer. *Nature Reviews Cancer*. https://doi.org/10.1038/nrc.2016.83

Davis, C. A., Haberland, M., Arnold, M. A., Sutherland, L. B., McDonald, O. G., Richardson, J. A., … Olson, E. N. (2006). PRISM/PRDM6, a Transcriptional Repressor That Promotes the Proliferative Gene Program in Smooth Muscle Cells. *Molecular and Cellular Biology*. https://doi.org/10.1128/mcb.26.7.2626-2636.2006

De Haas, T., Oussoren, E., Grajkowska, W., Perek-Polnik, M., Popovic, M., Zadravec-Zaletel, L., … Kool, M. (2006). OTX1 and OTX2 expression correlates with the clinicopathologic classification of medulloblastomas. *Journal of Neuropathology and Experimental Neurology*.

https://doi.org/10.1097/01.jnen.0000199576.70923.8a

Duan, Z., Zarebski, A., Montoya-Durango, D., Grimes, H. L., & Horwitz, M. (2005). Gfi1 Coordinates Epigenetic Repression of p21Cip/WAF1 by Recruitment of Histone Lysine Methyltransferase G9a and Histone Deacetylase 1. *Molecular and Cellular Biology*. https://doi.org/10.1128/mcb.25.23.10338-10351.2005

Duan, Zhijun, & Horwitz, M. (2003). Targets of the transcriptional repressor oncoprotein GFI-1. *Proceedings of the National Academy of Sciences of the United States of America*. https://doi.org/10.1073/pnas.1031694100

Dykhuizen, E. C., Hargreaves, D. C., Miller, E. L., Cui, K., Korshunov, A., Kool, M., … Crabtree, G. R. (2013). BAF complexes facilitate decatenation of DNA by topoisomerase IIα. *Nature*. https://doi.org/10.1038/nature12146

Ellison, D. W., Dalton, J., Kocak, M., Nicholson, S. L., Fraga, C., Neale, G., … Gilbertson, R. J. (2011). Medulloblastoma: Clinicopathological correlates of SHH, WNT, and non-SHH/WNT molecular subgroups. *Acta Neuropathologica*. https://doi.org/10.1007/s00401-011-0800-8

Endo, H., Okami, J., Okuyama, H., Kumagai, T., Uchida, J., Kondo, J., … Inoue, M. (2013). Spheroid culture of primary lung cancer cells with neuregulin 1/her3 pathway activation. *Journal of Thoracic Oncology*. https://doi.org/10.1097/JTO.0b013e3182779ccf

Fink, A. J., Englund, C., Daza, R., Pham, D., Lau, C., Nivison, M., & Kowalczyk, T. (2006). Development of the deep cerebellar nuclei: Transcription factors and cell migration from the rhombic lip. *Journal of Neuroscience*.

Forget, A., Martignetti, L., Puget, S., Calzone, L., Brabetz, S., Picard, D., … Ayrault, O. (2018). Aberrant ERBB4-SRC Signaling as a Hallmark of Group 4 Medulloblastoma Revealed by Integrative Phosphoproteomic Profiling. *Cancer Cell*, *34*(3), 379-395.e7. https://doi.org/10.1016/j.ccell.2018.08.002

Garancher, A., Lin, C. Y., Morabito, M., Richer, W., Rocques, N., Larcher, M., … Pouponnot, C. (2018). NRL and CRX Define Photoreceptor Identity and Reveal Subgroup-Specific Dependencies in Medulloblastoma. *Cancer Cell*. https://doi.org/10.1016/j.ccell.2018.02.006

Gholamin, S., Mitra, S. S., Feroze, A. H., Liu, J., Kahn, S. A., Zhang, M., … Cheshier, S. H. (2017). Disrupting the CD47-SIRPα anti-phagocytic axis by a humanized anti-CD47 antibody is an efficacious treatment for malignant pediatric brain tumors. *Science Translational Medicine*. https://doi.org/10.1126/scitranslmed.aaf2968

Gibson, P., Tong, Y., Robinson, G., Thompson, M. C., Currle, D. S., Eden, C., … Gilbertson, R. J. (2010). Subtypes of medulloblastoma have distinct developmental origins. *Nature*, *468*(7327), 1095–1099. https://doi.org/10.1038/nature09587

Gilbertson, R. J., & Ellison, D. W. (2008). The Origins of Medulloblastoma Subtypes. *Annual Review of Pathology: Mechanisms of Disease*. https://doi.org/10.1146/annurev.pathmechdis.3.121806.151518

Glazer, R. I., Hartman, K. D., Knode, M. C., Richard, M. M., Chiang, P. K., Tseng, C. K. H., & Marquez, V. E. (1986). 3-Deazaneplanocin: A new and potent inhibitor of S-adenosylhomocysteine hydrolase and its effects on human promyelocytic leukemia cell line HL-60. *Biochemical and Biophysical Research Communications*. https://doi.org/10.1016/0006-291X(86)90048-3

Goodrich, L. V., Milenković, L., Higgins, K. M., & Scott, M. P. (1997). Altered neural cell fates and medulloblastoma in mouse patched mutants. *Science*. https://doi.org/10.1126/science.277.5329.1109

Grammel, D., Warmuth-Metz, M., Von Bueren, A. O., Kool, M., Pietsch, T., Kretzschmar, H. A., … Schüller, U. (2012). Sonic hedgehog-associated medullobla stoma arising from the cochlear nuclei of the brainstem. *Acta Neuropathologica*. https://doi.org/10.1007/s00401-012-0961-0

Greer, E. L., & Shi, Y. (2012). Histone methylation: A dynamic mark in health, disease and inheritance. *Nature Reviews Genetics*. https://doi.org/10.1038/nrg3173

Gustafson, W. C., Meyerowitz, J. G., Nekritz, E. A., Chen, J., Benes, C., Charron, E., … Weiss, W. A. (2014). Drugging MYCN through an Allosteric Transition in Aurora Kinase A. *Cancer Cell*. https://doi.org/10.1016/j.ccr.2014.07.015

Haldipur, P., Aldinger, K. A., Bernardo, S., Deng, M., Timms, A. E., Overman, L. M., … Millen, K. J. (2019). Spatiotemporal expansion of primary progenitor zones in the developing human cerebellum. *Science*. https://doi.org/10.1126/science.aax7526

Hanahan, D., & Weinberg, R. A. (2000). The hallmarks of cancer. *Cell*. https://doi.org/10.1016/S0092-8674(00)81683-9

Hanahan, D., & Weinberg, R. A. (2011). Hallmarks of cancer: The next generation. *Cell*. https://doi.org/10.1016/j.cell.2011.02.013

Hendricks, K. B., Shanahan, F., & Lees, E. (2004). Role for BRG1 in Cell Cycle Control and Tumor Suppression. *Molecular and Cellular Biology*. https://doi.org/10.1128/mcb.24.1.362-376.2004

Hill, R. M., Kuijper, S., Lindsey, J. C., Petrie, K., Schwalbe, E. C., Barker, K., … Clifford, S. C. (2015). Combined MYC and P53 defects emerge at medulloblastoma relapse and define rapidly progressive, therapeutically targetable disease. *Cancer Cell*. https://doi.org/10.1016/j.ccell.2014.11.002

Hodges, C., Kirkland, J. G., & Crabtree, G. R. (2016). The many roles of BAF (mSWI/SNF) and PBAF complexes in cancer. *Cold Spring Harbor Perspectives in Medicine*.

https://doi.org/10.1101/cshperspect.a026930

Hoff, K. von, Hinkes, B., Gerber, N. U., Deinlein, F., Mittler, U., Urban, C., … Rutkowski, S. (2009). Long-term outcome and clinical prognostic factors in children with medulloblastoma treated in the prospective randomised multicentre trial HIT'91. *European Journal of Cancer*, *45*(7), 1209–1217. https://doi.org/10.1016/j.ejca.2009.01.015

Hovestadt, V., Ayrault, O., Swartling, F. J., Robinson, G. W., Pfister, S. M., & Northcott, P. A. (2019). Medulloblastomics revisited: biological and clinical insights from thousands of patients. *Nature Reviews Cancer*. Retrieved from https://www.nature.com/articles/s41568-019-0223-8

Hovestadt, V., Remke, M., Kool, M., Pietsch, T., Northcott, P. A., Fischer, R., … Jones, D. T. W. (2013). Robust molecular subgrouping and copy-number profiling of medulloblastoma from small amounts of archival tumour material using high-density DNA methylation arrays. *Acta Neuropathologica*. https://doi.org/10.1007/s00401-013-1126-5

Husain, A., Begum, N. A., Taniguchi, T., Taniguchi, H., Kobayashi, M., & Honjo, T. (2016). Chromatin remodeller SMARCA4 recruits topoisomerase 1 and suppresses transcription-associated genomic instability. *Nature Communications*. https://doi.org/10.1038/ncomms10549

Ishida, Y., Kawakami, H., Kitajima, H., Nishiyama, A., Sasai, Y., Inoue, H., & Muguruma, K. (2016). Vulnerability of Purkinje Cells Generated from Spinocerebellar Ataxia Type 6 Patient-Derived iPSCs. *Cell Reports*, *17*(6), 1482–1490. https://doi.org/10.1016/j.celrep.2016.10.026

Italiano, A., Soria, J. C., Toulmonde, M., Michot, J. M., Lucchesi, C., Varga, A., … Ribrag, V. (2018). Tazemetostat, an EZH2 inhibitor, in relapsed or refractory B-cell non-Hodgkin lymphoma and advanced solid tumours: a first-in-human, open-label, phase 1 study. *The Lancet Oncology*. https://doi.org/10.1016/S1470-2045(18)30145-1

Ivanov, D. P., Coyle, B., Walker, D. A., & Grabowska, A. M. (2016). In vitro models of medulloblastoma: Choosing the right tool for the job. *Journal of Biotechnology*. https://doi.org/10.1016/j.jbiotec.2016.07.028

Ivanov, D. P., Parker, T. L., Walker, D. A., Alexander, C., Ashford, M. B., Gellert, P. R., & Garnett, M. C. (2015). In vitro co-culture model of medulloblastoma and human neural stem cells for drug delivery assessment. *Journal of Biotechnology*, *205*, 3–13. https://doi.org/10.1016/j.jbiotec.2015.01.002

John, R. (2018). Global Cancer Facts & Figures 4 th Edition-Special section,the obesity epidemic. *American Cancer Society*, 76. https://doi.org/http://bit. ly/9NTLj6. Accessed 6 Aug 2017

Jones, D. T. W., N., J. J., M., K., T., Z., B., H., M., S. S., … Lichter, P. (2012). Dissecting the genomic complexity underlying medulloblastoma. *Nature*.

Jung, S., Kim, H. W., Lee, J. H., Kang, S. S., Rhu, H. H., Jeong, Y. Il, … Ahn, K. Y. (2002). Brain tumor invasion model system using organotypic brain-slice culture as an alternative to in vivo model. *Journal of Cancer Research and Clinical Oncology*. https://doi.org/10.1007/s00432-002-0366-x

Junhee, S., H. Shaw Warren, Alex, G. C., Michael, N. M., Henry, V. B., Xu, W., … Tompkins, R. G. (2013). Genomic responses in mouse models poorly mimic human inflammatory diseases. *Proceedings of the National Academy of Sciences of the United States of America*. https://doi.org/10.1073/pnas.1222878110

Kadoch, C., & Crabtree, G. R. (2015). Mammalian SWI/SNF chromatin remodeling complexes and cancer: Mechanistic insights gained from human genomics. *Science Advances*. https://doi.org/10.1126/sciadv.1500447

Kawauchi, D., Ogg, R. J., Liu, L., Shih, D. J. H., Finkelstein, D., Murphy, B. L., … Roussel, M. F. (2017). Novel MYC-driven medulloblastoma models from multiple embryonic cerebellar cells. *Oncogene*. https://doi.org/10.1038/onc.2017.110

Kawauchi, Daisuke, Robinson, G., Uziel, T., Gibson, P., Rehg, J., Gao, C., … Roussel, M. F. (2012). A Mouse Model of the Most Aggressive Subgroup of Human Medulloblastoma. *Cancer Cell*, *21*(2), 168–180. https://doi.org/10.1016/j.ccr.2011.12.023

Kia, S. K., Gorski, M. M., Giannakopoulos, S., & Verrijzer, C. P. (2008). SWI/SNF Mediates Polycomb Eviction and Epigenetic Reprogramming of the INK4b-ARF-INK4a Locus. *Molecular and Cellular Biology*. https://doi.org/10.1128/mcb.02019-07

Kim, J., Aftab, B. T., Tang, J. Y., Kim, D., Lee, A. H., Rezaee, M., … Rudin, C. M. (2013). Itraconazole and Arsenic Trioxide Inhibit Hedgehog Pathway Activation and Tumor Growth Associated with Acquired Resistance to Smoothened Antagonists. *Cancer Cell*. https://doi.org/10.1016/j.ccr.2012.11.017

Kim, K. H., Kim, W., Howard, T. P., Vazquez, F., Tsherniak, A., Wu, J. N., … Roberts, C. W. M. (2015). SWI/SNF-mutant cancers depend on catalytic and non-catalytic activity of EZH2. *Nature Medicine*. https://doi.org/10.1038/nm.3968

Kim, K. H., & Roberts, C. W. M. (2016). Targeting EZH2 in cancer. *Nature Medicine*. https://doi.org/10.1038/nm.4036

Kimura, M., Endo, H., Inoue, T., Nishino, K., Uchida, J., Kumagai, T., … Inoue, M. (2015). Analysis of ERBB ligand-induced resistance mechanism to crizotinib by primary culture of lung adenocarcinoma with EML4-ALK fusion gene. *Journal of Thoracic Oncology*. https://doi.org/10.1097/JTO.0000000000000381

Knutson, S. K., Kawano, S., Minoshima, Y., Warholic, N. M., Huang, K. C., Xiao, Y., … Keilhack,

H. (2014). Selective inhibition of EZH2 by EPZ-6438 leads to potent antitumor activity in EZH2-mutant non-Hodgkin lymphoma. *Molecular Cancer Therapeutics*. https://doi.org/10.1158/1535-7163.MCT-13-0773

Koelsche, C., Sahm, F., Capper, D., Reuss, D., Sturm, D., Jones, D. T. W., … Von Deimling, A. (2013). Distribution of TERT promoter mutations in pediatric and adult tumors of the nervous system. *Acta Neuropathologica*. https://doi.org/10.1007/s00401-013-1195-5

Kool, M., Jones, D. T. W., Jäger, N., Northcott, P. A., Pugh, T. J., Hovestadt, V., … Pfister, S. M. (2014). Genome sequencing of SHH medulloblastoma predicts genotype-related response to smoothened inhibition. *Cancer Cell*. https://doi.org/10.1016/j.ccr.2014.02.004

Kool, M., Korshunov, A., Remke, M., Jones, D. T. W., Schlanstein, M., Northcott, P. A., … Pfister, S. M. (2012). Molecular subgroups of medulloblastoma: An international meta-analysis of transcriptome, genetic aberrations, and clinical data of WNT, SHH, Group 3, and Group 4 medulloblastomas. *Acta Neuropathologica*, *123*(4), 473–484. https://doi.org/10.1007/s00401-012-0958-8

Kramer, M., Ribeiro, D., Arsenian-Henriksson, M., Deller, T., & Rohrer, H. (2016). Proliferation and survival of embryonic sympathetic neuroblasts by MYCN and activated ALK signaling. *Journal of Neuroscience*. https://doi.org/10.1523/JNEUROSCI.0183-16.2016

Kwong, J., Franky, L. C., Wong, K. K., Birrer, M. J., Archibald, K. M., Balkwill, F. R., … Mok, S. C. (2009). Inflammatory cytokine tumor necrosis factor α confers precancerous phenotype in an organoid model of normal human ovarian surface epithelial cells. *Neoplasia*. https://doi.org/10.1593/neo.09112

Lancaster, M. A., & Knoblich, J. A. (2014). Organogenesisin a dish: Modeling development and disease using organoid technologies. *Science*, *345*(6194). https://doi.org/10.1126/science.1247125

Lancaster, M. A., Renner, M., Martin, C. A., Wenzel, D., Bicknell, L. S., Hurles, M. E., … Knoblich, J. A. (2013). Cerebral organoids model human brain development and microcephaly. *Nature*. https://doi.org/10.1038/nature12517

Larson, J. D., & Largaespada, D. A. (2012). In vivo models for defining molecular subtypes of the primitive neuroectodermal tumor genome: Current challenges and solutions. *In Vivo*.

Łastowska, M., Trubicka, J., Niemira, M., Paczkowska-Abdulsalam, M., Karkucińska-Więckowska, A., Kaleta, M., … Matyja, E. (2018). Medulloblastoma with transitional features between Group 3 and Group 4 is associated with good prognosis. *Journal of Neuro-Oncology*. https://doi.org/10.1007/s11060-018-2797-5

Lau, J., Schmidt, C., Markant, S. L., Taylor, M. D., Wechsler-Reya, R. J., & Weiss, W. A. (2012).

Matching mice to malignancy: Molecular subgroups and models of medulloblastoma. *Child's Nervous System*, *28*(4), 521–532. https://doi.org/10.1007/s00381-012-1704-1

Lee, Y., Kawagoe, R., Sasai, K., Li, Y., Russell, H. R., Curran, T., & McKinnon, P. J. (2007). Loss of suppressor-of-fused function promotes tumorigenesis. *Oncogene*. https://doi.org/10.1038/sj.onc.1210467

Li, P., Du, F., Yuelling, L. W., Lin, T., Muradimova, R. E., Tricarico, R., … Yang, Z. J. (2013). A population of Nestin-expressing progenitors in the cerebellum exhibits increased tumorigenicity. *Nature Neuroscience*. https://doi.org/10.1038/nn.3553

Li, X., Nadauld, L., Ootani, A., Corney, D. C., Pai, R. K., O., G., … C.J., K. (2014). Oncogenic transformation of diverse gastrointestinal tissues in primary organoid culture. *Nature Medicine*. https://doi.org/10.1038/nm.3585

Liu, R. Z., Garcia, E., Glubrecht, D. D., Poon, H. Y., Mackey, J. R., & Godbout, R. (2015). CRABP1 is associated with a poor prognosis in breast cancer: Adding to the complexity of breast cancer cell response to retinoic acid. *Molecular Cancer*. https://doi.org/10.1186/s12943-015-0380-7

Louis, D. N., Perry, A., Reifenberger, G., von Deimling, A., Figarella-Branger, D., Cavenee, W. K., … Ellison, D. W. (2016). The 2016 World Health Organization Classification of Tumors of the Central Nervous System: a summary. *Acta Neuropathologica*, *131*(6), 803–820. https://doi.org/10.1007/s00401-016-1545-1

Lu, Y., Labak, C. M., Jain, N., Purvis, I. J., Guda, M. R., Bach, S. E., … Velpula, K. K. (2017). OTX2 expression contributes to proliferation and progression in Myc-amplified medulloblastoma. *American Journal of Cancer Research*.

Mabbott, D. J., Penkman, L., Witol, A., Strother, D., & Bouffet, E. (2008). Core Neurocognitive Functions in Children Treated for Posterior Fossa Tumors. *Neuropsychology*. https://doi.org/10.1037/0894-4105.22.2.159

Mabbott, D. J., Spiegler, B. J., Greenberg, M. L., Rutka, J. T., Hyder, D. J., & Bouffet, E. (2005). Serial evaluation of academic and behavioral outcome after treatment with cranial radiation in childhood. *Journal of Clinical Oncology*. https://doi.org/10.1200/JCO.2005.01.158

Manam, S., Oliphant, T., Henderson, A., Husain, A., & Rajan, N. (2018). Basaloid follicular proliferations and brain tumours: The tumour spectrum of SUFU mutation carriers. *British Journal of Dermatology*.

Margueron, R., & Reinberg, D. (2011). The Polycomb complex PRC2 and its mark in life. *Nature*. https://doi.org/10.1038/nature09784

Marzban, H., Del Bigio, M. R., Alizadeh, J., Ghavami, S., Zachariah, R. M., & Rastegar, M. (2015).

Cellular commitment in the developing cerebellum. *Frontiers in Cellular Neuroscience*. https://doi.org/10.3389/fncel.2014.00450

McCabe, M. T., & Creasy, C. L. (2014). EZH2 as a potential target in cancer therapy. *Epigenomics*. https://doi.org/10.2217/epi.14.23

McCabe, M. T., Ott, H. M., Ganji, G., Korenchuk, S., Thompson, C., Van Aller, G. S., … Diaz, E. (2012). EZH2 inhibition as a therapeutic strategy for lymphoma with EZH2-activating mutations. *Nature*. https://doi.org/10.1038/nature11606

Meng, W., Garnett, M. C., Walker, D. A., & Parker, T. L. (2016). Penetration and intracellular uptake of poly(glycerol-adipate) nanoparticles into three-dimensional brain tumour cell culture models. *Experimental Biology and Medicine*. https://doi.org/10.1177/1535370215610441

Menyhárt, O., Giangaspero, F., & Gyorffy, B. (2019). Molecular markers and potential therapeutic targets in non-WNT/non-SHH (group 3 and group 4) medulloblastomas. *Journal of Hematology and Oncology*. https://doi.org/10.1186/s13045-019-0712-y

Miele, E., Valente, S., Alfano, V., Silvano, M., Mellini, P., Borovika, D., … Ferretti, E. (2017). The histone methyltransferase EZH2 as a druggable target in SHH medulloblastoma cancer stem cells. *Oncotarget*. https://doi.org/10.18632/oncotarget.19782

Miranda, T. B., Cortez, C. C., Yoo, C. B., Liang, G., Abe, M., Kelly, T. K., … Jones, P. A. (2009). DZNep is a global histone methylation inhibitor that reactivates developmental genes not silenced by DNA methylation. *Molecular Cancer Therapeutics*. https://doi.org/10.1158/1535-7163.MCT-09-0013

Mizuhara, E., Minaki, Y., Nakatani, T., Kumai, M., Inoue, T., Muguruma, K., … Ono, Y. (2010). Purkinje cells originate from cerebellar ventricular zone progenitors positive for Neph3 and E-cadherin. *Developmental Biology*. https://doi.org/10.1016/j.ydbio.2009.11.032

Moreno, N., Schmidt, C., Ahlfeld, J., Pöschl, J., Dittmar, S., Pfister, S. M., … Schüller, U. (2014). Loss of Smarc proteins impairs cerebellar development. *Journal of Neuroscience*. https://doi.org/10.1523/JNEUROSCI.2560-14.2014

Morfouace, M., Shelat, A., Jacus, M., Freeman, B. B., Turner, D., Robinson, S., … Roussel, M. F. (2014). Pemetrexed and gemcitabine as combination therapy for the treatment of group3 medulloblastoma. *Cancer Cell*. https://doi.org/10.1016/j.ccr.2014.02.009

Morris, T. J., Butcher, L. M., Feber, A., Teschendorff, A. E., Chakravarthy, A. R., Wojdacz, T. K., & Beck, S. (2014). ChAMP: 450k Chip Analysis Methylation Pipeline. *Bioinformatics*. https://doi.org/10.1093/bioinformatics/btt684

Muguruma, K. (2018). Self-Organized Cerebellar Tissue from Human Pluripotent Stem Cells and Disease Modeling with Patient-Derived iPSCs. *Cerebellum*. https://doi.org/10.1007/s12311-

017-0905-2

Muguruma, K., Nishiyama, A., Kawakami, H., Hashimoto, K., & Sasai, Y. (2015). Self-organization of polarized cerebellar tissue in 3D culture of human pluripotent stem cells. *Cell Reports*, *10*(4), 537–550. https://doi.org/10.1016/j.celrep.2014.12.051

Muguruma, K., Nishiyama, A., Ono, Y., Miyawaki, H., Mizuhara, E., Hori, S., … Sasai, Y. (2010). Ontogeny-recapitulating generation and tissue integration of ES cell-derived Purkinje cells. *Nature Neuroscience*, *13*(10), 1171–1180. https://doi.org/10.1038/nn.2638

Murtagh, F., & Legendre, P. (2014). Ward's Hierarchical Agglomerative Clustering Method: Which Algorithms Implement Ward's Criterion? *Journal of Classification*. https://doi.org/10.1007/s00357-014-9161-z

Nakano, T., Ando, S., Takata, N., Kawada, M., Muguruma, K., Sekiguchi, K., … Sasai, Y. (2012). Self-formation of optic cups and storable stratified neural retina from human ESCs. *Cell Stem Cell*. https://doi.org/10.1016/j.stem.2012.05.009

Neal, J. T., & Kuo, C. J. (2016). Organoids as Models for Neoplastic Transformation. *Annual Review of Pathology: Mechanisms of Disease*, *11*(1), 199–220. https://doi.org/10.1146/annurev-pathol-012615-044249

Northcott, P. A., Buchhalter, I., Morrissy, A. S., Hovestadt, V., Weischenfeldt, J., Ehrenberger, T., … Lichter, P. (2017). The whole-genome landscape of medulloblastoma subtypes. *Nature*. https://doi.org/10.1038/nature22973

Northcott, P. A., Dubuc, A. M., Pfister, S., & Taylor, M. D. (2012). Molecular subgroups of medulloblastoma. *Expert Review of Neurotherapeutics*, *12*(7), 871–884. https://doi.org/10.1586/ern.12.66

Northcott, P. A., Jones, D. T. W., Kool, M., Robinson, G. W., Gilbertson, R. J., Cho, Y. J., … Pfister, S. M. (2012). Medulloblastomics: The end of the beginning. *Nature Reviews Cancer*, *12*(12), 818–834. https://doi.org/10.1038/nrc3410

Northcott, P. A., Korshunov, A., Witt, H., Hielscher, T., Eberhart, C. G., Mack, S., … Taylor, M. D. (2011). Medulloblastoma comprises four distinct molecular variants. *Journal of Clinical Oncology*. https://doi.org/10.1200/JCO.2009.27.4324

Northcott, P. A., Lee, C., Zichner, T., Stütz, A. M., Erkek, S., Kawauchi, D., … Pfister, S. M. (2014). Enhancer hijacking activates GFI1 family oncogenes in medulloblastoma. *Nature*. https://doi.org/10.1038/nature13379

Northcott, P. A., Shih, D. J. H., Peacock, J., Garzia, L., Sorana Morrissy, A., Zichner, T., … Taylor, M. D. (2012). Subgroup-specific structural variation across 1,000 medulloblastoma genomes. *Nature*. https://doi.org/10.1038/nature11327

Northcott, P. A., Shih, D. J. H., Remke, M., Cho, Y. J., Kool, M., Hawkins, C., … Taylor, M. D. (2012). Rapid, reliable, and reproducible molecular sub-grouping of clinical medulloblastoma samples. *Acta Neuropathologica*. https://doi.org/10.1007/s00401-011-0899-7

Pan, J., McKenzie, Z. M., D'Avino, A. R., Mashtalir, N., Lareau, C. A., St. Pierre, R., … Kadoch, C. (2019). The ATPase module of mammalian SWI/SNF family complexes mediates subcomplex identity and catalytic activity–independent genomic targeting. *Nature Genetics*. https://doi.org/10.1038/s41588-019-0363-5

Paterson, E., & Farr, R. F. (1953). Cerebellar Medulloblastoma: Treatment by Irradiation of the Whole Central Nervous System. *Acta Radiologica*. https://doi.org/10.1177/028418515303900407

Pei, Y., Liu, K. W., Wang, J., Garancher, A., Tao, R., Esparza, L. A., … Wechsler-Reya, R. J. (2016). HDAC and PI3K Antagonists Cooperate to Inhibit Growth of MYC-Driven Medulloblastoma. *Cancer Cell*. https://doi.org/10.1016/j.ccell.2016.02.011

Pei, Y., Moore, C. E., Wang, J., Tewari, A. K., Eroshkin, A., Cho, Y. J., … Wechsler-Reya, R. J. (2012). An Animal Model of MYC-Driven Medulloblastoma. *Cancer Cell*. https://doi.org/10.1016/j.ccr.2011.12.021

Perlman, R. L. (2016). Mouse Models of Human Disease: An Evolutionary Perspective. *Evolution, Medicine, and Public Health*. https://doi.org/10.1093/emph/eow014

Pierre, R. S., & Kadoch, C. (2017). Mammalian SWI/SNF complexes in cancer: emerging therapeutic opportunities. *Current Opinion in Genetics and Development*. https://doi.org/10.1016/j.gde.2017.02.004

Pöschl, J., Stark, S., Neumann, P., Gröbner, S., Kawauchi, D., Jones, D. T. W., … Schüller, U. (2014). Genomic and transcriptomic analyses match medulloblastoma mouse models to their human counterparts. *Acta Neuropathologica*, *128*(1), 123–136. https://doi.org/10.1007/s00401-014-1297-8

Ramaswamy, Nör, C., & Taylor, M. D. (2016). p53 and meduloblastoma. *Cold Spring Harbor Perspectives in Medicine*. https://doi.org/10.1101/cshperspect.a026278

Ramaswamy, V., Remke, M., Bouffet, E., Faria, C. C., Perreault, S., Cho, Y.-J., … Taylor, M. D. (2013). Recurrence patterns across medulloblastoma subgroups: An integrated clinical and molecular analysis. *The Lancet Oncology*.

Ramaswamy, Vijay, Remke, M., Bouffet, E., Bailey, S., Clifford, S. C., Doz, F., … Pomeroy, S. L. (2016). Risk stratification of childhood medulloblastoma in the molecular era: the current consensus. *Acta Neuropathologica*. https://doi.org/10.1007/s00401-016-1569-6

Ramaswamy, Vijay, & Taylor, M. D. (2017). Medulloblastoma: From myth to molecular. *Journal of*

Clinical Oncology. https://doi.org/10.1200/JCO.2017.72.7842

Rausch, T., Jones, D. T. W., Zapatka, M., Stutz, A. M., Zichner, T., Weischenfeldt Wasserman, J., … Korbel, J. O. (2012). Genome sequencing of pediatric medulloblastoma links catastrophic DNA rearrangements with TP53 mutations. *Cell*.

Remke, M., Ramaswamy, V., Peacock, J., Shih, D. J. H., Koelsche, C., Northcott, P. A., … A., V. D. (2013). TERT promoter mutations are highly recurrent in SHH subgroup medulloblastoma. *Acta Neuropathologica*.

Riggs, L., Bouffet, E., Laughlin, S., Laperriere, N., Liu, F., Skocic, J., … Mabbott, D. J. (2014). Changes to memory structures in children treated for posterior fossa tumors. *Journal of the International Neuropsychological Society*. https://doi.org/10.1017/S135561771300129X

Rivero-Hinojosa, S., Lau, L. S., Stampar, M., Staal, J., Zhang, H., Gordish-Dressman, H., … Rood, B. R. (2018). Proteomic analysis of Medulloblastoma reveals functional biology with translational potential. *Acta Neuropathologica Communications*. https://doi.org/10.1186/s40478-018-0548-7

Robinson, G., Parker, M., Kranenburg, T. A., Lu, C., Chen, X., Ding, L., … Gilbertson, R. J. (2012). Novel mutations target distinct subgroups of medulloblastoma. *Nature*, *488*(7409), 43–48. https://doi.org/10.1038/nature11213

Robinson, G. W., Rudneva, V. A., Buchhalter, I., Billups, C. A., Waszak, S. M., Smith, K. S., … Northcott, P. A. (2018). Risk-adapted therapy for young children with medulloblastoma (SJYC07): therapeutic and molecular outcomes from a multicentre, phase 2 trial. *The Lancet Oncology*. https://doi.org/10.1016/S1470-2045(18)30204-3

Roussel, M. F., & Hatten, M. E. (2011). Cerebellum: Development and Medulloblastoma. In *Current Topics in Developmental Biology*. https://doi.org/10.1016/B978-0-12-380916-2.00008-5

Saleque, S., Kim, J., Rooke, H. M., & Orkin, S. H. (2007). Epigenetic Regulation of Hematopoietic Differentiation by Gfi-1 and Gfi-1b Is Mediated by the Cofactors CoREST and LSD1. *Molecular Cell*. https://doi.org/10.1016/j.molcel.2007.06.039

Salero, E., & Hatten, M. E. (2007). Differentiation of ES cells into cerebellar neurons. *Proceedings of the National Academy of Sciences*, *104*(8), 2997–3002. https://doi.org/10.1073/pnas.0610879104

Sandén, E., Dyberg, C., Krona, C., Gallo-Oller, G., Olsen, T. K., Enríquez Pérez, J., … Darabi, A. (2017). Establishment and characterization of an orthotopic patient-derived Group 3 medulloblastoma model for preclinical drug evaluation. *Scientific Reports*. https://doi.org/10.1038/srep46366

Schüller, U., Heine, V. M., Mao, J., Kho, A. T., Dillon, A. K., Han, Y. G., … Ligon, K. L. (2008). Acquisition of Granule Neuron Precursor Identity Is a Critical Determinant of Progenitor Cell Competence to Form Shh-Induced Medulloblastoma. *Cancer Cell*. https://doi.org/10.1016/j.ccr.2008.07.005

Schwalbe, E. C., Lindsey, J. C., Nakjang, S., Crosier, S., Smith, A. J., Hicks, D., … Clifford, S. C. (2017). Novel molecular subgroups for clinical classification and outcome prediction in childhood medulloblastoma: a cohort study. *The Lancet Oncology*. https://doi.org/10.1016/S1470-2045(17)30243-7

Selvadurai, H. J., & Mason, J. O. (2011). Wnt/β-catenin signalling is active in a highly dynamic pattern during development of the mouse cerebellum. *PLoS ONE*. https://doi.org/10.1371/journal.pone.0023012

Seoane, J., Pouponnot, C., Staller, P., Schader, M., Eilers, M., & Massagué, J. (2001). TGFβ influences myc, miz-1 and smad to control the CDK inhibitor p15INK4b. *Nature Cell Biology*. https://doi.org/10.1038/35070086

Sharma, T., Schwalbe, E. C., Williamson, D., Sill, M., Hovestadt, V., Mynarek, M., … Clifford, S. C. (2019). Second-generation molecular subgrouping of medulloblastoma: an international meta-analysis of Group 3 and Group 4 subtypes. *Acta Neuropathologica*. https://doi.org/10.1007/s00401-019-02020-0

Shi, X., Wang, Q., Gu, J., Xuan, Z., & Wu, J. I. (2016). SMARCA4/Brg1 coordinates genetic and epigenetic networks underlying Shh-type medulloblastoma development. *Oncogene*. https://doi.org/10.1038/onc.2016.108

Shu, Q., Wong, K. K., Su, J. M., Adesina, A. M., Yu, L. T., Tsang, Y. T. M., … Li, X.-N. (2008). Direct orthotopic transplantation of fresh surgical specimen preserves CD133+ tumor cells in clinically relevant mouse models of medulloblastoma and glioma. *Stem Cells (Dayton, Ohio)*, *26*(6), 1414–1424. https://doi.org/10.1634/stemcells.2007-1009

Smits, M., Van Rijn, S., Hulleman, E., Biesmans, D., Van Vuurden, D. G., Kool, M., … Wurdinger, T. (2012). EZH2-regulated DAB2IP is a medulloblastoma tumor suppressor and a positive marker for survival. *Clinical Cancer Research*. https://doi.org/10.1158/1078-0432.CCR-12-0399

Spiegler, B. J., Bouffet, E., Greenberg, M. L., Rutka, J. T., & Mabbott, D. J. (2004). Change in neurocognitive functioning after treatment with cranial radiation in childhood. *Journal of Clinical Oncology*. https://doi.org/10.1200/JCO.2004.05.186

Stoppini, L., Buchs, P. A., & Muller, D. (1991). A simple method for organotypic cultures of nervous tissue. *Journal of Neuroscience Methods*. https://doi.org/10.1016/0165-

0270(91)90128-M

Stromecki, M., Tatari, N., Morrison, L. C., Kaur, R., Zagozewski, J., Palidwor, G., … Werbowetski-Ogilvie, T. E. (2018). Characterization of a novel OTX2-driven stem cell program in Group 3 and Group 4 medulloblastoma. *Molecular Oncology*. https://doi.org/10.1002/1878-0261.12177

Sun, W., Cornwell, A., Li, J., Peng, S., Osorio, M. J., Aalling, N., … Nedergaard, M. (2017). SOX9 Is an Astrocyte-Specific Nuclear Marker in the Adult Brain Outside the Neurogenic Regions. *The Journal of Neuroscience*, *37*(17), 4493–4507. https://doi.org/10.1523/JNEUROSCI.3199-16.2017

Suzuki, R., & Shimodaira, H. (2006). Pvclust: An R package for assessing the uncertainty in hierarchical clustering. *Bioinformatics*. https://doi.org/10.1093/bioinformatics/btl117

Taguchi, A., Kaku, Y., Ohmori, T., Sharmin, S., Ogawa, M., Sasaki, H., & Nishinakamura, R. (2014). Redefining the in vivo origin of metanephric nephron progenitors enables generation of complex kidney structures from pluripotent stem cells. *Cell Stem Cell*. https://doi.org/10.1016/j.stem.2013.11.010

Takahashi, K., Tanabe, K., Ohnuki, M., Narita, M., Ichisaka, T., Tomoda, K., & Yamanaka, S. (2007). Induction of Pluripotent Stem Cells from Adult Human Fibroblasts by Defined Factors. *Cell*. https://doi.org/10.1016/j.cell.2007.11.019

Tan, J., Yang, X., Zhuang, L., Jiang, X., Chen, W., Puay, L. L., … Yu, Q. (2007). Pharmacologic disruption of polycomb-repressive complex 2-mediated gene repression selectively induces apoptosis in cancer cells. *Genes and Development*. https://doi.org/10.1101/gad.1524107

Tang, Y., Gholamin, S., Schubert, S., Willardson, M. I., Lee, A., Bandopadhayay, P., … Cho, Y. J. (2014). Epigenetic targeting of Hedgehog pathway transcriptional output through BET bromodomain inhibition. *Nature Medicine*. https://doi.org/10.1038/nm.3613

Taylor, M. D., Northcott, P. A., Korshunov, A., Remke, M., Cho, Y. J., Clifford, S. C., … Pfister, S. M. (2012). Molecular subgroups of medulloblastoma: The current consensus. *Acta Neuropathologica*. https://doi.org/10.1007/s00401-011-0922-z

Taylor, R. E., Bailey, C. C., Robinson, K., Weston, C. L., Ellison, D., Ironside, J., … Lashford, L. S. (2003). Results of a randomized study of preradiation chemotherapy versus radiotherapy alone for nonmetastatic medulloblastoma: The International Society of Paediatric Oncology/United Kingdom Children's Cancer Study Group PNET-3 Study. *Journal of Clinical Oncology*, *21*(8), 1581–1591. https://doi.org/10.1200/JCO.2003.05.116

Tiberi, L., Bonnefont, J., VandenAmeele, J., LeBon, S.-D., Herpoel, A., Bilheu, A., & Baron, B. W. (2014). A BCL6/BCOR/SIRT1 Complex Triggers Neurogenesis and Suppresses Medulloblastoma by Repressing Sonic Hedgehog Signaling. *Cancer Cell*.

Uziel, T., Zindy, F., Xie, S., Lee, Y., Forget, A., Magdaleno, S., … Roussel, M. F. (2005). The tumor suppressors Ink4c and p53 collaborate independently with Patched to suppress medulloblastoma formation. *Genes and Development*, *19*(22), 2656–2667. https://doi.org/10.1101/gad.1368605

Vo, B. H. T., Li, C., Morgan, M. A., Theurillat, I., Finkelstein, D., Wright, S., … Roussel, M. F. (2017). Inactivation of Ezh2 Upregulates Gfi1 and Drives Aggressive Myc-Driven Group 3 Medulloblastoma. *Cell Reports*, *18*(12), 2907–2917. https://doi.org/10.1016/j.celrep.2017.02.073

Vong, K. I., Leung, C. K. Y., Behringer, R. R., & Kwan, K. M. (2015). Sox9 is critical for suppression of neurogenesis but not initiation of gliogenesis in the cerebellum. *Molecular Brain*, *8*(1), 0–17. https://doi.org/10.1186/s13041-015-0115-0

Wang, J., Garancher, A., Ramaswamy, V., & Wechsler-Reya, R. J. (2018). Medulloblastoma: From Molecular Subgroups to Molecular Targeted Therapies. *Annual Review of Neuroscience*. https://doi.org/10.1146/annurev-neuro-070815-013838

Wang, W., Yang, J., Liu, H., Lu, D., Chen, X., Zenonos, Z., … Liu, P. (2011). Rapid and efficient reprogramming of somatic cells to induced pluripotent stem cells by retinoic acid receptor gamma and liver receptor homolog 1. *Proceedings of the National Academy of Sciences of the United States of America*. https://doi.org/10.1073/pnas.1100893108

Ward, E., DeSantis, C., Robbins, A., Kohler, B., & Jemal, A. (2014). Childhood and adolescent cancer statistics, 2014. *CA: A Cancer Journal for Clinicians*, *64*(2), 83–103. https://doi.org/10.3322/caac.21219

Waszak, S. M., Northcott, P. A., Buchhalter, I., Robinson, G. W., Sutter, C., Groebner, S., … Pfister, S. M. (2018). Spectrum and prevalence of genetic predisposition in medulloblastoma: a retrospective genetic study and prospective validation in a clinical trial cohort. *The Lancet Oncology*, *19*(6), 785–798. https://doi.org/10.1016/S1470-2045(18)30242-0

Wetmore, C., Eberhart, D. E., & Curran, T. (2001). Loss of p53 but not ARF accelerates medulloblastoma in mice heterozygous for patched. *Cancer Research*. https://doi.org/10.1158/0008-5472.can-10-2876

Wilson, B. G., Wang, X., Shen, X., McKenna, E. S., Lemieux, M. E., Cho, Y. J., … Roberts, C. W. M. (2010). Epigenetic antagonism between polycomb and SWI/SNF complexes during oncogenic transformation. *Cancer Cell*. https://doi.org/10.1016/j.ccr.2010.09.006

Wu, Y., Ferguson, J. E., Wang, H., Kelley, R., Ren, R., McDonough, H., … Patterson, C. (2008). PRDM6 is enriched in vascular precursors during development and inhibits endothelial cell proliferation, survival, and differentiation. *Journal of Molecular and Cellular Cardiology*.

https://doi.org/10.1016/j.yjmcc.2007.06.008

Yan, W., Herman, J. G., & Guo, M. (2016). Epigenome-based personalized medicine in human cancer. *Epigenomics*. https://doi.org/10.2217/epi.15.84

Yang, Z. J., Ellis, T., Markant, S. L., Read, T. A., Kessler, J. D., Bourboulas, M., … Wechsler-Reya, R. J. (2008). Medulloblastoma Can Be Initiated by Deletion of Patched in Lineage-Restricted Progenitors or Stem Cells. *Cancer Cell*, *14*(2), 135–145. https://doi.org/10.1016/j.ccr.2008.07.003

Yusa, K., Zhou, L., Li, M. A., Bradley, A., & Craig, N. L. (2011). A hyperactive piggyBac transposase for mammalian applications. *Proceedings of the National Academy of Sciences of the United States of America*. https://doi.org/10.1073/pnas.1008322108

Zeltzer, P. M., Boyett, J. M., Finlay, J. L., Albright, A. L., Rorke, L. B., Milstein, J. M., … Packer, R. J. (1999). Metastasis stage, adjuvant treatment, and residual tumor are prognostic factors for medulloblastoma in children: Conclusions from the Children's Cancer Group 921 randomized phase III study. *Journal of Clinical Oncology*. https://doi.org/10.1200/jco.1999.17.3.832

Zhang, H., Zhu, D., Zhang, Z., Kaluz, S., Yu, B., Devi, N. S., … Van Meir, E. G. (2019). EZH2 targeting reduces medulloblastoma growth through epigenetic reactivation of the BAI1/p53 tumor suppressor pathway. *Oncogene*. https://doi.org/10.1038/s41388-019-1036-7

Acknowledgments

Desidero ringraziare Luca Tiberi, per avermi dato la possibilità di crescere all'interno di una nuova realtà e di un laboratorio nato con noi.
Tutto ciò non potrebbe essere stato possibile senza i miei compagni di viaggio: Claudio e Giuseppe. Le ore passate a non vedere la luce del sole sono indecifrabili, ma la fatica era avvolta da un'ironia e una leggerezza di pensiero che invidierò nei prossimi anni.
Ringrazio anche i seguenti componenti del laboratorio per gli scambi fondamentali di idee: Chiara Lago, Matteo Gianesello, Francesco Antonica, Marina Cardano.